# THE APPLICATION OF THE GENERALIZED IMPACT PARAMETER METHOD TO A NUMBER OF CHEMICAL PROCESSES

by

Bruce Alan Roy Kuppers

A Thesis Submitted to

The Faculty of Graduate Studies and Research

University of Manitoba

In Partial Fulfillment of the Requirements

for the Degree

Doctor of Philosophy

# THE APPLICATION
# OF THE
# GENERALIZED IMPACT PARAMETER METHOD
# TO A NUMBER OF
# CHEMICAL PROCESSES

BY

BRUCE ALAN ROY KUPPERS

A dissertation submitted to the Faculty of Graduate Studies of the University of Manitoba in partial fulfillment of the requirements of the degree of

DOCTOR OF PHILOSOPHY

DEDICATED

to

my parents

ACKNOWLEDGEMENTS

To say the least, my stay at the University of Manitoba has been educational. It has also included many good times and memories that will be cherished.

To give thanks individually to all those that assisted in this work, directly and indirectly, would be a task in itself. I therefore hereby acknowledge and thank these silent partners in this work.

Of course, special thanks goes to my supervisor, Dr. R. Wallace, whose patience has been tried often by my sometimes exasperating inability ' to learn'.

The other members of staff also bear mention, and, of course, the department's financial assistance in the form of Teaching Assistantships is duly appreciated.

## PREFACE

The work reported in this thesis is part of a collaborative investigation, involving R. Wallace, B. Pettitt, B. Corrigall, and A. Penner among others, aiming at the development of practical methods in the theoretical treatment of collisional processes. The author was involved in the evaluation of a number of models, but his major effort was directed at the development and testing of the semi-classical Generalized Impact Parameter method. The emphasis has been in general on qualitative and semi-quantitative rather than quantitative treatments since most chemical problems become intractable if attacked in an 'ab initio' manner. The general success of the method has been its applicability to a variety of processes including among others atom-atom collisions and photo-induced molecular rearrangement. A continued investigation of the application of this method to the study of de-excitation processes could be fruitful.

## ABSTRACT

A generalization of a well known method, the impact parameter method, is investigated and the feasibility of its application to reactive collision theory considered. The basis of choice of a semi-classical method is discussed.

A general form of the equations are developed and various features of the equations discussed. The use and advantages of various representations and transformations are examined.

This is followed by a discussion of the numeric and computational aspects of the problem which is concluded by the choice of the Runge-Kutta-Gill algorithm as the integration procedure to be applied to the general system of equations.

The method was applied in its classical limit form to the study of bimolecular vibrational energy exchange in highly excited oxygen molecules.

Next the proton-hydrogen system was studied using the general method. Both low and high energy collisions were analyzed. The photo-decomposition of $H_2^+$ was also simulated. The agreement of the high energy results with available experimental information was one of the more satisfying aspects of this study. The photo-decomposition study lead to an estimate of the lifetime of the excited species.

The next two investigations were model studies of molecular systems. The first study was of photo-induced cis-trans isomerization of simple ethylenes. The role of vibration and rotation of the methylene groups in the de-excitation process was considered. An estimate of the de-excitation time was obtained. The second study examined

the factors involved in electronic energy exchange in the bimolecular collision of pi bonded systems. The system coupling was taken to be short range and coulombic in nature.

The study is concluded by a summary and brief discussion of the results of the study and future possibilities.

TABLE OF CONTENTS

LIST OF TABLES

## LIST OF FIGURES

# Chapter I

## INTRODUCTION

## I.1 General Background

The dynamics of atomic and molecular processes have for some time presented the chemist, both experimentalist and theoretician, with an area of study which is both intriguing and difficult but also of fundamental importance to the discipline. The belief that a predictive understanding of chemical dynamics can be gained through a knowledge of fundamental collisional phenonema is the main motivation for the work offered herein.

The following discussion is intended to provide a qualitative overall view of the field of collision theory within the context of its application to the study of chemical processes. The practical impossibility of providing a more quantitative treatment is made manifest by the number of texts (1-7) and reviews (8-13*) available; the more formal aspects being examined in some detail in the former. It will perhaps clarify the following discussion to mention that the work reported in this dissertation was aimed at the development of a theory capable of application to actual physical systems, an objective receiving considerable support from Levine (10).

Collision theory describes an event in three distinct stages (4). One starts with an initial system which then undergoes an interaction leading to a final system. The system may consist of two initially isolated molecules which are allowed to approach, interact, and produce a system of molecule(s) as a result of the interaction. Such collisions are termed bimolecular. Alternately, the system may be an

---

* These references are only indicative. For a more comprehensive list see introduction of (10).

unstable molecule prepared at some starting time which undergoes an intra-molecular interaction leading to the formulation of a stable system, often called a unimolecular process.

Physically, it is possible to observe the initial reactants and final products but not the interaction complex of a collision (4). A quantum mechanical wave function which satisfies the boundary conditions imposed by the definition of the starting and final compounds of a reaction is called an asymptotic state. Since such states have a physical interpretation it is useful to describe the collision in terms of such states (3). The interaction is then described in terms of couplings among the various asymptotic states. Unfortunately the analytic aspects of such a description can become extremely complex and it is often necessary to develop the theory so it takes into account the special features of a given process.

Collision theories take advantage of the specifics of a given system by employing classical and semi-classical treatments rather than the more complex quantum mechanical treatment. However, two central problems are common to all approaches. The first is the handling of the translational modes of the collision while the other is the difficulty of managing the strong coupling of asymptotic states. These two difficulties are related. The absence of coupling amongst the electronic asymptotic states in the interaction region reduces the problem to one electronic channel, that is only one chemical product is expected from the reaction. The presence of such couplings introduces the possibility of alternate electronic channels and associated with each channel is a translational mode. In quantum and semi-classical

nuclear treatments these translational modes tend in general to be coupled. This difficulty may be expressed in other fashions, as in the case of classical nuclear treatments which require some form of statistical averaging of initial conditions to produce physically meaningful results, but the central problem remains.

To avoid this dual difficulty, total quantum theories, that is both the nuclei and electrons are treated as quantum particles, have commonly adopted either the adiabatic or Born-Oppenheimer approximations. Kolos (14) gives an analytic definition of these two related approximations but physically these two approximations take that the electronic and nuclear behaviours are independent; each only "seeing" a static potential representing the other set of particles. As has been mentioned (15), this is a static model which attempts to describe dynamic events. This approximation will fail whenever there are degeneracies in the electronic states involved in the process (16). Kolos (14) has considered the accuracy of the adiabatic approximation and some calculations have been attempted which include non-adiabatic behaviour (17-19). The main reason for imposing such a constraint is the resulting reduction in the complexity of the equations. Also, a number of events can be adequately described by such a model.

However, besides this pair of approximations one other approximation appears rather frequently in total quantum treatments, this being the use of perturbation theory. The formal aspects of this topic will not be considered here, the reader being referred to Messiah (1), but instead some general comments will be made. The extensive use of perturbation theory (8-10) reflects the fact that this method is one of

the more powerful analytic techniques available for the analysis of Schrodinger's equation. For a variety of phenomena which satisfy conditions described in (20) this method is indeed useful.

As a result of the common adoption of these approximations, almost all work using total quantum treatments have been restricted to non-rearrangement collisions. Emphasis has been on the analysis of translational-vibrational and/or rotational energy transfer; the usual systems being atom-diatom and diatom-diatom collisions. The reviews of Takayanagi (8), Rapp and Kassel (9), and Levine (10) indicate the level of present interest in this topic. Recently, with the advent of exact quantum calculations by Johnson and Secrest (21) and Clark and Dickinson (22) a great deal of effort has been directed toward a comparison of exact and various approximate methods.

However, some work has been done on rearrangement or reactive collisions with total quantum models. For instance, the system ($H+H_2$) has received considerable attention (23-24). Though other systems have been investigated the treatments employed generally incorporate adiabatic electronic potential energy surfaces and consider the reaction to be dominated by the collinear event.

Other work that has been done which is of relevance to this thesis is the study of electronic relaxation by a full quantum treatment by Jortner et al (25-28). However, this work has been more qualitative than computational in nature.

Not wishing to incorporate the adiabatic potential surface approximation in the general method, and seeing at the present time no way to manage the quantal description of translational modes in a

computationally oriented study, the full quantum treatment was abandoned.

The difficulties associated with total quantum descriptions has led to the re-investigation of the use of total classical theories to describe atomic and molecular events. Until recently this area has been largely neglected after the advent of quantum mechanics (see introduction of 29). However, interest has expanded rapidly as may be discerned from the review articles by Burgess and Percival (11), Bates and Kingston (12) and Keck (13). It is to be noted that few classical treatments actually consider the electron as a particle. However, both Abrines and Percival (29, 30) and Pettitt (31) have analyzed the system (p, H) wherein the electron was treated as a charged classical particle. Pettitt commented that "The ability to employ rotating classical electrons in the representation of low quantum atomic states is startling", (P. 42; 31). However, this approach is severly limited by the possibility of the electrons colliding with the nuclei, an almost unavoidable difficulty for systems of many electrons.

The more common approach is to represent the electrons by a suitable potential field. The use of Monte Carlo and statistical averaging techniques are common. The advantage of the total classical treatments is that the problem is solvable if somewhat time consuming. The disadvantages are associated with interpretation and choice of the proper potential surfaces (13). These methods tend to depend heavily on empirical and semi-empirical curve fits to define the potential surfaces and it has been noted (31) that the potential parameters are rather arbitrary yet their choice has significant effect on the interactions of the system. This difficulty will be elucidated by the study

reported in Chapter IV. Having no desire to be so limited from the start in the treatment of electronic behaviour, the semi-classical theories were considered.

Semi-classical theories divide naturally in two groups; the division being based on whether a classical or semi-classical nuclear treatment is employed. The latter treatment will be considered first.

The use of this group of semi-classical collision theories has been quite limited. However, there has been a recent renewal of interest in this particular approach. For example, Pechukas (32) and more recently Miller (33) have undertaken studies of vibrational phenomena within this semi-classical framework. Others such as Eu (126), Eu and Tsien (127), and Marcus (128) have developed methods for analyzing both non-rearrangement and rearrangement processes. Cross (129) divides the available methods into two general catagories, the perturbed elastic trajectory methods (130) where the inelastic scattering is treated as a time dependent perturbation, and the exact semi-classical method (32,33,128 ) in which quantum mechanical information is obtained by integrating a phase over the exact classical trajectory. However, these studies have been concerned more with the development of techniques than the study of actual systems and it is too early to draw conclusions on the general usefulness of this model (34). For a more complete discussion of this approach to the collisional problem the reader is referred to the work of the author's co-workers Penner and Wallace (35,36). However, considering the difficulties encountered in these developmental studies this approach was deemed inadvisable.

A variety of semi-classical theories which treat the nuclei as classical particles have been developed. Their range of application has

been rather extensive. For instance, Watson et al (37-39) have adapted the eikonal approximation to a semi-classical theory and applied it to reactive collisions. The study of classical trajectories along representative potential surfaces has received considerable attention from Polanyi et al (40-45) amongst others (46-47). A variety of processes have been studied including reactive collisions. Much effort has been directed towards an analysis of the effect of the shape of the potential surface on the reaction.

Unfortunately, these studies tend to adopt in one fashion or another the adiabatic approximation in that most studies consider only one electronic state. For this reason the study of Gallaher and Wilets (48) was of particular interest since it allowed the possibility of contribution from the electronic excited states in the evaluation of the transition possibilities. Their method, however, is not directly applicable to chemical systems since they were analyzing the collision of medium energy protons (KeV) with hydrogen atoms by a standard impact-parameter method. It is known that these methods fail when the initial and final state trajectories are significantly different (49), behaviour expected in chemical processes.

However, the more general existance of semi-classical methods (classical nuclei) which have been used to analyze reactive collisions and the ability of the impact-parameter method to investigate simultaneously the importance of various electronic states in a given process suggested the investigation of the possibility of developing a generalization of the impact-parameter method which would not be limited to relatively high energy events.

This thesis reports the development of a method and its application to a number of systems resulting from such an investigation.

I.2 Scope of Dissertation

In the next chapter the equations of motion representative of the generalized impact parameter method are developed. The general form and necessary properties of the multi-electron functions are discussed followed by the introduction of the general use of transformation theory on this set of equations.

Chapter three undertakes to find the optimum method of solving the systems of equations developed in Chapter two. Taking into consideration both numeric and computer aspects of the problem, the fourth order Runge-Kutta Gill method was chosen and program coding was done in the Fortran IV computer language.

In the first study employing the generalized impact parameter method the equations were developed to a form appropriate for the total classical limit and applied to the analysis of the collision of oxygen molecules in highly excited vibrational states. The study employed empirical potentials and the results are indicative of the difficulties associated with their use.

Chapter five undertakes the study of low and high energy collisions of the proton-hydrogen (p-H) system as well as the photo-decomposition of excited states of $H_2^+$ using the generalized impact parameter method. The results of the high energy collision study are perhaps most signifigant.

In the next chapter, the cis-trans isomerization of photo-excited ethylenes is examined. This is a unimolecular reaction involving non-radiative de-excitation processes. The relative importance of the various available modes for energy transfer is considered and the time for

the process to take place estimated.

Chapter seven contains an investigation of intermolecular electronic energy transfer in $\pi$ bonded systems. This final study examines the factors which control short range electrostatically induced electronic energy transfer in the collision of ethylene like molecules where one of the colliding partners is electronically excited.

The dissertation is concluded by a general discussion of results and possible directions for development.

# Chapter II

## DEVELOPMENT OF GENERALIZED IMPACT PARAMETER METHOD

## II.1 Introductory Comments

Standard impact parameter methods usually employ the approximations that the relative velocity is constant and that the particles follow straight line trajectories. As a result these methods are implicitly limited to the study of relatively high energy events since it is realized that non-linear motion will be important for low energy collisions (2, 49).

It was apparent, therefore, that a method applicable to low energy collisions could employ neither of these approximations. The resulting theory takes the nuclei to be classical particles moving along trajectories determined by an electronic potential which dynamically depends on the internal states of the colliding molecules and these states have an implicit dependence on the nuclear motion through their explicit dependence on the potentials defined in terms of the time dependent nuclear positions. In this way, all changes happening during the collision are coupled, and these time dependent couplings represent the interactions which result in the processes that are to be investigated. The use of numeric methods and standard approximate electronic treatments resulted in it being feasible to undertake at least model calculations of actual chemical systems.

Before proceeding it is perhaps appropriate to deal briefly with the questions raised by the employment of a classical nuclear treatment for collisions of such low energy. First, one may wonder how valid such a treatment is for low energy processes. Thorson and Delos (50) investigated the applicability of the classical equations of motion and concluded that they were valid in situations in which the classical

picture did not apply. They were able to derive sufficient conditions to guarantee the validity of the classical equations but did not show them to be necessary conditions. The other major question is the practicality of a method that inherently requires multiple trajectory calculations for statistical averaging in the calculation of physical quantities such as cross sections. This point will not present this research with much difficulty since the present interest lies more in revealing the basic mechanism of the reaction than obtaining quantitative calculations of physically unmeasurable events.

In the following chapters, two alternative reference frames are used. The first is the laboratory frame, denoted by the set $\{\tilde{q}^i\}$ while the other is the centre of mass frame specified by the set $\{\tilde{R}^i\}$. The relation between the two frames for a two body case is shown in figure one.

The derivation presented in this chapter is general in nature. The quantum mechanical equations are developed in the centre of mass frame (1) while the classical equations can be considered to lie in either frame.

Throughout the rest of this thesis atomic units are used in which Planck's constant $\hbar$, the electronic mass m, and charge e are unity. For the definition of these units see Appendix A.

Figure 1

Relation between the laboratory $(\tilde{q}^1, \tilde{q}^2)$ and centre of mass (R) frames of reference for a two body system where

$$R = | \tilde{q}^1 - \tilde{q}^2 |$$
$$= \sqrt{(\tilde{q}^1 - \tilde{q}^2) \cdot (\tilde{q}^1 - \tilde{q}^2)}$$

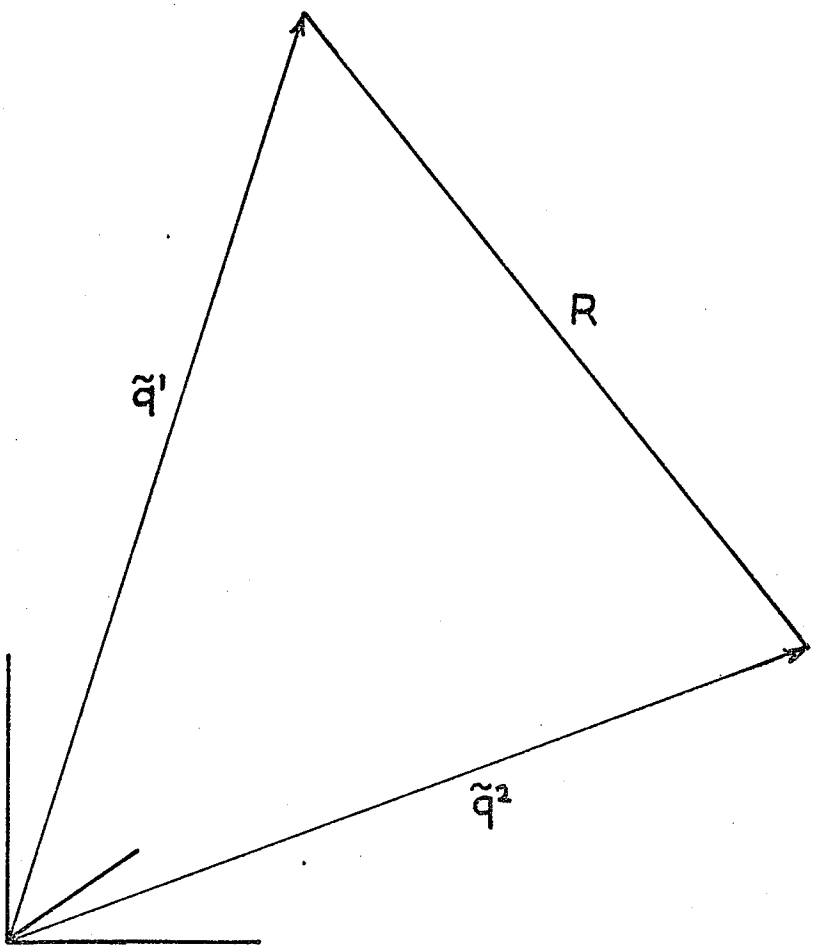
R
$\tilde{q}^1$
$\tilde{q}^2$

## II.2 Development of Equations Describing Electronic Dynamics

The time evolution of the electronic wave function $|\Psi(\tilde{r},t)>$ is given by the time-dependent Schrödinger equation

$$i\,(\partial_t)_{\tilde{r}}\,|\,\Psi\,(\tilde{r},t)> = H\,|\,\Psi\,(\tilde{r},t)> \qquad \text{(II.1)}$$

where H is the Hamiltonian describing the motion of the electrons in the centre of mass frame, $\tilde{r}$ represents all electronic co-ordinates in the centre of mass frame, t is the variable time, and $(\partial_t)_{\tilde{r}}$ is the partial differential operator with respect to time under the constraint that $\tilde{r}$ remains fixed. To develop from (II.1) a manageable set of equations, it is necessary to examine the forms of H and $|\,\Psi\,(\tilde{r},t)>$.

The Hamiltonian H is defined for a given system by a set of rules which are well established (1). However the present interest is not in the specific resolution of H but the general separation

$$H = H_o + V \qquad \text{(II.2)}$$

which has general applicability.

The choice of an appropriate form for the multi-electron function $|\,\Psi\,(\tilde{r},t)>$ is a more difficult problem, the scope of the topic being suggested by the extensive work that has been done for its time-independent counter-part ( 51 - 54 ). Certain ramifications of this topic will be discussed in the next section but it will be taken that $|\,\Psi\,(\tilde{r},t)>$ has the form

$$|\,\Psi\,(\tilde{r},t)> \;=\; \sum_i b_i\,(\tilde{R},t)\;|\,\chi_i\,(\tilde{r})> \qquad \text{(II.3)}$$

where $\tilde{R}$ represents all nuclear co-ordinates and $\{\,|\,\chi_i\,(\tilde{r})>\,\}$ is a set of time independent multi-electron functions. The coefficients $b_i\,(\tilde{R},t)$ contain all the time dependence of the many electron wave function. The choice of the set $\{\,|\,\chi_i\,(\tilde{r})>\,\}$ is somewhat arbitrary but it is often

convenient to relate the resolutions (II.2) and (II.3) such that

$$H_o \mid \chi_i (\tilde{r})> = E_i \mid \chi_i (\tilde{r})> \tag{II.4}$$

where

$<\chi_i \mid \chi_j> = \delta_{ij}$, $\delta_{ij}$ being the Kronecker delta. It perhaps bears mention at this point that in a given problem there may be no unique resolution for H of the form (II.2) and in fact a number of such resolutions may be used. This technicality will not present the general derivation with any difficulty but this point must be kept in mind in actual applications.

Having chosen the general form (II.3) for the wave function, and noting the mathematical relationship

$$(\partial_t)_{\tilde{r}} = (\partial_t)_{\tilde{r},\tilde{R}} + d_t\tilde{R}\,(\partial_{\tilde{R}})_{\tilde{r},t} \tag{II.5}$$

(II.1) can be rewritten by first applying (II.5) to (II.3) giving

$$(\partial_t)_{\tilde{r}} \mid \Psi (\tilde{r},t)> = \sum_i d_t\, b_i (\tilde{R},t) \mid \chi_i (\tilde{r})> + \sum_i b_i\, d_t\tilde{R} \cdot(\partial_R \mid \chi_i (\tilde{r})>) \tag{II.6}$$

which upon substitution into (II.1) followed by the formation of the inner product on the left with $<\chi_k|$ results in the equation

$$i \sum_i <\chi_k \mid \chi_i> d_t\, b_i = \sum_i \{<\chi_k|H|\, \chi_i> - i\, d_t\, \tilde{R} \cdot<\chi_k \mid \partial_{\tilde{R}} \mid \chi_i>\}b_i \tag{II.7}$$

Since there is such a set of equations for each $<\chi_k|$ the complete set of equations are

$$d_t\, \underline{b} = \underline{N}^{-1} \{-i\, \underline{H} - d_t\, \tilde{R}\, \underline{G}\}\underline{b} \tag{II.8a}$$

or

$$d_t\, \underline{b} = \underline{N}^{-1} \{-i\, H_o - i\underline{V} - d_t\, \tilde{R}\, \underline{G}\}\underline{b} \tag{II.8b}$$

where $\underline{b}$ is a column vector composed of elements $b_i(\tilde{R},t)$ of equation (II.3) and the matrices are defined as follows

$$\underline{N}(i,j) = \langle \chi_i \mid \chi_j \rangle \tag{II.9a}$$

$$\underline{H}(i,j) = \langle \chi_i \mid H \mid \chi_j \rangle \tag{II.9b}$$

$$\underline{H_o}(i,j) = \langle \chi_i \mid H_o \mid \chi_j \rangle \tag{II.9c}$$

$$\underline{V}(i,j) = \langle \chi_i \mid V \mid \chi_j \rangle \tag{II.9d}$$

$$\underline{G}(i,j) = \langle \chi_i \mid \partial_{\tilde{R}} \mid \chi_j \rangle \tag{II.9e}$$

Solving (II.8), which describes the time evolution of electronic wave function and may be called the electronic force law is the central task to be considered. Its solution, after defining the Hamiltonian H or equivalently the system of study, requires the specification of

a) a basis set of multi-electron functions

b) a nuclear force law.

These two topics are the subjects considered in the next two sections.

Before proceeding there are some general relationships that can be obtained from the equation derived to this point. For instance, choosing the set $\{ |\chi_i\rangle \}$ such that (II.4) is true gives one the equation

$$\underline{H_o} = \underline{N}\,\underline{E} \tag{II.10}$$

where $\underline{E}(i,j) = E_i\,\delta_{ij}$. Also, one obtains by comparison of (II.5) and (II.8) the relationships

$$(\partial_t \underline{b})_{\tilde{r},\tilde{R}} = -\,i\,\underline{N}^{-1}\,\underline{H}\,\underline{b} \tag{II.11a}$$

$$(\partial_{\tilde{R}} \underline{b})_{t,\tilde{r}} = -\,i\,\underline{N}^{-1}\,\underline{G}\,\underline{b} \tag{II.11b}$$

It is also useful to know that conservation with respect to time of the normalization condition

$$\langle \Psi \mid \Psi \rangle = \underline{b}^{+}\,\underline{N}\,\underline{b} = 1 \tag{II.12}$$

where $\underline{b}^+$ is the complex conjugate of $\underline{b}$ requires that

$$\underline{G}^+ = - \underline{G} \tag{II.13}$$

Finally it is noted that associated with $| \Psi >$ and H is the quantity

$$\bar{\bar{E}} (\tilde{R}) = \underline{b}^+ \underline{H} \underline{b} \tag{II.14a}$$

$$= b^+ (\underline{H}_o + \underline{V}) b \tag{II.14b}$$

which is the mean internal energy of the colliding system (excluding nuclear kinetic energy). The derivation of the nuclear force law will make use of this quantity. It is interesting to note $\bar{\bar{E}}$ depends only upon configuration and not time for

$$\begin{aligned} \partial_t \bar{\bar{E}}(\tilde{R}) &= \partial_t (\underline{b}^+ (\tilde{R},t) \underline{H} (\tilde{R}) \underline{b} (\tilde{R},t)) \\ &= (\partial_t \underline{b}^+) H b + \underline{b}^+ \underline{H} (\partial_t \underline{b}) \\ &= i \underline{b}^+ \underline{H}^+ \underline{N}^{+-1} \underline{H} \underline{b} - i b^+ \underline{H} \underline{N}^{-1} \underline{b} \\ &= 0 \end{aligned}$$

since $\underline{H}$ and $\underline{N}$ are hermitian. The third line used the relation given in (II.11a).

## II.3 Basis Set for Multi-Electron Functions

The topic to be initially considered in this section is the appropriate choice of form for the wave function $|\Psi>$ of (II.1) or equivalently for the wave function $|\chi_i(\tilde{r})>$ of (II.3). Since the objective of this study is the development of a theory which will deal with reaction dynamics there is no need that the selected form be quantitatively accurate but it need only provide a physically realistic if simplified description of the system. Therefore, there would be little benefit from an examination of the myriad of approaches to the solution of this problem (51, 52). Instead, the following treatment will present the reasoning by which one may choose a proper basis set.

It is perhaps best to start by discussing equation (II.3). It takes that the general solution $|\Psi>$ may be expressed as a linear combination of a set of multi-electron functions, an approach common to a number of the most sophisticated molecular energy calculations (55-57). The question is then resolved to the choice of an appropriate set of multi-electron functions.

First, the form of a given function of the set will be defined. It is well known that an electronic wave function must be anti-symmetric with respect to permutations of the electron (1). Then it is taken that

$$|\chi_i(\tilde{r})> = |\chi_i(\tilde{r}^1, \tilde{r}^2 \cdots, \tilde{r}^n)>$$

$$= \frac{1}{\sqrt{n!}} \| |\phi_1(\tilde{r}^1)> \cdot |\phi_2(\tilde{r}^2)> \cdots |\phi_n(\tilde{r}^n)> | \qquad \text{(II.15)}$$

where $|\chi_i(\tilde{r})>$ is an n electron function and the final form on the right hand side is a Slater determinant constructed from a set of one electron functions $\{|\phi_i>\}$ and $\tilde{r}^i$ is the position of the i-th electron. This

form of the multi-electron function is well established (1, 51, 58). Upon choice of the set $\{|\phi_i\rangle\}$ which usually has more than n members, it is possible to create a set of multi-electron functions simply by choosing different members of the set in using (II.15).

There remains, then, the choice of form of the single electron functions. The two general categories are single centre and multi-centre functions. Since it is common practice to build multi-centre functions by forming linear combinations of single centre functions, the starting point of the discussion is the development of an appropriate set of single centre functions.

The study of molecular electronic structure has resulted in the development and use of a number of general sets of single electron functions. Unfortunately to date the only known way to find the best set of functions has been essentially "trial and error". For the purposes of the present study it was considered adequate to employ previously developed treatments which had the appropriate properties.

This brings the discussion to the central question in the choice of the basis functions, both single and multi-electron. Basically one desires a basis set that leads to easy interpretation of results and at the same time results in the maximal simplification of (II.8) with the second requirement being the more critical.

One of the more straightforward simplications is to choose an orthonormal set of multi-electron functions $\{ | \chi_i > \}$ which in practice usually requires the use of an orthonormal set of single electron functions. The result is the elimination of $\underline{N}$ from (II.8). An often related option is to choose the $\{ | \chi_i > \}$ such that (II.4) is true, resulting in

a diagonal $\underline{H}_o$ whose elements are often elementary to solve.

Another property which is necessary for a basis set to be practical is that it must be possible to keep the number of states down to a small number and still produce meaningful results. Although the proper choice is found mainly by trial and error, there are a few criteria that are generally employed. These criteria are physical in origin, for example, the state energies and expected initial and final products are parameters that may prove useful in limiting the set of functions.

There is one more general question to examine in choosing a basis set, this being the choice of representation. This topic has been investigated by Nitzan and Jortner (28) and Smith (59), with particular emphasis on the diabatic and adiabatic representations.

The adiabatic representation is defined by choosing $\{ \mid \chi > \}$ such that

$$H \mid \chi_n > = E_n (\tilde{R}) \mid \chi_n > \qquad \text{(II.16)}$$

Then (II.8) becomes

$$d_t \underline{b} = -(i \underline{E} + d_t \tilde{R} \underline{G}) \underline{b} \qquad \text{(II.17)}$$

where

$$\underline{E} (i,j) = \underline{E}_i (\tilde{R}) \delta_{ij}$$

By this choice the inter-state couplings are all contained in $\underline{G}$. Then the one matrix $\underline{G}$ describes the behaviour of the electronic system. Unfortunately the evaluation of $\underline{G}$ can be difficult. However, this form of the equations is considered appropriate for low velocities or $d_t \tilde{R} \to 0$ or for cases in which the operator V varies slowly with changes in $\tilde{R}$ (P. 302, 6).

The diabatic representation is defined by choosing $\{ \mid \chi > \}$ such that

$$\underline{G} = \underline{0} \text{ for all } \tilde{R} \tag{II.18}$$

Then (II.8b) becomes

$$d_t \underline{b} = -i \underline{H} \underline{b} \tag{II.19a}$$

$$= -i (\underline{H}_o + \underline{V}) \underline{b} \tag{II.19b}$$

This avoids the evaluation of $\underline{G}$ but results in a non-diagonal $\underline{H}$ matrix. Using a number of resolutions of the operator of the form (II.2) it may be possible to resolve $\underline{H}$ to the form (II.19b). This representation is considered appropriate when V changes quickly with $\tilde{R}$.

The actual choice between the two representations is a matter of judgement depending heavily on the form of the potential (60), nor are these two representations necessarily the only feasible choices. Also, it may be desirable to change from one representation to another as the behaviour of V dictates. This is possible by the use of transformation theory, the last topic to be considered in this section.

It is possible to relate any two general representations by the equations

$$\underline{b}' = \underline{U} \underline{b} \tag{II.20}$$

$$\underline{A}' = \underline{U} \underline{A} \underline{U}^{+} \tag{II.21}$$

where $\underline{U}$ is a unitary matrix, $\underline{b}'$ and $\underline{b}$ are column vectors while $\underline{A}'$ and $\underline{A}$ are matrices.

This is termed a unitary transformation and for a formal treatment of the topic one is referred to Messiah (1). The equations are general in nature but to relate to the previous discussion one could take $\underline{b}'$ to be a column vector representing the diabatic basis set and $\underline{b}$ the

adiabatic basis set.

Just as it is possible to remove a certain dependence from the wave function by such a unitary transformation, it is possible to introduce new variable dependence. For example, in the adiabatic representation defined by (II.12) it is generally found that $\underline{E} \rightarrow \underline{E}_\infty$ as $\tilde{R} \rightarrow \tilde{\infty}$ where

$$\underline{E}_\infty \ (i,j) = E_i \ (\tilde{R}=\tilde{\infty}) \ \delta_{ij}$$

the $E_i$ again being defined by (II.16). If one defines the transformation matrix

$$\underline{U} \ (i,j) = \ e^{\ i \ E_i \ (\tilde{R}=\tilde{\infty})t} \ \delta_{ij} \qquad \text{(II.22)}$$

and applies (II.20) and (II.21)

$$\underline{E}' = \underline{U} \ \underline{E} \ \underline{U}^+ \qquad \text{(II.23)}$$

and

$$d_t \underline{b}' = - d_t \tilde{R} \ \underline{G}' \ \underline{b}' \qquad \text{(II.24)}$$

which in the limit of large $\tilde{R}$ becomes zero. The mean energy of (II.14) becomes

$$\bar{E} = \underline{b}'^{+} \underline{H}' \ \underline{b}' \qquad \text{(II.25)}$$

with $\underline{b}'$, $\underline{G}'$ and $\underline{H}'$ being defined by equations (II.22), (II.20) and (II.21).

In summary, the multi-electron set $\{ \ | \ \chi_i > \}$ is constructed from a set of single electron functions $\{ \ | \ \phi_i > \}$, whose choice is guided by the discussion of this section. The set $\{ \ | \ \phi_i > \}$ may be composed of single centre or multi-centred functions. In the present work, however, the prevelence of multi-centre function or molecular orbital treatments has lead to their predominant use in this thesis.

## II.4 Development of Equations Describing Nuclear Dynamics

Since the electronic potential energy defined by (II.14) is time-independent, the equations of motion for the nuclei may be derived by application of Newtonian mechanics. Then starting with Hamilton's canonical equations which in vector form are

$$d_t\, \tilde{r}^m = \partial_{\tilde{p}^m} H_c \qquad m = 1,n \tag{II.26a}$$

$$d_t\, \tilde{p}^m = \partial_{\tilde{r}^m} H_c \qquad m = 1,n \tag{II.26b}$$

where in cartesian coordinates

$$\partial_{\tilde{p}^m} = \partial_{p_i^m}\, \bar{i} + \partial_{p_j^m}\, \bar{j} + \partial_{p_k^m}\, \bar{k}$$

$$\partial_{\tilde{r}^m} = \partial_{r_i^m}\, \bar{i} + \partial_{r_j^m}\, \bar{j} + \partial_{r_k^m}\, \bar{k}$$

and $\tilde{p}^n$ and $\tilde{r}^n$ are, respectively, the generalized momentum and coordinate vectors of the m-th particle of n particles. $H_c$ is the total classical Hamiltonian for the system and has the form

$$H_c = \sum_{m=1}^{n} \tilde{p}^m \cdot \tilde{p}^m / 2M^m + \bar{E}\,(\tilde{R}) \tag{II.27}$$

where $M^m$ is the mass of the m-th particle and $\bar{E}\,(\tilde{R})$ the electronic potential energy defined by (II.14). Substituting (II.27) into (II.26) one arrives at the equations

$$d_t\, \tilde{r}^m = \tilde{p}^m / M^m \qquad m = 1,n \tag{II.28a}$$

$$d_t\, \tilde{p}^m = - \partial_{\tilde{q}^m} \bar{E} \qquad m = 1,n \tag{II.28b}$$

The second set of equations is readily solved by use of the relationship

$$\partial_{\tilde{q}^m} = (\partial_{\tilde{q}^m} \tilde{R})\, \partial_{\tilde{R}} \tag{II.29}$$

## II.5 Concluding Remarks on General Equations of Generalized Impact Parameter Method

This completes the derivation of the general equations of the Generalized Impact Parameter Method. Equations (II.8) and (II.28) are a complete set of coupled differential equations which require only a definition of the operator H of (II.2) and the Hamiltonian $H_c$ of (II.27), and the choice of basis set $\{|\chi_i\rangle\}$ to be completely defined. The first two are defined upon the choice of the system, while the last item is more arbitrary but limited by the considerations discussed in this chapter.

It is perhaps useful to note at this time that the conservation laws associated with the normalization of the function $|\Psi\rangle$ and the total energy defined by (II.27) can be used to check the accuracy of the solutions obtained from this set of coupled equations.

The necessary simplifications that must be introduced to deal with systems of any complexity have not been discussed in this chapter. Instead a general framework has been presented which will be adopted to the individual systems to be examined in later chapters.

However, to analyze any system, it is necessary to develop a method of integrating the equations (II.8) and (II.28) with respect to time; the topic of the next chapter.

# Chapter III

## A GENERAL METHOD OF SOLUTION FOR THE EQUATIONS OF THE GENERALIZED IMPACT PARAMETER METHOD

## III.1 Introductory Comments

In the previous chapter a set of differential equations (II.8) and (II.28) was developed which formally are capable of providing a quantitative description of any chemical reaction in which the nuclei are not expected to exhibit quantum behaviour. The complexity of this set of differential equations is emphasized by the close relationship between each equation in the set (II.8) and the differential equation analyzed by those who are interested in molecular electronic structure, and in fact the equations in this form are insoluble by analytic techniques. It was decided, therefore, partially through necessity, to incorporate the use of computer based techniques, that is numerical analysis, into the general method employed to solve this system of equations.

The development and availability of sophisticated computer technology in the last decade is "mirrored" in the literature by the appearance of a number of studies which inherently depend on this technique. For instance, the calculations of Johnson and Secrest (21), Locker and Endres (61), and Locker and Wilson (62) incorporate numeric methods in the integration of differential equations. More recently Goodwin (63, 64) has applied a similar approach to the study of response in Magnetic Resonance. Many of the classical trajectory calculations (40-45) depend heavily on computer technology.

There are two considerations in undertaking a computation of the magnitude being considered; the choice of numeric method, and computer hardware and software capabilities. These two elements may be considered separately but in practice they are interrelated. The more formal as-

pects will be avoided where possible. Instead it is the intention of the writer to give a general idea of the factors involved in assessing and applying this approach to the solution of differential equations.

Since (II.8) and (II.28) are all first order equations and a specific system is defined by a set of initial conditions, the next section on numeric analysis will examine methods developed for the treatment of the initial value problem for first order differential equations. This is followed by a discussion of a number of relevant aspects of computer technology and some general remarks.

## III.2 A Discussion on the Numeric Solution of the Initial Value Problem

The concern here will not be with the formal aspects of numerical analysis but with the practicality of various algorithms in solving equations (II.8)&(II.28). For a formal treatment of this problem the reader is referred to the various texts in this field (65-68).

Equations (II.8, II.28) are a set of differential equations of the form

$$d_t\, y_i = f_i\,(t, y_1, \ldots, y_n) = f_i\,(t, \underline{y}),\ i = 1,n \qquad \text{(III.1)}$$

It is assumed that all $f_i\,(t, \underline{y})$ are continuous single valued functions, and that the initial conditions $(t_o, \underline{y}_o)$ are known. The general problem is the integration of (III.1) to find the final conditions $(t_n, \underline{y}_n)$. Numerically this is approached in a step-wise fashion. The interval $(t_o, t_n)$ is divided into a number of segments, n, of size h, such that

$$t_{i+1} = t_i + h \qquad \text{(III.2)}$$

and each of these subintervals is integrated by the application of a chosen algorithm. An algorithm is a computational procedure which approximates the solution of the above problem and in general is developed by truncating the Taylor's series expansion solution and rewriting the resulting equations in terms of the first order derivatives. The accuracy and reliability of a given algorithm can be determined from its convergence and stability properties.

Assuming the existance of a unique solution, the convergence properties of an algorithm are determined by truncation error. Truncation error of a particular algorithm can generally be defined analytically (65). Qualitatively, this error is the difference between using a finite step

size and infinitely small step size (exact solution) in the computation. It is possible to analyze both local truncation error, that is the error resulting from one application of the method, and total truncation error (65). In most cases, the local truncation error is more signifigant since a method is considered to be convergent if in the limit of h tending to zero the local truncation error goes to zero.

The other factor generally considered important is the stability of a method. Qualitatively it is related to error propagation; a method being considered stable if the error propagation remains within defined bounds. Of course, stability has been defined analytically (65,66). One can derive a stability diagram (69) for a given algorithm which defines a region of the complex number plane in which all the products

$$h\,\lambda_i,\ i = 1,\ n$$

must lie where the $\lambda_i$ are the eigenvalues of the Jacobian matrix $\underline{A}$ defined

$$\underline{A}\ (i,j) = \partial f_i \ / \ \partial y_j \qquad \text{(III.3)}$$

It can be seen that this type of analysis can determine the maximum step size h for which the method can be expected to produce a unique, consistent solution for a given set of functions $(f_i)$. It is to be emphasized that this analysis is only indicative of expected behaviour. Use of a step size larger than that found by this analysis might lead to the correct solution but it also could produce spurious solutions.

Having suggested the minimal properties a given method must possess, it is now appropriate to discuss the general classes of algorithm that are available. There are infact only two general classes; single step and multi-step.

The single step methods require only one set of conditions or the conditions of one step $(t_i, \underline{y}_i)$ to generate the solution at time $(t_i + h)$. This class of methods is usually designated by the term Runge-Kutta. There is in fact a whole family of Runge-Kutta methods of varying orders (70-73). For the purposes considered here, only fourth and higher order methods will provide the necessary accuracy for reasonable step size.

The general features of this group of algorithms are the following. First, they are self starting since they require only one set of conditions and as a result definition of initial conditions automatically provides all the information necessary for this class of algorithms to integrate a given set of differential equations. This leads to a second useful feature, an ability to change the step size at any point in the calculation without excessive loss of effort since the integration at one point is independent of what has been done previously. Most importantly these methods are highly stable exhibiting at most partial instability which is easily corrected by reduction of the step size.

The drawbacks associated with these methods are mainly associated with the lack of automatic error estimates and the related difficulty that a check is not provided on the solution being generated. It is generally necessary to repeat the solution with a smaller step size or use criteria based on expected system behaviour to establish the accuracy of the solution. Also, an n-th order method of this class requires n evaluations of the first derivatives in a given integration step. For systems whose derivatives are difficult to evaluate this is a serious consideration. The multi-step methods define the solution at time $t_{i+1}$ in terms of a number of previous equally spaced solutions. There

are two general approaches, these being explicit methods in which the value can be found directly, and implicit methods where the desired value is contained on the right hand side of the equation for the algorithm. The latter group are quite often called predictor corrector methods.

There are a number of advantages associated with these methods. First, an estimate of the truncation error is calculated automatically as an integral part of the algorithm. Also, most algorithms, say of order n where n is even, require only n/2 evaluations of the derivative.

These methods have balancing disadvantages. They are not self-starting but instead must employ an additional procedure to produce the necessary sets of conditions from one set of initial conditions. It follows that changing the step size becomes a much more involved and expensive procedure than is the case for the Runge-Kutta methods. But most importantly the stability of this group of algorithms is a more complex question. Whereas, the Runge-Kutta methods exhibited at worst partial instability, the multi-step methods can be weakly stable or display partial or inherent instability. A weakly stable method is one in which a "parastic" solution may introduce errors into the desired solution, while an algorithm possessing inherent instability will diverge from the desired solution (65).

Pages intentionally omitted.

III.3 Other Remarks

A discussion of elementary software and hardware considerations is given in Appendix B.1.

Appendix B.2 gives a brief account of the factors which lead to the choice of the Runge-Kutta-Gill algorithm (66).

The question of cost forced the choice of the Fortran language for bulk of the programming. All work was done in double precision and compiling was done mainly on the IBM Fortran H level compiler. A few routines were written in assembler, generally with the help of the staff at the computer centre. The general structure of all programs is the same but for efficiency the coding tended to be highly specialized for each system studied. A number of logic flow charts for the system of programs is provided in Appendix B.4. It was felt that the logic flow charts would be of more use and interest than the actual coded programs, the logic of which are difficult to understand as a result of size and certain features of the Fortran language.

This concludes the discussion of the practical aspects of finding numeric solutions for sets of coupled equations of the form of (II.8) and (II.28). In the remaining sections the establishment of the specific forms of the $f_i$ $(t,\underline{y})$ for the various systems to be studied will be considered the major task, after which it will be taken to be only necessary to define appropriate initial conditions for a given event to establish the transition probability.

# Chapter IV

## CLASSICAL LIMIT OF GENERALIZED IMPACT PARAMETER

## IV.1 Introductory Comments

The interrelation between the Generalized Impact Parameter method and the Classical Trajectory method (single potential surface) will be illustrated.

Historically, the work reported in this chapter was done in conjunction with B. A. Pettitt previous to the development of the Generalized Impact Parameter method but it is informative to include it at this point as a special case of the Generalized Impact Parameter method.

A brief study of the collision of $O_2$ molecules in highly excited vibration states is presented as a test application of the equations developed in this chapter. Only collinear collisions were considered since it was not the intent of this study to produce physical quantities such as cross sections but to exhibit the model's ability to deal with bimolecular energy exchange, if only under these constrained conditions, and to examine the dependence of this exchange on the form of the potential used to describe the interaction.

## IV.2 General Classical Model

The classical collision theory considered here takes that the electronic behaviour can be effectively represented by some potential field. In short, equation (II.8) becomes trivial by the simplifying assumption that only one electronic state is ever populated. Only non-rearrangement collisions are considered.

Then the question is the form of the potential $\overline{E}$ (R) in (II.27). It is noted that a general potential function for a system of N particles can have the form

$$V'(\tilde{q}) = \sum_{i}^{N} V_i(\tilde{q}_i) + 1/2! \sum\sum_{i\neq j} V_{ij}(\tilde{q}_i,\tilde{q}_j) + 1/3! \sum\sum\sum_{i\neq j\neq k} V_{ijk}(\tilde{q}_i,\tilde{q}_j,\tilde{q}_k) + \quad (IV.1)$$

Omitting the self energy term $\sum_{i}^{N} V_i(\tilde{q}_i)$ one obtains the interaction potential

$$V(\tilde{q}) = 1/2! \sum\sum_{i\neq j} V_{ij}(\tilde{q}_i,\tilde{q}_j) + 1/3! \sum\sum\sum_{i\neq j\neq k} V_{ijk}(\tilde{q}_i,\tilde{q}_j,\tilde{q}_k) + \quad (IV.2)$$

Then (II.27) becomes

$$H = \sum_{i}^{N} \tilde{p}_i \cdot \tilde{p}_i / M_i + V(\tilde{q}) \quad (IV.3)$$

Since a classical model is distinguished by its characteristic interaction potential, it is only necessary to choose the appropriate models for a system to define the potential $V(\tilde{q})$.

A molecular system in motion (or collision) can be usefully modelled by retaining selective terms in (IV.2) Visualization of the geometry is most easily accomplished in terms of "valence coordinates" (77) (bond angles and distances) and intermolecular separations. These coordinates will be used here.

Bonded-pair (nuclei) interactions are considered to be represented adequately by the empirical Morse function (78)

$$V^{m}_{ij}\ (\tilde{q}_i,\ \tilde{q}_j) = D_{ij}\ \{1 - K_{ij} \cdot \exp\ (-\beta_{ij}|\tilde{q}_i-\tilde{q}_j|)\}^2 \qquad \text{(IV.4)}$$

where $K_{ij} = \exp\ (\beta_{ij}|\tilde{q}^{o}_i-\tilde{q}^{o}_j|)$, where $(\tilde{q}^{o}_i-\tilde{q}^{o}_j)$ is the equilibrium bond distance, $\beta_{ij}$ the range parameter, and $D_{ij}$ the bond dissociation energy.

Non-bonded intermolecular pairwise interactions are taken to be Morse (79, 80) or Leonard-Jones (81) potentials.

$$V_{ij}\ (\tilde{q}_i,\ \tilde{q}_j) = 4\ \varepsilon_{ij}\ \{(\sigma_{ij}/|\tilde{q}_i-\tilde{q}_j|)^{12} - (\sigma_{ij}/|\tilde{q}_i-\tilde{q}_j|)^{6}\} \qquad \text{(IV.5)}$$

where $\varepsilon_{ij}$ is the depth of attractive well, and $|\tilde{q}^{o}_i-\tilde{q}^{o}_j|$ is the position of the minimum in the attractive well while $\sigma_{ij} = 2^{1/6}\ |\tilde{q}^{o}_i-\tilde{q}^{o}_j|$.

To represent the bending mode for atoms i and k bonded to atom j, the following three body potential may be used

$$V^{a}_{ijk}\ (\theta_{ijk}) = 1/2\ \delta_{ijk}\ (\theta_{ijk}-\theta^{o}_{ijk})^2 \qquad \text{(IV.6)}$$

where $\delta_{ijk}$ is the bending force constant, $\theta_{ijk}$ the bond angle, and $\theta^{o}_{ijk}$ is the equilibrium bond angle. That this is a three-body interaction can be seen from the relation $\theta_{ijk} = \arccos\ [\tilde{q}_{ji} \cdot \tilde{q}_{jk}/|\tilde{q}_{ji}||\tilde{q}_{jk}|]$. It is assumed that all inter-molecular forces arise as a result of pair-wise interactions.

One can introduce four-body interactions to represent hindered out-of-plane motion by species such as $NO_3^-$ in a fashion similar to that used for the bending modes. However, the resulting equations are cumbersome.

The general classical model is now defined since H of (IV.3) and (II.27) is resolved once the system of study and choice of coordinate system is defined. Equation (II.28) now becomes

$$d_t\tilde{q}_i = \tilde{p}_i/M_i \qquad \text{(IV.8a)}$$

$$d_t\tilde{p}_i = - \partial_{\tilde{q}_i} V(\tilde{q}) \qquad \text{(IV.8b)}$$

The detailed equations are given in Appendix C. These are solved numerically using the Runge-Kutta-Gill algorithm. The model is a dynamic classical picture of molecular translations, vibrations and rotations described by model potentials. Principally it was developed to study energy transfer processes.

## IV.3 Study System - Collision of $O_2$ Molecules in Highly Excited Vibrational States

To keep computer time of the study within reason only collinear collisions were considered. This reduces the number of independent variables since the impact parameter and relative angular orientation of the two molecules is fixed. The choice of the laboratory frame in cartesian coordinates proved most convenient and is shown in Figure 2. A further specification of the relative and internal energies and phases of the vibrations defines the initial state with the last element being somewhat arbitrary. It will prove convenient to define the terms, where $E_\nu^i$(1 or 2) is the initial vibrational energy of (1 or 2), $E_\nu^f$(1 or 2) is the final vibrational energy of (1 or 2), $E_R^i$(1 or 2) is the initial relative kinetic energy and $\Delta E_\nu = E_\nu^f - E_\nu^i$.

The potential function $V(\tilde{q})$ consists of two intramolecular and four intermolecular Morse terms. The choice of Morse function to describe the intermolecular interaction is discussed in some detail by Pettitt (31), and revolves mainly around the dependence of energy transfer on potential energy surface shape. The choice of parameters and sources of the same are given below.

Bonded $O_2$ Morse Parameters

equilibrium bond distance ... 2.282 au (82)

range parameter ..... 1.404 au (83)

dissociation energy ..... 1.917 au (84)

Non-bonded 0-0 Interaction

position of minimum ..... 7.28 au (85)

range parameter ..... see following discussion

well depth ..... $0.356 \times 10^{-3}$ au (85)

The literature reports the use of a number of range parameters for the non-bonded interaction; some of these being $\beta = 1.02$ (86), 1.03 (87), 1.06 (88), 1.20 (85) and 1.24 (89).

Since the shape of the potential is quite signifigant in determining the collision dynamics, and this shape is effected by changes in $\beta$, it was decided that a quantitative investigation of the effect of the intermolecular range parameter might be illuminating. Figure 3 demonstrates the effect of variation in $\beta$ on $\Delta E$ for three initial phases and initial conditions $E_v^i(1) = E_v^i(2) = 0.99$ D, $E_R^i = 4 \cdot 10^{-3}$ au = 0.11 eV, R = 50 au. As can be discerned from Figure 3 the largest energy transfer occurs when the diatomic vibrations are out of phase. It is also this case which is most drastically effected by changes in $\beta$.

Definitive conclusions can hardly be drawn from such a limited investigation. However, the work is somewhat suggestive of some general features or difficulties in this field and this will be commented on briefly in the next section.

In closing, it is noted that the study presented here is a classical mechanical description of the evolution of a single event involving two diatomic molecules near the dissociation limit. This picture can be claimed to be correct since at this limit the vibrational level spacing of most diatomics is small when compared to thermal energies.

Figure 2

Cartesian and relative co-ordinates for

$O_2$-$O_2$ collinear collision study

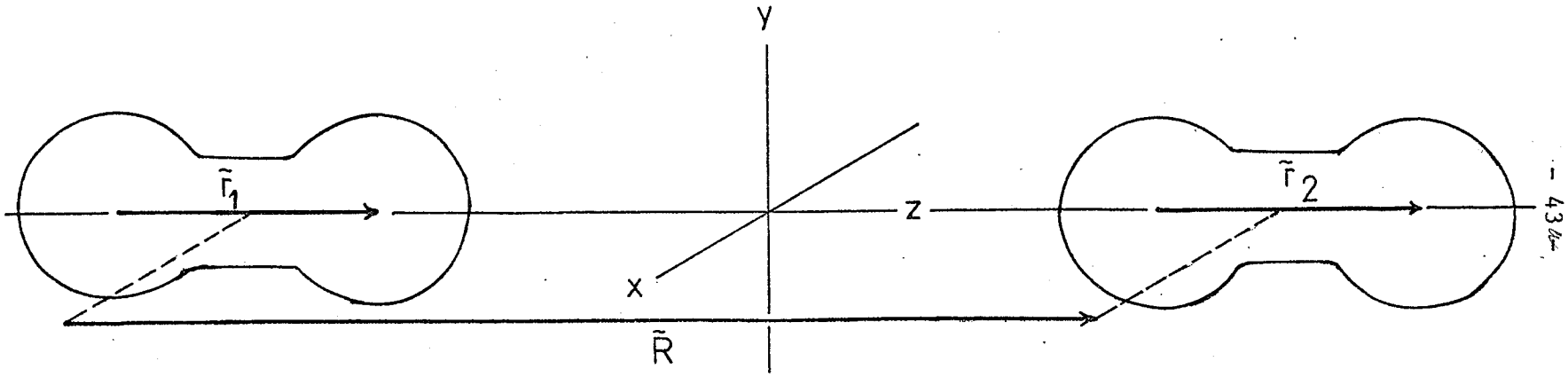
y
$\tilde{r}_1$
z
$\tilde{r}_2$
x
$\tilde{R}$
Molecule 1
Molecule 2

Figure 3

This graph shows the dependence of vibrational energy changes in $O_2$ - $O_2$ collisions upon the range parameter in the Morse terms of the intermolecular potential for three phases.

Curve I: The phases are determined by the initial condition $|\tilde{r}_1|=|\tilde{r}_2|$= minimum classical turning point for $E_v^i$(1 and 2) = 0.99D.

Curve II: In this case, both molecules begin at their maximum classical turning points.

Curves III and IV correspond to molecules 1 and 2 in a collision in which molecule 1 began at its maximum classical turning point and molecule 2 at its minimum.

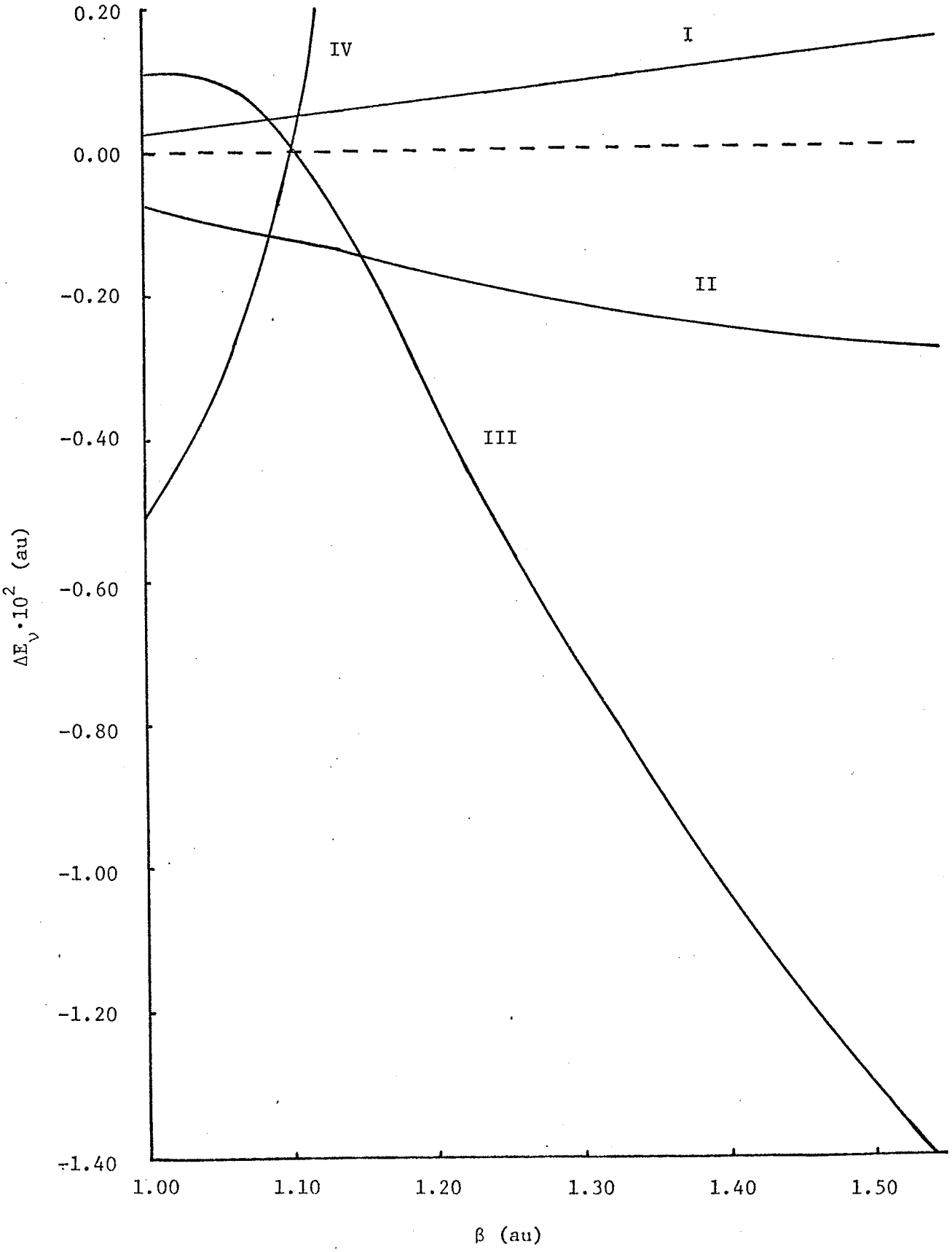
0.20
0.00
-0.20
-0.40
-0.60
-0.80
-1.00
-1.20
-1.40
$\Delta E_\nu \cdot 10^2$ (au)
1.00
1.10
1.20
1.30
1.40
1.50
β (au)
I
II
III
IV

## IV.4 Some Concluding Remarks

The significance of this particular study can be appreciated more fully by remembering that this was a preliminary investigation predating the development of the generalized impact parameter method.

The immediate intent of this study was to test whether the model could describe energy exchange processes. The results do indicate the model was capable of analyzing this system but the difficulties which were demonstrated to be associated with the use of empirical functions cast doubt on the usefulness of extending this study as the results at best would be of a qualitative nature and would not likely be more enlightening than the results of the present study. It is not suggested that this feature of empirical potentials was not known but few researches emphasize how citical this factor can become.

The study does indicate, however, that for reactions in which the quantum nature of nuclei is not expected to play a large role or can be approximated in some way such as phase averaging (see 90, 91, 87, 92, 93), the dynamics of the nuclei can be accurately represented by a set of differential equations which incorporates a potential field dependence on electronic behaviour and which can be solved accurately by numeric methods.

In summation, this investigation suggested that the development of a more fundamental approach in the treatment of electronic behaviour was necessary. Also, the results were suggestive that the use of numeric methods could provide a flexible, computationally useful model.

# Chapter V

## THE PROTON-HYDROGEN SYSTEM

## V.1 Preliminary Statement

The proton-hydrogen (p-H) system study was the first which employed the generalized impact parameter methods. There are a number of reasons for choosing this system for study. First, it is the simplest system of chemical interest consisting of only two nuclei and one electron and as a result the system is relatively easy to analyze. Besides this there is in existance an experimental ( 94 ) as well as a number of theoretical studies ( 95-101 ) which makes it possible to make a comparative estimate of the value of the present study.

The development of the specific equations for the p-H system from the general system equations is presented in the next section. This is followed in the next two sections by studies of low energy collision (<10eV), photodissociation of $H_2^+$, and high energy collisions (KeV). Finally, the signifigance of the results of this study is discussed.

## V.2 p-H System Equation of Motion

The application of the equations developed in chapter II requires the definition of the system and the co-ordinate system describing the relative position of the particles making up the system. The p-H system consists of three particles with the relative co-ordinates being given in figure 4 while figure 1 gives the co-ordinates in the laboratory frame. Then the Hamiltonian for this one electron system may be written

$$H = -\frac{\nabla^2}{2} - \sum_{n=1}^{2} 1/r_n + 1/R \qquad (V.1)$$

where the subscript n refers to the nucleus. This Hamiltonian has two physically meaningful resolutions of the type suggested by (II.2), these being

$$H = H_o^\alpha + V^\alpha \qquad (V.2a)$$

$$H = H_o^\beta + V^\beta \qquad (V.2b)$$

where

$$H_o^\alpha = -\frac{\nabla^2}{2} - 1/r_1$$

$$V^\alpha = -1/r_2 + 1/R$$

$$H_o^\beta = -\frac{\nabla^2}{2} - 1/r_2$$

$$V^\beta = -1/r_1 + 1/R$$

It will be taken that $\alpha$ is the non-rearrangement channel while $\beta$ is the rearrangement channel, that is in each channel a hydrogen atom sees the potential field of a proton in collision with itself but the role of two protons is interchanged. For either channel the set of eigenfunctions for the Hamiltonian in the asymptotic limit is the set of eigenfunctions for the hydrogen atom or

$$H_o^{(\alpha,\beta)} |\phi_j^{(\alpha,\beta)}(\tilde{r})\rangle = E_j^{(\alpha,\beta)} |\phi_j^{(\alpha,\beta)}(\tilde{r})\rangle \qquad (V.3)$$

Figure 4

Relative co-ordinate system for p-H system.

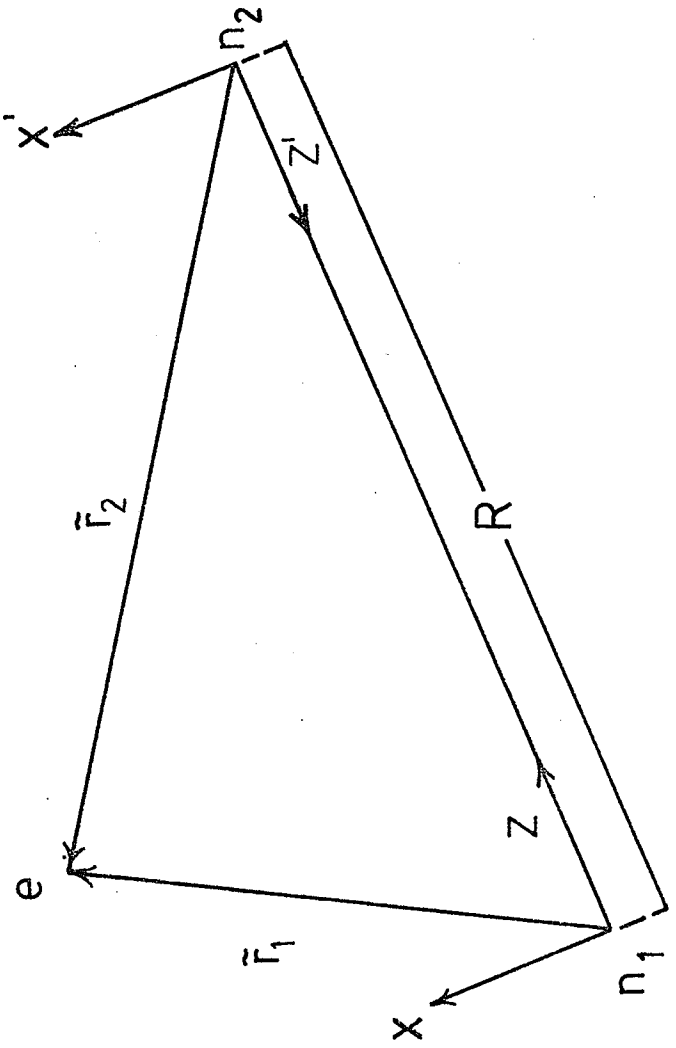
n2
x'
Z'
r̃2
R
Z
e
r̃1
n1
x

where $|\phi_j>$ is the j-th hydrogenic eigenfunction and $E_j$ the eigenenergy. Then using these functions (II.3) becomes

$$|\Psi(\tilde{r},t)> = \sum_{c}^{\alpha,\beta} \sum_{j}^{(c)} b_j^c(R,t)\,|\phi_j^c(\tilde{r})> \qquad (V.4)$$

It was necessary to truncate this set for (II.8) to be manageable and for the low energy collision only the (1s, 2s, 2pz) functions were used at each nuclear centre. It was not necessary to include the (2px,2py) functions since the symmetry of the system allows a two dimensional treatment. The analytic form of these functions is given in appendix D.

Having resolved the forms of H and $\{|\chi>\}$ of equations (II.2) and (II.3), respectively, in equations (V.1), (V.2), and (V.3), the matrices of equation (II.9) and, of course, the equations of motion for the electrons (II.8) are completely defined. Noting the complex form the $\underline{G}$ matrix would take from (II.9e) the approximation that

$$\underline{G} \approx \underline{b}^{+}\,(\partial_R \underline{N})\,\underline{b}\,/2 \qquad (V.5)$$

was used. This form was expected to give the correct behaviour and have the correct order of magnitude. Then equation (II.8b) becomes upon substituting (V.5) and (II.10)

$$d_t\underline{b} = \underline{N}^{-1}\left[-i\,\underline{NE} - i\,\underline{V} - \frac{d_t R}{2}\,\{\underline{b}^{+}\,\partial_R \underline{N}\,\underline{b}\}\right]\underline{b} \qquad (V.6)$$

where $\underline{E}$ is defined by (V.3) and the explicit form of the matrices in (V.6) are given in Appendix D.

To understand this equation more fully consider the form of the matrix $\underline{V}$. It may be written

$$\underline{V} = \begin{bmatrix} \underline{V}^{\alpha\alpha} & \underline{V}^{\alpha\beta} \\ \underline{V}^{\beta\alpha} & \underline{V}^{\beta\beta} \end{bmatrix} \qquad (V.7)$$

and the various submatrices can be interpreted as follows:

1) The diagonal blocks represent the perturbation within that coupling states of that channel or

$$\underline{V}_{ij}^{\alpha\alpha} = \langle\phi_i^{\alpha}|V^{\alpha}|\phi_j^{\alpha}\rangle$$

Transitions within a channel are determined by these diagonal blocks in $\underline{V}$ and $\partial_R\underline{N}$.

2) An off-diagonal block, say $V^{\alpha\beta}$, represents the perturbation $V^{\beta}$ of channel $\beta$ coupling the states of channel $\beta$ to the states of channel $\alpha$, or

$$V_{ij}^{\alpha\beta} = \langle\phi_i^{\alpha}|V^{\beta}|\phi_j^{\beta}\rangle$$

Therefore, transitions between the channels are determined by these off-diagonal blocks in $\underline{V}$ and $\partial_R\underline{N}$.

It is computationally useful to simplify equation (V.6) further. It is noted, that although the present basis set is a non-orthogonal set belonging to neither the adiabatic nor the diabatic representation, at the limit $R = \infty$ where $\underline{N} = \underline{I}$, $\partial_R\underline{N} = \underline{0}$, and $\underline{V} = \underline{0}$, (V.6) has the form $d_t\underline{b} = i\,\underline{E}\,\underline{b}$. This behaviour suggests the use of the transformation (II.22); the $E_i$ in Equation (II.22) being defined by (V.3). The resulting simplified equation is

$$d_t\underline{b}' = \underline{N}'^{-1}[-i\underline{V}' - \frac{d_tR}{2}\{\underline{b}'+(\partial_R\underline{N}')\underline{b}'\}]\underline{b}' \qquad (V.8)$$

$\underline{b}'$, $\underline{N}'$, $\underline{N}'^{-1}$, $\underline{V}'$ are easily obtained by use of (II.22) in equations (II.20) and (II.21). Upon substituting (II.10) into (II.14b) and applying equations (II.20) and (II.21), the mean energy is given by the expression

$$\bar{E}(R) = \underline{b}'+ [\underline{N}'\underline{E}' + \underline{V}']\underline{b}' \qquad (V.9)$$

It is noted that $\underline{E} = \underline{E}'$.

Next, one defines in the laboratory frame the cartesian coordinates $(x_1,y_1,z_1)$ and $(x_2,y_2,z_2)$ (where the subscript refers to the particle) which in turn defines the internuclear separation

$$R = \{(x_1-x_2)^2 + (y_1-y_2)^2 + (z_1-z_2)^2\}^{1/2} \tag{V.10}$$

Then substituting (V.9) into (II.27), one obtains from (II.28) the equations of motion for the nuclei which consist of three sets of the form

$$d_t x_i = p_{x_i}/M \tag{V.11a}$$

$$i = 1, 2$$

$$d_t p_{x_i} = -\partial_{x_i} \bar{E}(r) \tag{V.11b}$$

where the x co-ordinate is replaced in turn by the y and z co-ordinates. $p_{x_i}$ is the momentum of the i-th particle along the x cartesian co-ordinate while M is the mass of a proton. The solution of (V.11b) is straightward involving the use of (II.29) and the relation

$$\partial_R \bar{E}(R) = (\partial_R b^+)\ \underline{H}\ \underline{b} + b^+ (\partial_R H)\underline{b} + b^+\ \underline{H}\ (\partial_R \underline{b}) \tag{V.12}$$

The matrix $\partial_R \underline{H}$ can be evaluated analytically from $\underline{H}$ while the other two derivatives with respect to R can be found by use of (II.10b) and (V.5) which gives

$$\partial_R \underline{b} = -i\ \underline{N}^{-1}\ (\underline{b}^+ (\partial_R \underline{N})\underline{b})\ \underline{b}/2 \tag{V.13}$$

The primes have been dropped for convenience from the last three equations.

## V.3 Test Cases, Energy Surfaces, and Low Energy Collisions

The equations (V.8) and (V.11) are a set of coupled equations which fully describe the time evolution of the p-H system in time. Besides the accepted limitation of the classical nuclear treatment in the development of this theory, the only approximations are the adoption of a truncated basis set and approximate form for the $\underline{G}$ matrix. It is to be noted that neither of the representations discussed in Chapter II has been used to develop equation (V.6) or (V.8). This choice of basis set may therefore appear inappropriate but perhaps it can be considered to be the "intuitive" choice for this system. The adiabatic representation can be found by solving the eigenvalue problem

$$\underline{H} = \underline{N}\,\underline{E} + \underline{V} \qquad (V.14)$$

The resulting eigenfunctions are the molecular functions for the $H_2^+$ system. The potential energy surfaces for these functions are shown in figure 5.

It was found that the symmetry properties of the molecular functions provided a convenient internal check on the consistency of equation (V.8) and (V.11) and the computer program. The anti-symmetric and symmetric states (with respect to co-ordinate space) will not couple at any point in a collision. Therefore a collision with initial conditions such that the system is in the $1\sigma_u^*$ or $1\sigma_g$ electronic molecular state, with an impact parameter $\rho = 0$, and relative incident energy significantly less than the energy separation to the next state of the same symmetry (choice was 4eV = .148 au) will be expected to have a dynamic potential energy surface of the appropriate state. Such test collisions were run and the expected behaviour observed.

The relationship between the symmetry classification of a molec-

Figure 5

The molecular potential energy surfaces for $H_2^+$.

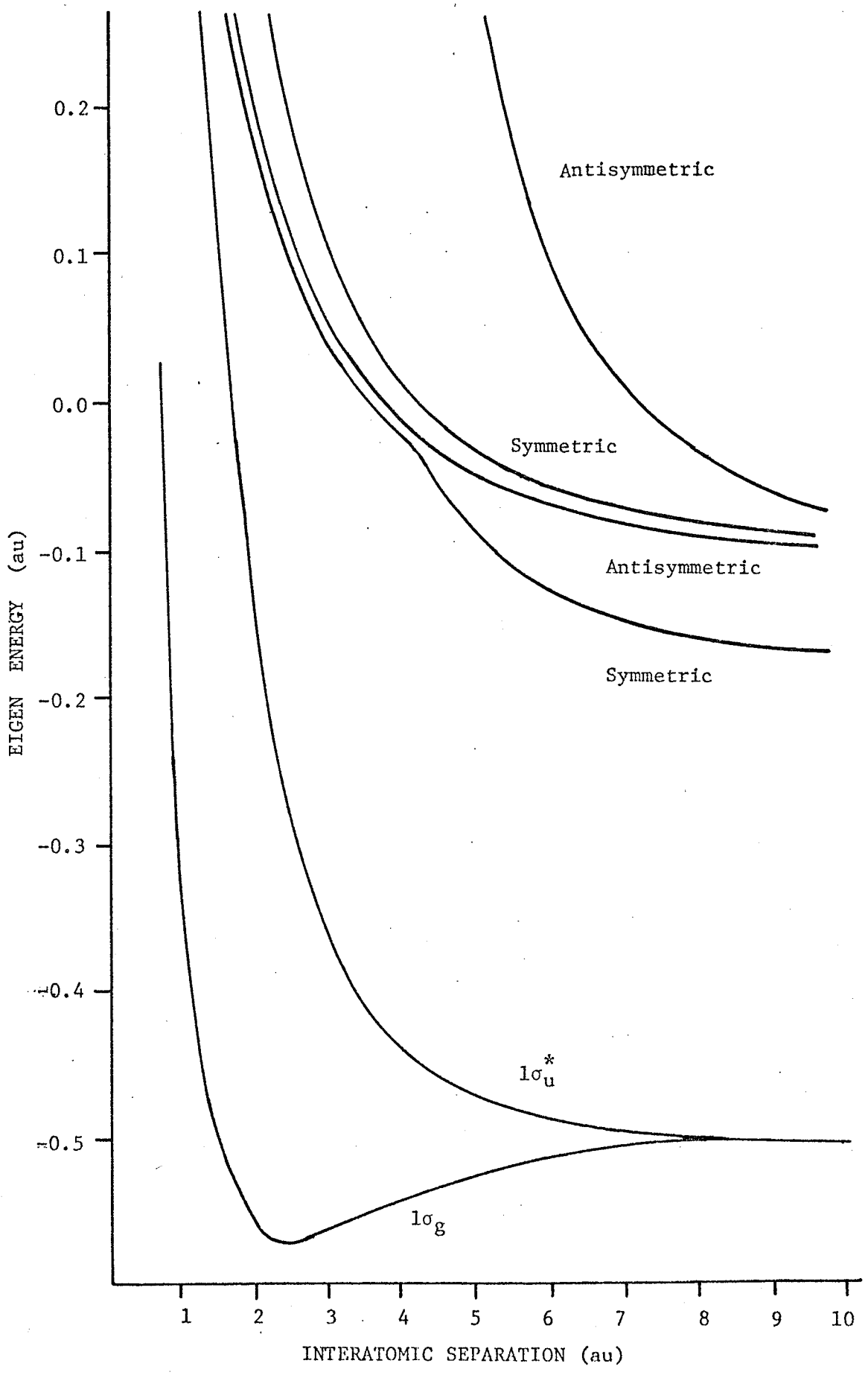
0.2
0.1
0.0
-0.1
-0.2
-0.3
-0.4
-0.5
EIGEN ENERGY (au)
Antisymmetric
Symmetric
Antisymmetric
Symmetric
$1\sigma_u^*$
$1\sigma_g$
1
2
3
4
5
6
7
8
9
10
INTERATOMIC SEPARATION (au)

ular function and its couplings can be demonstrated analytically (102), and it is informative to present this analysis at this point. For simplicity, only the (1s) functions, one on each center, will be considered since the inclusion of more states would make little difference to the following discussion. Then transforming from the atomic orbital basis set to the adiabatic basis set by the use of the relations (II.20) and (II.21), and not using (V.5) equation (II.8) becomes

$$d_t \underline{b} = (-i\underline{H}_o - i\underline{V} - d_t\underline{R}\underline{G})\underline{b} \qquad (V.15)$$

where $\underline{H}_o$ and $\underline{V}$ are diagonal or zero matrices and the molecular functions associated with the coefficient matrix $\underline{b}$ are

$$|\chi_1\rangle = \frac{2^{-1/2}}{(1 + \langle\phi_1|\phi_2\rangle)1/2} \quad (|\phi_1\rangle + |\phi_2\rangle) \quad (1\sigma_g) \qquad (V.16a)$$

$$|\chi_2\rangle = \frac{2^{-1/2}}{(1 - \langle\phi_1|\phi_2\rangle)1/2} \quad (|\phi_1\rangle - |\phi_2\rangle) \quad (1\sigma_u^*) \qquad (V.16b)$$

Then the only coupling between these two states is contained in $\underline{G}$ but

$$\underline{G}(1,2) = \langle\chi_1|\partial_R|\chi_2\rangle$$

$$= \frac{2\{(\langle\phi_1| + \langle\phi_2|)\partial_R(|\phi_1\rangle - |\phi_2\rangle)\}}{(1 + \langle\phi_1|\phi_2\rangle)1/2\ (1 - \langle\phi_1|\phi_2\rangle)^{1/2}}$$

$$= 0$$

since the center of mass is identical with the midpoint of the two centers. Then the states of different symmetry are completely uncoupled in the exact treatment. However, there is more than one state of each symmetry type being used in (V.8). Therefore, the dynamic surface will be a mixture of static or adiabatic states of the same symmetry with an implicit dependence on the relative velocity of the two nuclei.

For the low energy collisions, it was taken that the proton labelled one was the target hydrogen atom, and therefore the initial electronic state is

$$|\psi(R)\rangle = |\phi_1\rangle = \{1\sigma_g\ (R=\infty) + 1\sigma_u^*\ (R=\infty)\} \qquad (V.17)$$

It becomes clear on considering equation (V.17) that the initial conditions are critical. In particular, it is necessary in numeric calculations to choose R finite, yet large enough as not to cause the system to follow an erroneous potential surface. This difficulty was overcome by repeating the calculation for a given energy with increasing R until the dynamic potential energy surface became independent of this parameter. For these collisions, an initial separation of 150 to 200 au was found to be suitable. A further check of the results was obtained by testing the system's invariance to time reversal. The accuracy with which this could be done was quite remarkable in that the electronic behaviour became quite complex in the interaction region.

The initial study was of low energy, zero impact parameter collisions. Figure 6 is a plot of the dynamic potential energy surfaces for various initial collision energies. From the previous discussion on symmetry conservation, one can deduce from the form of the initial state given by (V.17) that these dynamic surfaces should not lie below the 50-50 mixture of the surfaces for the two states $1\sigma_g$ and $1\sigma_u^*$. The departure of the surfaces from this expectation is in effect a reflection on the accuracy of the approximation (V.5). It is to be noted that this approximation appears to be more accurate for the higher energy collisions. To compensate for the approximation (V.5), the normalization condition (II.12) was forced at

Figure 6

The dynamic potential energy Surfaces for the p-H collision. The collision energies are given on the right and $1\sigma_g$ and $1\sigma_u^*$ static potential surfaces are included for reference.

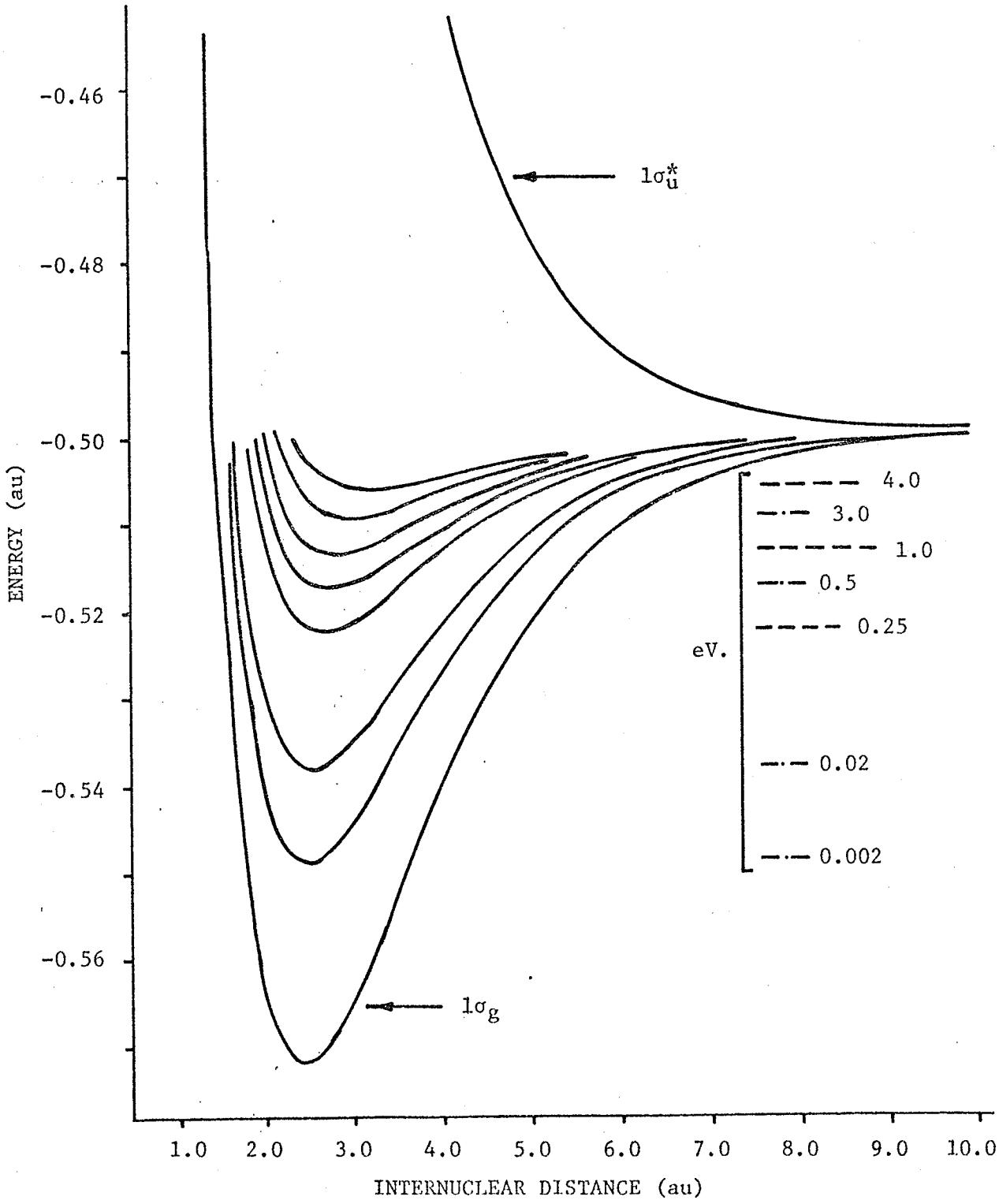
-0.46
-0.48
-0.50
-0.52
-0.54
-0.56
ENERGY (au)
$1\sigma_u^*$
$1\sigma_g$
4.0
3.0
1.0
0.5
0.25
eV.
0.02
0.002
1.0
2.0
3.0
4.0
5.0
6.0
7.0
8.0
9.0
10.0
INTERNUCLEAR DISTANCE (au)

each step in the calculation. In spite of this inaccuracy in the surfaces some interesting qualitative features were demonstrated by these calculations.

A usual theoretical approach for low energy collisions is to assume the adiabatic approximation (103) in which it is taken that the two colliding systems interact so slowly that the static molecular eigenfunctions for the whole system adequately describe the electronic wave function; that is, the potential energy surface for the interacting system is taken to be one of the static molecular potential energy surfaces of the whole system. This approximation has not been incorporated into the GIP method and as demonstrated by the trial runs of Figure 6 it is possible that the dynamic surface can be a combination of static surfaces. This method,in fact, allows one to include a number of electronic states in the analysis of a system. This difference between the static and dynamic approaches is reflected in the behaviour of the electronic density during the collision. Whereas a method employing the adiabatic approximation implicitly assumes the electronic density changes slowly, the GIP method is capable of handling collisions in which the electronic density is constant during the collision (symmetry property check,initial electronic state $1\sigma_u^*$ or $1\sigma_g$) or cases such as that shown in Figure 7 for the p-H low energy collision where the electron density fluctuates rapidly (resonant charge exchange) into and out of the rearrangement channel. It perhaps bears mention that the description of the process, particularly in the interaction region, is a characteristic of the basis set chosen, and only the initial and final conditions are measurable. However, it is sometimes useful to be able to describe the interaction in terms of a "mechanism". This often allows one to resolve which factors control the reaction.

A number of collisions with non-zero impact parameters were run. The especially interesting feature of these collisions were the trajectories followed by the nuclei. Figure 8 shows the trajectory of a collision with an impact parameter of 1 au and incident energy of 5 eV. The co-ordinates are given in the laboratory frame. In particular, the strong deviation from a linear path and the changing form of interaction - initial and final interaction are attractive while intermediate interaction is repulsive - are to be noted.

These studies, though limited, suggest the flexibility of the GIP method. The consistency of the equations has been tested and the limitations of one of the approximations employed has been intimated. In as much as there is no available experimental information on the p-H system at the collision energies discussed in this section, there was no effort made to generate cross sections and other measurable quantities.

Figure 7

Behaviour of the electron density during the collision for $\rho = 0$.

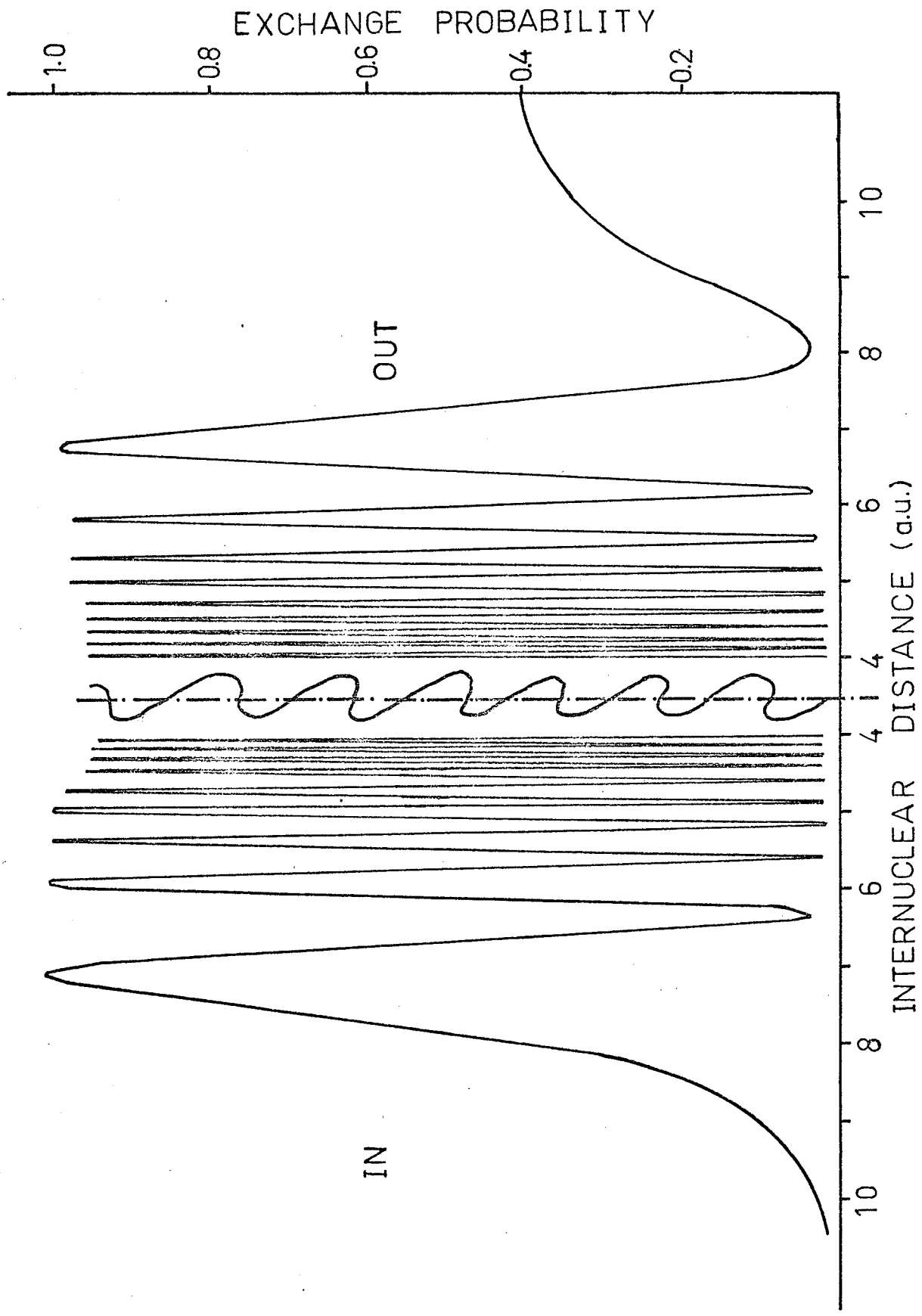
EXCHANGE PROBABILITY
1.0
0.8
0.6
0.4
0.2
OUT
IN
4
6
8
10
4
6
8
10
INTERNUCLEAR DISTANCE (a.u.)

Figure 8

A typical trajectory produced by the generalized impact parameter model in low energy scattering. The co-ordinates refer to the laboratory frame.

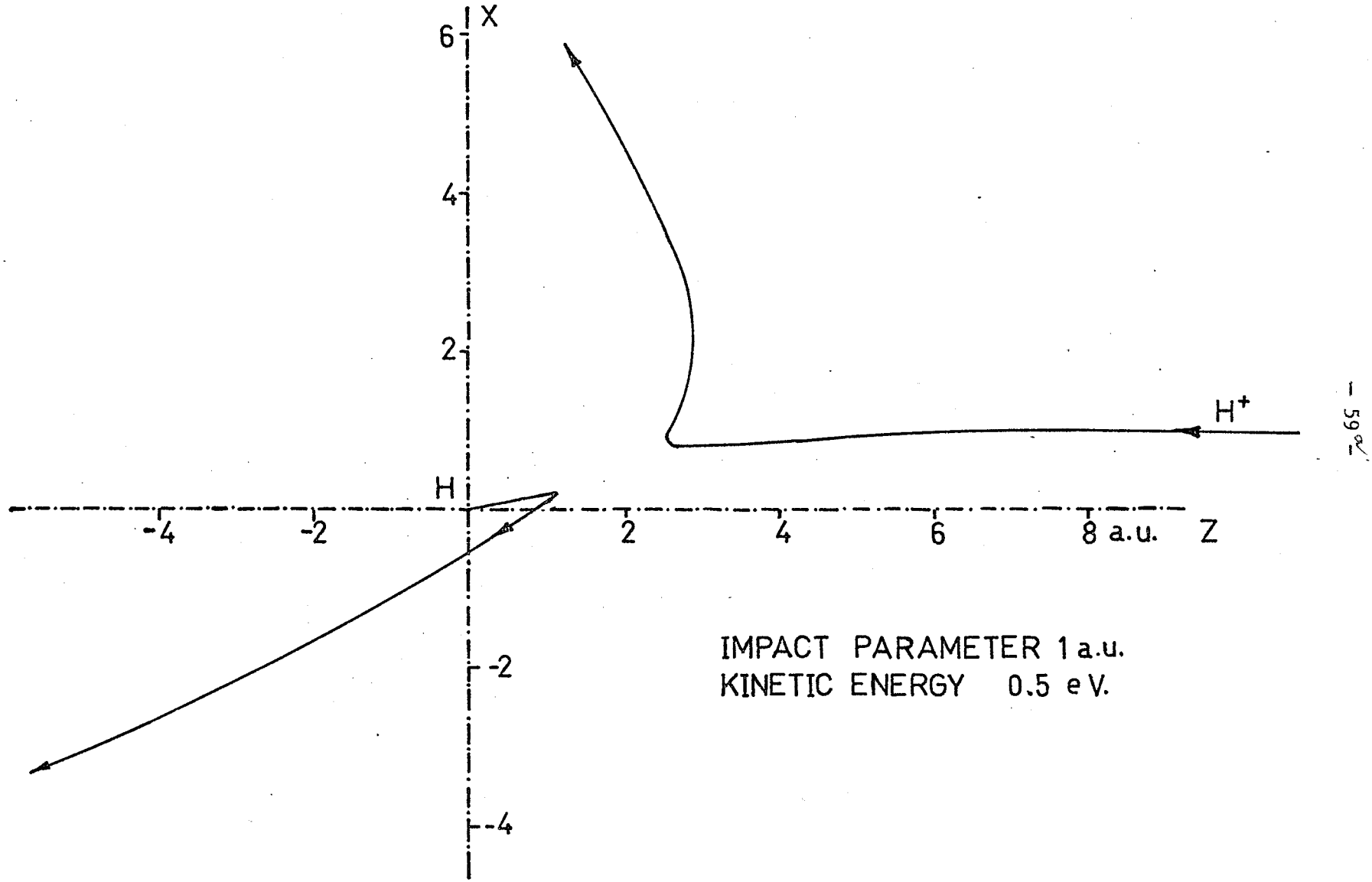
X
6
4
2
H
H+
-4
-2
2
4
6
8 a.u.
Z
-2
-4
IMPACT PARAMETER 1 a.u.
KINETIC ENERGY 0.5 e V.

## V.4 Photodissociation of $H_2^+$ and p-H High Energy Collision

The system of equations developed for the low energy p-H collisions is used to analyze two other processes. Though the major portion of this work was done by B. Corrigall, the results are of interest to the present thesis and will be briefly presented. For more details the reader is referred to the thesis of B. Corrigall (104) or the paper(s) by Corrigall and Wallace (105, 106).

The first process to be discussed is the photodecomposition of $H_2^+$. This can be simulated in the generalized impact parameter method by setting the nuclei at the equilibrium separation for the ground state $1\sigma_g$ and putting the system in the electronically excited state $1\sigma_u^*$ (Frank-Condon transition). By following the evolution of this system with time, one can estimate the life-time for the excited species which turned out to be of the order of $10^{-14}$ sec. This quantity was of some interest to one of the researchers, R. Wallace, since he had previously developed an expression for the probability of photodecompostion involving this lifetime (107), a quantity very difficult to calculate analytically or measure experimentally.

The other study of the p-H system undertaken was high energy scattering. This particular system was chosen so that the GIP method could be compared with both experiment and other models.

Some extension of equations is required to analyze this system since the translation mode of the electrons becomes significant in high velocity encounters. In fact, it is pointed out by Bates and McCarroll (131) that the usual electronic eigenfunctions for the hydrogen atom do not satisfy

the time-dependent Schrödinger equation even asymptotically for this situation. Without going into a detailed derivation of the new equations for which one may refer to (104) and (106), the proper time dependent form of the electronic wavefunction is

$$|\chi_j^c(\tilde{r},t)\rangle = |\phi_j^c\rangle \exp\{-i(E_j^c + \frac{v_{xj}^2}{8} + \frac{v_{yj}^2}{8} + \frac{v_{zj}^2}{8})t\}$$

$$\times \exp(\mp iv_{xj}x/2)\exp(\mp iv_{yj}y/2)\exp(\mp iv_{zj}z/2) \qquad (V.18)$$

where $\{|\phi_j^c\rangle\}$ is the set of stationary eigenfunctions of the hydrogen atom and $v_{xj}$, $v_{yj}$, $v_{zj}$ are the translational velocities of the electron in the x, y, z directions. Then (V.18) takes the form

$$d_t\underline{b} = \underline{N}^{-1}\{-i\,\underline{V} - \underline{N}\,\underline{v} - \frac{d_tR\{\underline{b}^+(\partial_R\underline{N})\underline{b}\})\underline{b} \qquad (V.19)$$

The only change other than the matrix elements is the introduction of the matrix $\underline{v}$ which is diagonal with its non-zero elements being $v_j^2/8$, where $v_j$ is the translational velocity of the electron in state j.

There are some practical considerations that bear mention. At high energies the two nuclei approach quite closely in the case of zero impact parameter collisions. This forces the use of a small step size in the numeric integration and gives rise to extremely long computation times. It was decided, therefore, to restrict the study to two representative cases.

First, a series of calculations were performed for a variety of impact parameters at 20 KeV. It was found that, although the total exchange probability did not become independent of impact parameter, the variation with change in impact parameter became quite small at small impact parameters. This observation is important since it was also found that only extremely small impact parameters would lead to scattering

angles of the order of degrees( Helbig and Everhart's experimental measurements were at scattering angles of the order of a degree(108)) and computation time increased drastically as $\rho \to 0$. Since the total exchange probabilites at these small impact parameters would not be significantly different from those at larger impact parameters in the region in which the above condition applied, a series of calculations were performed for collision energies of 2, 4, 8, 14, and 20 KeV in which the impact parameter was reduced until the total exchange probability changed insignificantly with variation of the impact parameter. The results of this series of calculations is presented in figure 9 along with the experimental results of Helbig and Everhart(108) and the original calculations of Wilets and Gallaher(95). Although the number of points calculated by the GIP method is limited, the agreement with experiment is excellent, particularly in matching the oscillatory dependence on the impact parameter of the exchange probability.

Finally, the cross section for a given excitation or exchange process from level i to level f was calculated from the equation

$$\sigma_{i\to f} = 2\pi \int_0^\infty d\rho \; \rho \; P_{i\to f}(\rho, E_p) \qquad (V.20)$$

where $P_{i\to f}$ is the probability of excitation or exchange from level i to level f and is defined

$$P_{i\to f} = \left| b_f^c \; (R=\infty) \right|^2 \qquad (V.21)$$

It is a function of impact parameter $\rho$ and incident proton energy $E_p$. $b_f^c(R=\infty)$ is the asymptotic coefficient of level f in channel c after the collision. A number of cross sections were calculated from the 20 KeV series of calculations and are tabulated in in Table 1 along with ex-

perimental measurements and results of other calculations. In this case the superiority of one calculation over all others is not apparent but the GIP results are as accurate as any of the other calculations presented.

As can be discerned from Table 1, a fair number of calculations have been attempted on this system (95-101) with a variety of results. The work of Gallaher and Wilets(96) using Sturmian functions produced significantly better results than previous calculations using hydrogenic functions but recently Rapp et al (99,100) have reexamined the use of the hydrogenic basis set and, though plagued by convergence difficulties for certain conditions, they felt their calculations compared favorably with experiment. However, the quoted data of Rapp and Dinwiddie (100) does not correspond with that of Table 1 nor do they elucidate on the source of their data. It is assumed by the author that the corrections suggested by Kaupilla et al(109) have been incorporated. Since the study reported here predates that of Rapp et al (99,100), comparisons were originally made only to the work of Gallaher et al (95,96,98). At that time it was felt that the calculations using the hydrogenic basis set and GIP method compared favorably with these calculations. The poor results of (95) using hydrogenic functions were not understood since the GIP calculation indicated that the linear trajectory, constant velocity approximation was appropriate, and it was concluded, assuming the calculations were accurate, that various terms were improperly coupled. Recently, Rapp (100) reported that there were numeric errors in the work reported by Wilets and Gallaher (95) which explains this particular inconsistency.

In conclusion, the verification and improvement of experimental data would make it possible to decide which approach is most accurate. The

repetition of the calculations carried out with the generalized impact parameter method using a more accurate $\underline{G}$ matrix is suggested, but there is little point until better experimental information is available.

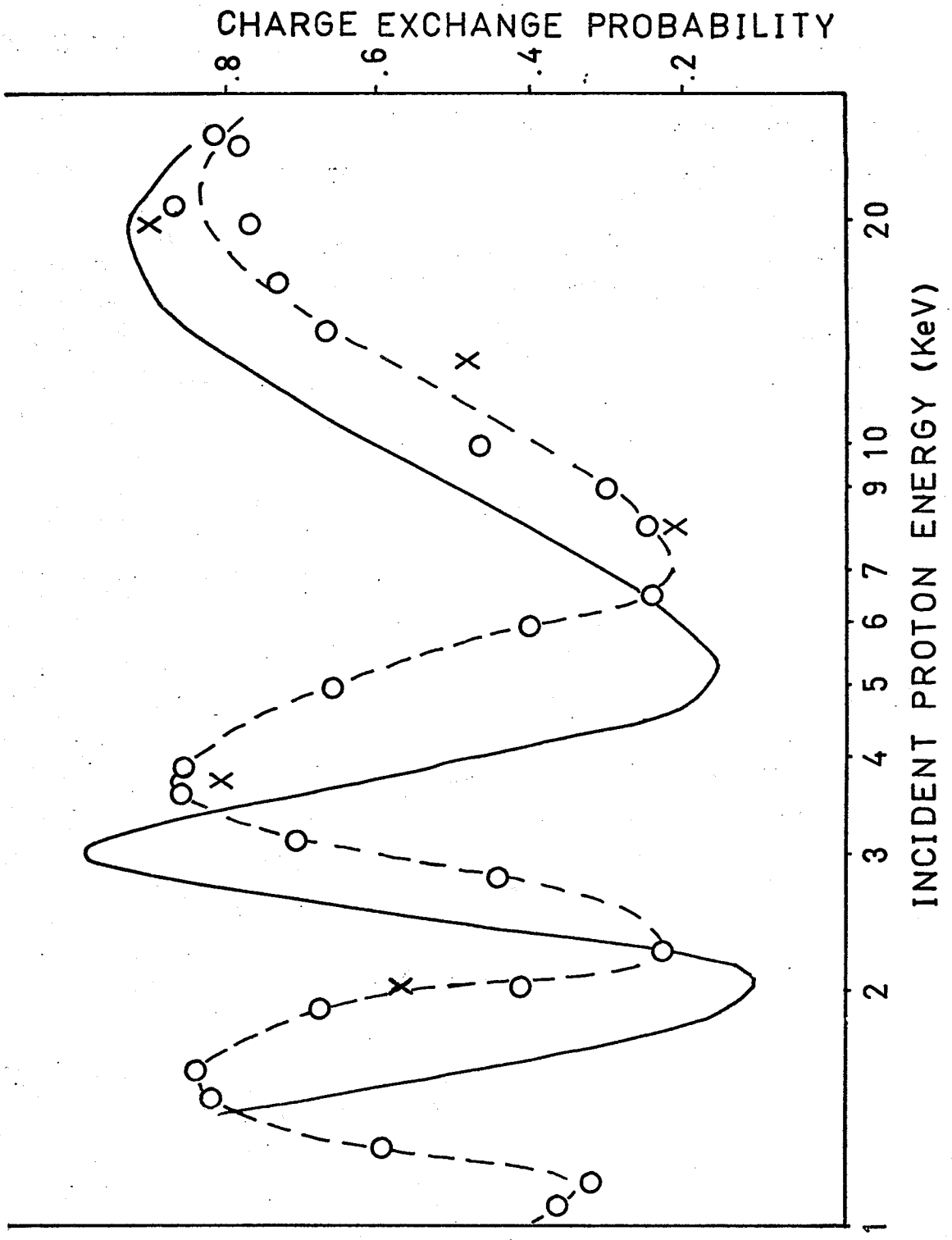
CHARGE EXCHANGE PROBABILITY
.8
.6
.4
.2
INCIDENT PROTON ENERGY (KeV)
1
2
3
4
5
6
7
9
10
20

Figure 9

Electron exchange probability as a function of incident proton energy.

-- o -- curve through experimental points of Helbig and Everhart (108).

..... ...

_____ the calculation of Wilets and Gallaher (95).

X the generalized impact parameter calculation.

Table 1

Excitation (D) and Charge Exchange (E) Cross Sections in Units of $10^{-17}$ cm $^2$.

| Process | Linear-Trajectory Approximation with | | | Generalized Impact Parameter Model | Experiment | L-T Approx. |
|---|---|---|---|---|---|---|
| | Hydrogenic Basis (95) | Pseudo-state Basis (98) | Sturmian Basis (96) | | | Rapp (100) |
| 2s(D) | 1.076 | 0.943 | 1.3 | 3.400 | - | 1.12 |
| $2p_z$(D) | 1.816 | 3.425 | 4.6 | 3.577 | 4.5 | 1.18 |
| 1s(E) | 38.730 | 41.400 | 40.0 | 47.950 | - | 40.4 |
| 2s(E) | 3.327 | 3.760 | 3.6 | 4.002 | 4.2 | 3.4 |
| $2p_z$(E) | 1.085 | 1.633 | 3.2 | 2.531 | 3.1 | .66 |



The values for the hydrogenic and the pseudo-state bases are from a tabulation in reference 98; the experimental values are from the work of Stebbings et al (94), except for the value for 2s(E) which is from Figure 4 in reference 95.

## V.5 Significance of the p-H Study

In as much as this was the first use of the GIP method, two major areas of concern were examined in this study of the p-H system; the consistency and flexibility of the GIP method, and its ability to produce a realistic description of a physical situation.

To demonstrate the consistency of the GIP equations, tests were run on symmetry conservation and invarience to time reversal. Both properties were exhibited by the solutions found by the GIP method. The flexibility of the method was established in that it was shown that the GIP method could simultaneously evaluate the importance of a number of electronic states in a collisional process, handle non-linear trajectories, non-exchange, and exchange processes.

In addition, the crude approximation taken for the matrix $\underline{G}$ was tested thoroughly and found to be not quite adequate, particularly for very low energy collisions. This observation lead to a more careful treatment of this matrix in the following studies.

The calculation of the photodecomposition lifetime is indicative not only of the flexibility and range of processes that may be analyzed using the GIP method but also of its ability to produce at least a qualitative estimate of an elusive physical quantity.

The study of the high energy scattering of the p-H system, though quite selective and restricted in range of energies and impact parameters studied, did show that the GIP method could produce numbers just as meaningful as those produced by other methods, and relatively good agreement with known experimental results was demonstrated.

These positive indications of the method's accuracy and flexibility lead to its utilization in the study of molecular processes. These studies are reported in the next two chapters.

Chapter VI

# CIS-TRANS ISOMERIZATION IN SIMPLE ETHYLENES

## VI.1 Introductory Remarks for the Ethylene Study

The theory of cis-trans (CS) isomerization of ethylene compounds has received considerable attention in recent years ( 110-112 ). Experimentally CS isomerization is induced by direct photo-excitation of ethylene or indirectly by the use of various "triplet sensitizers". The process can be considered to be an intramolecular rearrangement in which a molecule in an excited electronic state transfers energy to other modes in the molecule in order to return to a stable ground electronic state. These types of processes are termed non-radiative transitions and are broken into two classes (113). Transitions between states of the same spin multiplicity are called internal conversions while those between states of different multiplicity are termed intersystem crossing. Both mechanisms will be considered in this study.

If we accept the commonly held model for cis-trans isomerism (110, 111, 112) which, to a large extent, is a semi-intuitive rationalization of experimental information related to cis-trans ratios, etc., there remain many questions which are incompletely or unsatisfactorily answered. For example,

i) In the case of the simple ethylenes, does photo-induced isomerization proceed via $S^1 \rightarrow S^0$ or by $S^1 \rightarrow T^1 \rightarrow S^0$? It would appear to be tacitly assumed on "minimization of energy" criteria alone that the molecule will get into $T^1$ from which it will have little difficulty in crossing to $S^0$.

ii) The current model includes only rotational distortion of the methylene groups, even though it is realized that relaxation from the Franck-Condon excited state $S^1$ (C-C distance that of the equilibrium configura-

tion of $S^0$) will involve extension of the C-C bond to single bond length with resultant C-C vibration. One might ask to what extent such vibration will be important in the isomerization.

iii) It would appear to be assumed that in the sensitized reactions the action of the sensitizer is to produce the $T^1$ state of ethylene which then decays via a unimolecular mechanism. However, there is experimental evidence which indicates that it is highly unlikely that the relaxation process is this simple. Therefore, a model study of ethylene like systems was undertaken in an attempt to resolve some of these questions.

There were two major reasons for modelling rather than dealing with this problem in an exact manner. First, the system is of such a size that the order of the electronic energy levels has not been resolved by a series of ab initio calculations. Secondly, there are so many degrees of freedom in the original problem that to deal with them all simultaneously would probably obscure which modes were of importance to the relaxation processes.

The specifics of the model are given in the next section. However, some comments on the limits of this model might be appropriate. The treatment of the electronic state is extremely simplified, in fact almost naive. This results in an inability of the model to examine the $S^1 \rightarrow T^1$ process since the distribution of the two states is indistinguishable in this simplified approach. Also the use of such simplified excited states may result in certain modes of possible de-excitation being neglected by being absent from the model.

However, on the other hand it was possible to make a rudimentary evaluation of the lifetime for the decay processes $S^1 \rightarrow S^0$ and $T^1 \rightarrow S^0$. Also, the role of the vibrational and rotational modes of the methylene groups was examined.

## VI.2 Development of Ethylene System Equations

Noting that the ethylene system consists of twelve electrons and six nuclei, it does not take much thought to realize some simplifications will have to be introduced to have a computationally manageable system of equations. This point is emphatically demonstrated by the molecular orbital calculations performed on this system. One of the original calculations was done by Mulliken and Roothaan (114) in which semi-empirical methods were used to calculate the various energy levels for varying configurations of the molecule in a determination of the energy barrier for thermal cis-trans isomerization. More recently, Robin et al (115) and Buenker et al (116, 117) have performed calculations on this system. Robin (et al) has reviewed the various assignments of the "mystery band" and presented his own assignment. Buenker's calculations give another explanation. Other calculations are available (118, 119). Most interestingly, Levy and Ridard (119) conclude that energy criteria alone are not going to resolve the dilemma presented by the myriad of conflicting calculations.

Having no desire to become involved in such a controversy, and realizing that practical considerations would not allow the use of such complex functions as those employed by Robin or Buenker, it was decided that a simplified model of the ethylene system would be employed.

The model chosen has the following features:

1) the nuclear behaviour is treated as a two center problem, with each center having the mass and inertia of a methylene ($CH_2$) group. The two types of motion which will be considered relevent to cis-trans isomerization are:

a) Rotation of one methylene group relative to the other, characterized by angle $\alpha$ and velocity $\omega$.

b) Vibration of one methylene with respect to the other, characterized by the carbon-carbon bond length R, and velocity $\nu$.

The co-ordinate system is shown in figure 10.

2) Only the pi ($\pi$) electrons are treated explicitly. The sigma bond (C-C) is represented by an empirical function.

3) A one-electron (semi-empirical) treatment is employed in the $\pi$ electronic description.

This simplified description of the ethylene molecule was motivated by the assumption that photo-excitations primarily involve the pi electron system and the success that has been achieved by theories which consider only the pi electrons (51). This choice of model is reflected by the Hamiltonian having the form;

$$H = H^{o} + V^{so} + E_{\sigma} \qquad \text{(VI.1)}$$

where $H^{o}$ is the usual Born-Oppenheimer electronic Hamiltonian including electrostatic nuclear interactions and $V^{so}$ is the spin-orbit interaction for the $\pi$ electrons while $E_{\sigma}$ describes the behaviour of the other electrons.

The appropriate basis set of single electron functions which are consistent with the level of treatment being considered are the eigenfunctions of the one electron operator $H_i^{o}$ where

$$H^{o} = \sum_{i} H_i^{o} \qquad \text{(VI.2)}$$

These functions have the form

$$|\pi> \; = \; N \{ |p_{x_a}> + |p_{x_b}'> \} \qquad \text{(VI.3a)}$$

$$|\pi^*\rangle = N^* \{|p_{x_a}\rangle - |p'_{x_b}\rangle\} \quad \text{(VI.3b)}$$

The form of $H_i^o$, N, $N^*$ and the Slater functions $\{|p_{x_i}\rangle\}$ are given in Appendix E. The basis set of multi-electron functions that will be employed are the Slater determinants.

$$|S^o\rangle = |\pi\ \tilde{\pi}| \quad \text{(VI.4a)}$$

$$|S^1\rangle = 2^{-1/2} \{|\pi\ \tilde{\pi}^*| - |\tilde{\pi}\ \pi^*|\} \quad \text{(VI.4b)}$$

$$|T_1^1\rangle = |\pi\ \pi^*| \quad \text{(VI.4c)}$$

$$|T_2^1\rangle = 2^{-1/2} \{|\pi\ \tilde{\pi}^*| + |\tilde{\pi}\ \pi^*|\} \quad \text{(VI.4d)}$$

$$|T_3^1\rangle = |\tilde{\pi}\ \tilde{\pi}^*| \quad \text{(VI.4e)}$$

where $\pi = |\pi\rangle|\alpha\rangle$

$\tilde{\pi} = |\pi\rangle|\beta\rangle$

$|\alpha\rangle$, and $|\beta\rangle$ being spin functions. Using (VI.1) and (VI.4) and noting that the set $\{\phi_j\}$ defined by (VI.4) is an orthonormal set, equation (II.8) becomes

$$d_t \underline{b} = -[i\ \underline{H}^o + i\ \underline{V}^{so} + \omega \underline{G}_\alpha + \nu \underline{G}_R]\underline{b} \quad \text{(VI.5)}$$

where

$$\underline{H}^o\ (i,j) = \langle\phi_i|H^o + \delta_{ij}\ E_\sigma|\phi_j\rangle \quad \text{(VI.6a)}$$

$$\underline{V}^{so}\ (i,j) = \langle\phi_i|V^{so}|\phi_j\rangle \quad \text{(VI.6b)}$$

$$\underline{G}_\alpha\ (i,j) = \langle\phi_i|(\partial_\alpha)_{r,R,t}|\phi_j\rangle \quad \text{(VI.6c)}$$

$$\underline{G}_R\ (i,j) = \langle\phi_i|(\partial_R)_{r,\alpha,t}|\phi_j\rangle \quad \text{(VI.6d)}$$

To reduce the computation time of the calculations the transformations defined by (II.20) and (II.21) were applied to (VI.5) using the transformation matrix

$$\underline{U}\ (i,j) = e^{i(E_\sigma + C)t}\ \delta_{ij} \quad \text{(VI.7)}$$

where C =-3.46. The resulting equation is identical to (VI.5) except that

Figure 10

The co-ordinate system used to describe electronic and nuclear motion of ethylene with $x_b' = x_b \cos \alpha + y_b \sin \alpha$, and $x_a = x_b$.

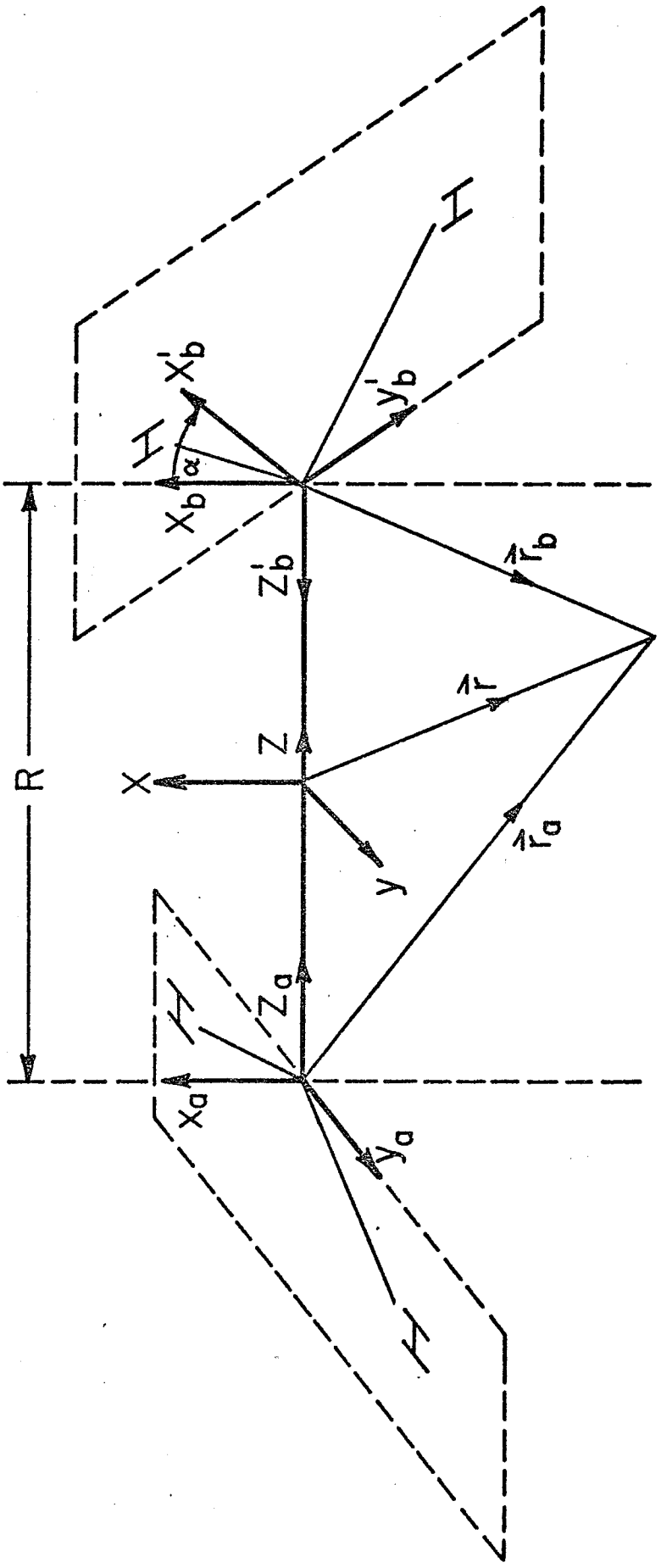
I
$X'_b$
$Y'_b$
I
α
$X_b$
$Z'_b$
$1r_b$
1r
Z
X
R
Y
$1r_a$
$Z_a$
I
$X_a$
$Y_a$
I

$\underline{H}^o$ is replaced by

$$\underline{H}^{o\,\prime} = \underline{H}^o - (E_\sigma + C)\,\underline{I} \qquad \text{(VI.8)}$$

where $\underline{I}$ is the identity matrix.

For the explicit form of the matrices of (VI.5) refer to Appendix E. The mean internal molecular energy, excluding nuclear kinetic energy, is found by substituting (VI.8) into (II.14b) and is given by the equation:

$$\bar{E}(\alpha,R) = C + E_\sigma\,(\alpha,R) + \bar{E}_\pi\,(\alpha,R) \qquad \text{(VI.9)}$$

where

$$\bar{E}_\pi\,(\alpha,R) = \underline{b}^+\,(H^{o\,\prime} + \underline{V}^{so})\,\underline{b}$$

The empirical function $E_\sigma$ was chosen by fitting $\bar{E}$ to the results obtained from CNDO/2 calculations (58) choosing $\partial_\alpha E_\sigma = 0$. Then

$$E_\sigma\,(\alpha,R) \equiv E_\sigma\,(R) = -12.575 + 0.446\,(R-2.92)^2 \qquad \text{(VI.10)}$$

The resultant potential energy surfaces for the first two states are shown in Figure 11. It is to be noted that the simple molecular orbital theory used in this study does not give the correct $T^1$, $S^1$ energy separation. This inaccuracy was corrected empirically and will be discussed in a later section.

The motion of the nuclei can be analyzed conveniently in the center of mass and center of inertia frames in which only the relative motion of the two particles are considered (121,122). The nuclear co-ordinates $(\alpha,R)$ of Figure 10 are convenient and using (II.28)

$$d_t R = \nu \qquad \text{(VI.11a)}$$

$$d_t \alpha = \omega \qquad \text{(VI.11b)}$$

$$d_t \nu = -\frac{1}{\mu_{CH_2}}\,[\partial_R E_\sigma + \partial_R \bar{E}_\pi] \qquad \text{(VI.11c)}$$

$$d_t \omega = -\frac{1}{I_{CH_2}}\,[\partial_\alpha E_\sigma + \partial_\alpha \bar{E}_\pi] \qquad \text{(VI.11d)}$$

Using (VI.10) and (II.11)

$$d_t \nu = - \frac{1}{\mu_{CH_2}} \{0.892\ (R-2.92) + \underline{b}^+ \{\partial_R \underline{H} + [G_R, \underline{H}]\}\underline{b} \qquad \text{(VI.12a)}$$

$$d_t \omega = - \frac{1}{I'_{CH_2}} \{\underline{b}^+ \{\partial_\alpha \underline{H} + [\underline{G}_x, \underline{H}]\}\underline{b} \qquad \text{(VI.12b)}$$

where $\underline{H} = \underline{H}^o + \underline{V}^{so}$, [A,B] is the commutator of A and B, and $\mu_{CH_2}$ and $I'_{CH_2}$ are the methylene reduced mass and reduced inertia respectively. It was found that the variation of $\underline{V}^{so}$ was so slow that the approximations $\partial_R \underline{V}^{so} = \partial_\alpha \underline{V}^{so} = \underline{0}$ were reasonable.

This completes the derivation of the equations describing the model ethylene system for equations (VI.5), (VI.11a + b) and (VI.12) are a complete set of differential equations which can be solved by the method described in Chapter III.

Figure 11

Born Oppenheimer potential energy surfaces for states $S^0$ and $S^1$ (Energy contours in atomic units).

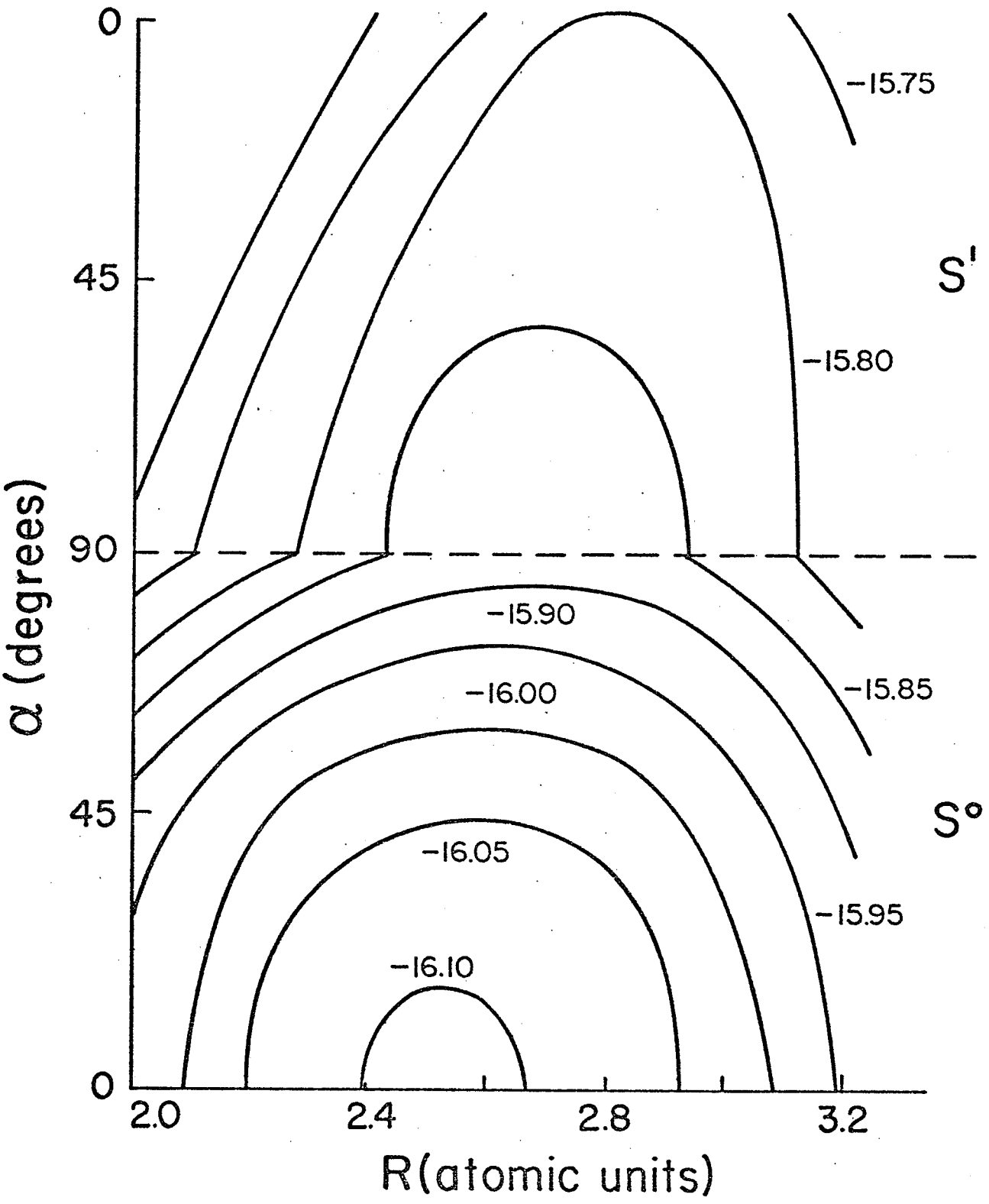
0
45
90
45
0
α (degrees)
2.0
2.4
2.8
3.2
R(atomic units)
-15.75
-15.80
-15.85
-15.90
-15.95
-16.00
-16.05
-16.10
S'
S°

## VI.3 Direct and Indirect Coupling. Structure of the Coupling Matrices

This section deals explicitly with the various matrices occurring in Equation (VI.5). Since the elements of the basis set (VI.3) are eigenstates of $H_i^o$, it follows from (VI.2) that the matrix $\underline{H}$ is diagonal. Thus, if $\underline{V}^{so}$ was negligible and $\omega$ and $\nu$ were zero (stationary nuclear configuration) each state (each $b_j$) would simply change its phase in time but there would be no flow of probability from one state to another. All transitions occur via the matrices $\underline{V}^{so}$, $\underline{G}_\alpha$ and $\underline{G}_R$. If a non zero matrix element between two states a and b exists in any of these three matrices, one says that a and b are directly coupled. Even if two states a and c are not directly coupled, it is still possible for level c to be populated from level a, but only if, say, a is directly coupled to b, and b is directly coupled to c. One refers to this type of coupling as indirect.

It is to be noted from the preceding statements and section II.3 that (VI.5) has been obtained by the use of the orthonormal, adiabatic basis set (VI.4). The discussion that follows is inherently dependent upon this choice, and the analysis that follows reflects the usefulness of this representation.

It is interesting to note the "selection" rules which apply to direct coupling. Since the operators occurring in $\underline{G}_\alpha$ and $\underline{G}_R$ act upon the wavefunctions as spin-independent one electron operators, $\underline{G}_\alpha$ and $\underline{G}_R$ can only couple states of a given multiplicity to other states of the same multiplicity, $S \leftrightarrow S^1$, $T \leftrightarrow T^1$, etc. In no way, for example, can nuclear motion couple $T^1$ with $S^0$. Similarly, $\underline{V}^{so}$ can only couple states differing in multiplicity, S with T, etc.

In the present studies, there are two specific processes of interest, namely $S^1 \leftrightarrow S^0$ and $T^1 \leftrightarrow S^0$. Because direct coupling for both of these processes is small, indirect coupling is essentially negligible. This permits one to study $S^1 \leftrightarrow S^0$ and $T^1 \leftrightarrow S^0$ separately. In itself, this is largely a matter of convenience, as it allows one to employ only a partial basis set which makes the dimensions of all matrices smaller and this in turn greatly speeds computations. Hence, in the computations which will be reported, it is considered that $S^1 \leftrightarrow S^0$ proceeds via $\underline{G}_\alpha$ and $\underline{G}_R$ and $T^1 \leftrightarrow S^0$ via $V^{SO}$.

$S^1 \leftrightarrow S^0$ Coupling:

Because $\underline{G}_\alpha$ and $\underline{G}_R$ are anti-Hermitian matrices, their diagonal elements are zero. The off diagonals are given in Appendix E but are repeated here

$$-\underline{G}^{\alpha}_{S1}{}_{So} = \underline{G}^{\alpha}_{SoS1} = S \sin \alpha/2^{1/2} (1-S^2\cos^2\alpha)^{1/2} \qquad \text{(VI.14)}$$

$$-\underline{G}^{R}_{S1}{}_{So} = \underline{G}^{R}_{SoS1} = A \cos \alpha/(1-S^2\cos^2\alpha)^{1/2} \qquad \text{(VI.15)}$$

S and A are integrals which are solved in Appendix E. Expressions (VI.14) and (VI.15) are interesting since they show the features of the $S^1 \leftrightarrow S^0$ coupling. Vibrational coupling is strongest at $0^o$ and zero at $90^o$ when $S^1$ and $S^o$ are degenerate. As coupling is usually only signifigant when two energy levels cross or lie close to each other, one would expect (and find) that vibrational coupling of $S^1$ and $S^o$ is not important. (This does not mean that vibrational motion itself plays no role in cis-trans isomerism as shall be seen later). The angular coupling on the other hand is strongest at $90^o$ where the levels are degenerate for all R. As it happens this is also where $\omega$ is greatest for the $S^1$ state, so that one expects

strong coupling of $S^1 \leftrightarrow S^o$ when the methylene groups are at right angles.

$T^1 \leftrightarrow S^0$ Coupling:

In terms of the basis set employed the only non-zero matrix elements are between $T_2^1$ and $S^0$ for which

$$V_{31}^{SO*} = V_{13}^{SO}$$

$$= \frac{i\,Z}{2^{3/2}\,(137)^2} \frac{1}{(1-S^2\cos^2\alpha)} \langle p_{x_a} | r^{-3} | p_{x_b} \rangle \sin\alpha \qquad \text{(VI.16)}$$

Again it can be seen that the coupling depends upon sin $\alpha$ so that this interaction is similar in form to the angular coupling in $S^1 \leftrightarrow S^o$ except that the magnitude of the coupling is not velocity dependent.

## VI.4 Transition Probabilities

The procedure by which one studies transition probabilities using equations (V.6) & (V.11) is relatively simple. At time zero, the system is put into a given state with unit probability and some given nuclear configuration, then the iterative solution of the equations is initiated. The nuclear configuration alters due to the forces acting on the nuclei, and as nuclear velocities develop, so coupling occurs between different electronic states which in turn alters the probabilities (the $|b_j|^2$'s) of these states. The output from the program consists of state probabilities, nuclear configurations, nuclear velocities, energies etc. as a function of time. Accuracy of computation is again assured by energy conservation and stability of the solutions with respect to time reversal.

Interpretation of the transition probabilities obtained using the present model in which the nuclei move as classical particles is somewhat complicated. This is well known, however, and is common to all methods employing point particle descriptions of the nuclei. The difficulty arises because the transition probabilities for all points on the nuclear trajectory are not equal. This "inequivalence" causes the transition probability to exhibit irregular fluctuations as a function of time as shown in Figure 12 for the $S^1 \leftrightarrow S^0$ transition. The frequency of these fluctuations is of the order of $10^{-14}$ seconds which is somewhat shorter than the $10^{-12}$ seconds which one might consider to be of the order of a collision time. What is physically relevant is really the "long time" or "average" transition probability which reflects the passage of the nuclear configuration through all energetically accessible trajectories as illustrated in Figure 13. It can be seen from Figure 12 that

Figure 12

$S^1 \leftrightarrow S^0$ exchange probabilities due to nuclear motion as a function of time.

(a) $\alpha$, R, variable. No collisional deactivation. Actual exchange probability.

(b) Average exchange probability corresponding to (a).

(c) $\alpha$, R, variable. With collisional deactivation.

(d) $\alpha$ variable. R fixed.

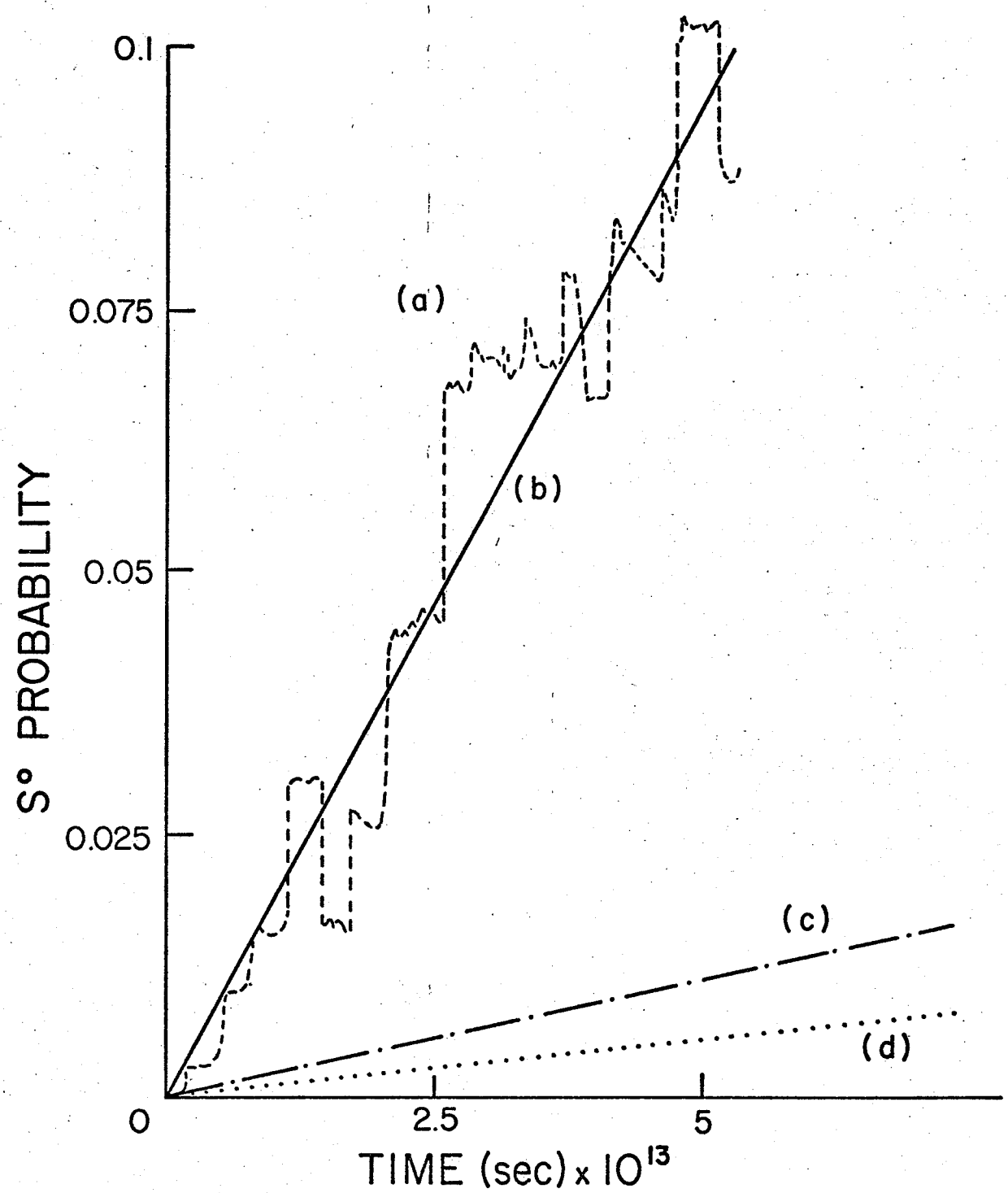
0.1
0.075
0.05
0.025
0
S° PROBABILITY
(a)
(b)
(c)
(d)
2.5
5
TIME (sec) x 10^13

this average increases linearly in time, at least for the interval of time studied. This means that the transition probability per unit time is constant.

These fluctuations of the transition probability are an inherent manifestation of the GIP method which, in solving a problem, examines the moment by moment changes in the coupling terms and reflects these changes in the transition probability.

The $S^1 \leftrightarrow S^0$ Transition

Three separate types of calculations were performed related to the $S^1 \leftrightarrow S^0$ transition.

The first run permitted only the angle $\alpha$ to vary as a function of time, the carbon-carbon distance being fixed at the equilibrium internuclear distance of the excited state $S^1$. This run was considered to be comparable to the commonly accepted qualitative model.

The second calculation permitted both $\alpha$ and R to vary as functions of time and started out by assuming a direct Franck-Condon transition from the equilibrium configuration of $S^0$ vertically upwards to $S^1$. In this run the total molecular energy lay just above the rotational barrier height so that rotation by $n\pi$ was possible. This run was considered to simulate unimolecular rearrangement in the absence of collisional deactivation.

The third run was similar to the second but started out by presuming that the molecule in state $S^1$ had been collisionally deactivated and possessed only 0.02 eV of energy above the bottom of the $S^1$ well. The trajectory for this run is shown in Figure 13. The average exchange

probability as a function of time for the above three runs is shown in Figure 12. Rather than discuss these transition rates themselves, it is perhaps more appropriate to discuss the $S^1$ decay time, $t_{1/2}$ ($S^1$) for the various calculations. From the slopes, these were calculated to be as follows:

| RUN | $t_{1/2}$ ($S^1$) |
|---|---|
| i) α only | $40 \times 10^{-12}$ sec. |
| ii) α, R, no deactivation | $2.6 \times 10^{-12}$ sec. |
| iii) α, R, deactivation | $21.8 \times 10^{-12}$ sec. |

It can be seen from these figures that it is necessary to consider vibrational as well as angular motion to account in quantitative terms for the transition probability. Decay by a molecule which is not collisionally deactivated is seen to be about ten times faster than for one which is, the reasons for this undoubtedly lying in the higher average velocities, $\omega$ and $\nu$, in the former.

An attempt was made to rationalize the importance of vibrational motion by plotting nuclear angular and vibrational kinetic energy (Figures 14a, 14b) as functions of time and comparing these directly with the exchange probability (Figure 11).

Some features of the relaxation process are obvious from such a comparison. These are:

i) The cis-trans isomerization time (Figure 14a) is about $2.7 \times 10^{-14}$ sec.

ii) The period of one C-C vibration (Figure 14b) is about $1.9 \times 10^{-14}$ sec.

Figure 13

Nuclear trajectory for the collisionally deactivated calculation from zero time to $2.5 \times 10^{-13}$ sec.

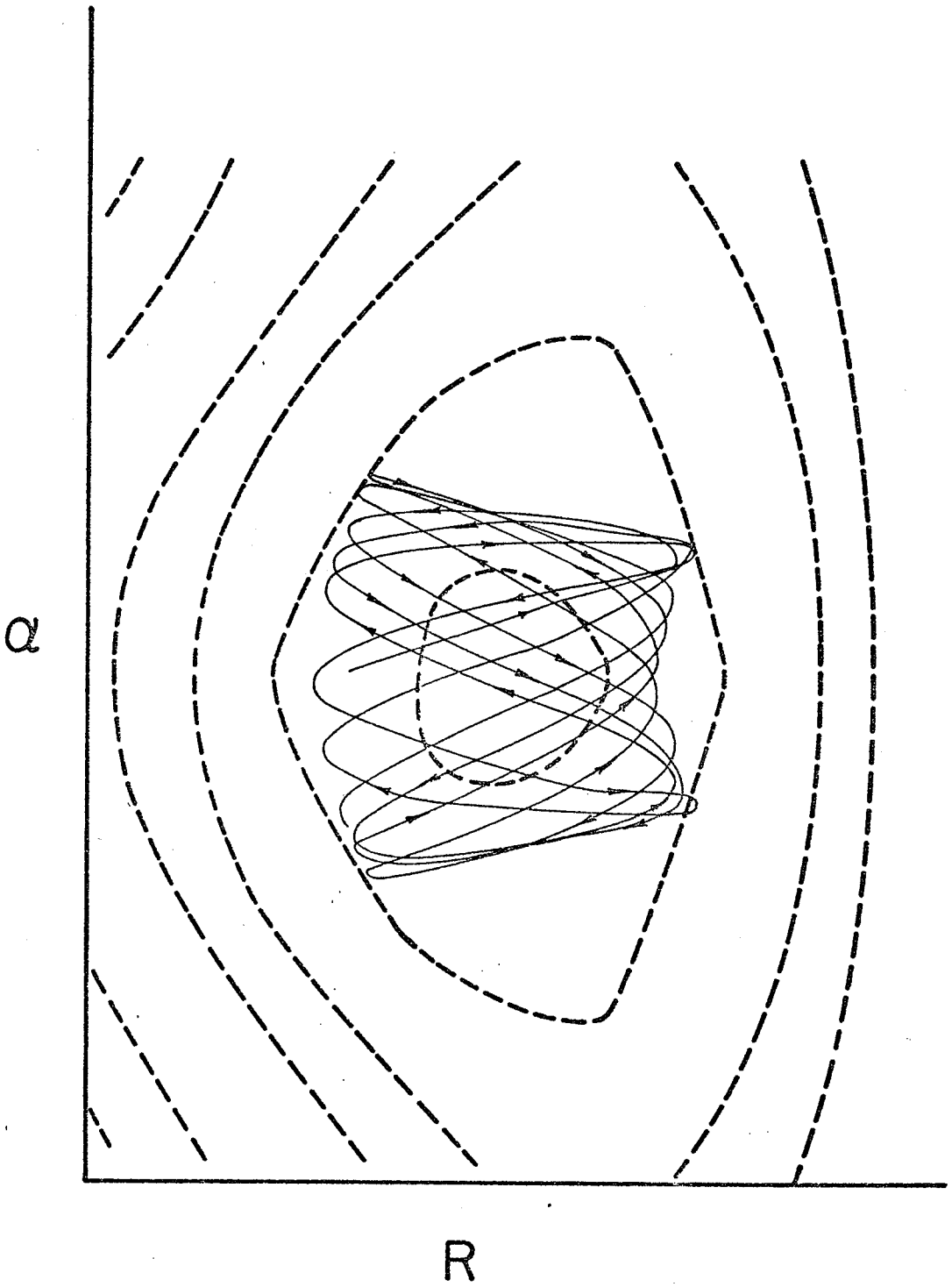
α
R

iii) There is an exchange between angular and vibrational kinetic energy as one might expect from the shape of the $S^1$ potential surface.

iv) There is no obvious correlation between high or low angular or vibrational kinetic energy and electronic relaxation ($S^1 \leftrightarrow S^0$) probability.

The conclusion would then be that the vibrational mode of motion simply serves as an energy sink for electronic energy as it is converted into nuclear kinetic energy during the relaxation process.

The $T^1 \leftrightarrow S^0$ Transition

The probability of exchange between $T^1$ and $S^0$ is expected to depend to a considerable extent upon the nature of the crossing of the $T^1$ and $S^0$ energy surfaces. As mentioned earlier, the level of MO theory employed in this paper does not lead to the energies of the $S^1$ and $T^1$ states being different. On the other hand,it is known that the $T^1$ state lies between the $S^0$ and $S^1$ states in energy. This was taken into account in the present calculation in a somewhat ad hoc fashion. The $T^1$ energy surface was simply lowered by subtracting 0.137 au from the $S^1$ energy. This separation was chosen so that, at the ground state equilibrium configuration,the relative positions of the three energy levels agreed with the assignment of Turro (110). Other choices are possible, for example, one could preferentially use the energy level assignment of Parr (51) or those given by Buenker (56). However, the final $T^1 \rightarrow S^1$ energy separation would not likely vary by more than ten percent from the present assignment, no matter which approach was employed. Though this factor will effect the

Figure 14a

Angular kinetic energy $T_\omega$ as a function of time.

Figure 14b

Vibrational kinetic energy $T_R$ as a function of time.

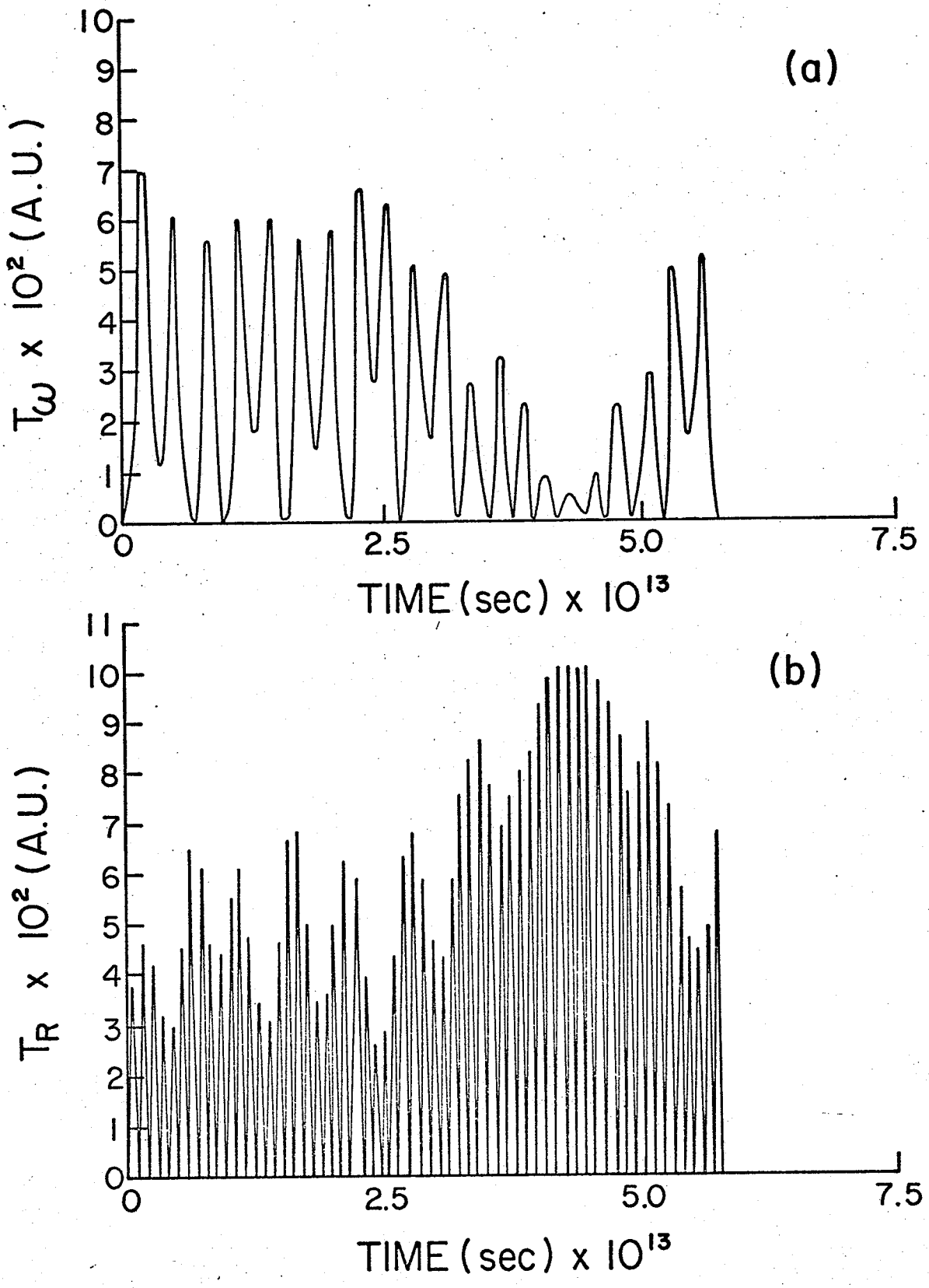
(a)
$T_\omega \times 10^2$ (A.U.)
0
1
2
3
4
5
6
7
8
9
10
0
2.5
5.0
7.5
TIME (sec) x $10^{13}$
(b)
$T_R \times 10^2$ (A.U.)
0
1
2
3
4
5
6
7
8
9
10
11
0
2.5
5.0
7.5
TIME (sec) x $10^{13}$

results somewhat, the qualitative behaviour would not be effected a great deal.

A run was carried out with the system initially in the $T^1$ state and $S^0$ state's nuclear equilibrium configuration. Both $\alpha$ and R were allowed to vary with time. The calculated exchange probability in this case was somewhat more difficult to interpret than for $S^1 \leftrightarrow S^0$ coupling since the fluctuations in the exchange probability were much larger than before and a "long-time" average could not be obtained. The origin of these fluctuations is not difficult to comprehend, and depends upon a strong relationship between the relative phases of the electronic wave-functions and the detailed nature of the nuclear trajectories. Ideally one should average over all allowable nuclear trajectories (phase average of classical motion). In practice this difficulty was overcome by carrying out a set of four calculations in which the initial angular velocity of the nuclei was given slightly different values. This had the effect of randomizing the trajectories. An average exchange probability was computed simply by averaging the exchange probabilities from each separate run. The resultant average showed much smaller fluctuations than any individual run and did increase linearly with time. $t_{1/2}(T^1 \leftrightarrow S^0)$ was calculated to be $1.99 \times 10^{-9}$ sec.

VI.5 Discussion of Results

To ascertain the significance of this set of calculations, one should examine the physical implications of the approximation employed to develop the model. There were three major approximations taken in this particular study.

First, the nuclear behaviour was described in terms of only two variables. This forces the neglect of distortions in the methylene groups. However, these motions are usually considered minor in importance and their neglect would not likely result in a loss of physical reality for the model. However, this treatment of the nuclear behaviour does limit the model in that it cannot be applied directly to oddly substituted ethylenes. There is also, of course, the question raised by the use of a classical nuclear treatment which generally requires some Monte Carlo averaging technique to produce meaningful results. However, in the present study the expected range in the variables defining initial conditions would be small, and Figure 13 demonstrates that a large range of nuclear configurations are found in any given trajectory calculation suggesting that the present study may not display the usual critical dependence on initial conditions that is a characteristic of classical methods.

The more serious approximations with respect to the physical reality of the model are those dealing with the electronic treatment. The treatment of only the pi electrons assumes that the sigma framework has no role in the de-excitation. The use of a one-electron theory approach implicitly assumes the use of semi-empirical methods. The accuracy of such a description is certainly open to question.

However, a more sophisticated treatment would probably be unmanageable computationally at this time, and the present model does provide an estimate of the lifetimes of the two excited states, and suggests some of the factors which control this rate.

For ethylene it is difficult to compare theoretical and experimental results since the latter do not exist. Ethylene does not fluoresce which means that relaxation from the $S^1$ state must be faster than $10^{-9}$ sec. and the present result is certainly consistent with that. The calculated $T^1 \leftrightarrow S^0$ relaxation time is of the correct order of magnitude.

In the case of ethylene itself it would seem from the model calculation that unimolecular $S^1 \leftrightarrow S^0$ exchange is sufficient to account for the observed relaxation of the photo-excited molecule. This might not be the case, however, for substituted ethylenes for which the moment of inertia governing rotation about the C-C bond is much greater than for ethylene itself. Regarding the $T^1 \leftrightarrow S^0$ relaxation process, it is doubtful if unimolecular triplet-singlet coupling is sufficient to account for triplet sensitizer cis-trans isomerization. It seems that the $10^{-9}$ second relaxation time is much too long and that some other process such as a bimolecular relaxation process involving the sensitizer would take precedence. This might well account for the observed dependence of the cis-trans ratio upon the nature of the sensitizer. This possibility is the topic of study in the next chapter.

# Chapter VII

# INTERMOLECULAR ELECTRONIC ENERGY TRANSER IN pi BONDED SYSTEMS

## VII.1 Introduction

In the last chapter only unimolecular photo-induced processes were considered. There are, however, an important group of photo-induced bimolecular processes which are called sensitized reactions (110, 111, 112).

The sensitized photo-isomerization of ethylene-like compounds is considered to take place in three steps, these being:

1. the photo-excitation of the sensitizer, generally some aromatic compound, to an excited state.
2. the transfer of the electronic excitation to the ethylene-like compound.
3. the non-radiative deactivation of the ethylene-like compound.

The first step shall be considered to be instanteous while the third step has been considered in the last chapter.

Therefore, the present concern will be with an analysis of the second step which is clearly bimolecular in nature. However, little else is understood. It is generally assumed that step one includes an inter-system crossing, and that the energy transfer involves triplet states. This aspect of the problem will not be considered in this study but instead it is the intent here to investigate the possible role of a "damped" or short range coulombic interaction in the energy exchange processes.

The system will be taken to consist of two of ethylene model molecules of the last study which are fixed in the equilibrium configuration for the ground state colliding along their centers of mass. The allowed states will be the singlet states considered in the previous investigation. since, within the approximations used in the treatment of the

ethylene problem, the electronic distribution of the $S^1$ and $T^1$ states is identical, and the simple testing of the possibility that energy exchange between molecules could take place through the interaction of excited states seemed to be the first step in the analysis of step two. The physical implications of the constraints imposed on the system study and detailed in the next section will be dealt with in the general discussion of results.

As in the last chapter, this is a model study, in this case of a four-body collision, rather than a quantitative analysis of the collision of two ethylene molecules. The lack of an accurate description of intermolecular forces or the molecules themselves forces this choice. The need for clarification of the reaction pathways and some qualitative estimate of the time scale of this reaction validates the use of the simple study presented here.

Besides determining the feasibility of this reaction pathway, the study will consider the influence of changes in various physical quantities such as:

1. relative orientation of the two molecules during the collision.
2. relative kinetic energy.
3. energy of the excited electronic state of the sensitizer.

## VII.2 System Equations for Bimolecular Collision

To avoid unmanageable complexity and to be consistent with the treatment used on the ethylene molecules, the following constraints were imposed on the system of study.

1. Only energy exchange processes will be considered. No rearrangement channels will be included in the treatment.
2. Each molecule will be taken to be a rigid two body rotor.
3. Only collinear collisions will be considered.
4. Only one class of geometries will be considered, those in which the pi bond of molecule 1) is taken to be fixed in the plane of collision, while the pi bond of molecule 2) is fixed such that it lies parallel to the place of collision.
5. Only the $\pi$ electrons will be considered specifically.
6. A one-electron theory will be employed to deal with the electrons.

Applying these constraints, the electronic Hamiltonian operator may be written

$$H = H_{\pi} + H_{\varepsilon} + V_{\pi\varepsilon} + V_{\sigma_1\sigma_2} \qquad \text{(VII.1)}$$

where the symbol $\pi$ is associated with molecule 1 of Figure 15 and $\varepsilon$ with molecule 2. $H_{\pi}$ and $H_{\varepsilon}$ are identical with the Hamiltonian of (VI.1) except that the spin-orbit term has been dropped. The other two terms represent the intermolecular interaction where $V_{\pi\varepsilon}$ is associated with the pi electrons and $V_{\sigma_1\sigma_2}$ with the sigma electrons. The use of a one electron treatment and specific treatment of only the pi electrons forces the adoption of semi-empirical and empirical forms for the operators $V_{\pi\varepsilon}$ and $V_{\sigma_1\sigma_2}$ respectively. Their forms are

Figure 15

A planar view of bimolecular system giving relative co-ordinate systems for analysis of the collision. R is the separation of center of masses while $\alpha_1$ is the relative orientation of molecule one with respect to the line joining the two center of masses. $\alpha_2$ is the relative orientation of molecule 2.

Also the relative cortesian co-ordinate frames associated with the methylene center of masses are given. The pi bond of each molecule is taken to lie in the Z plane which is common to both centers.

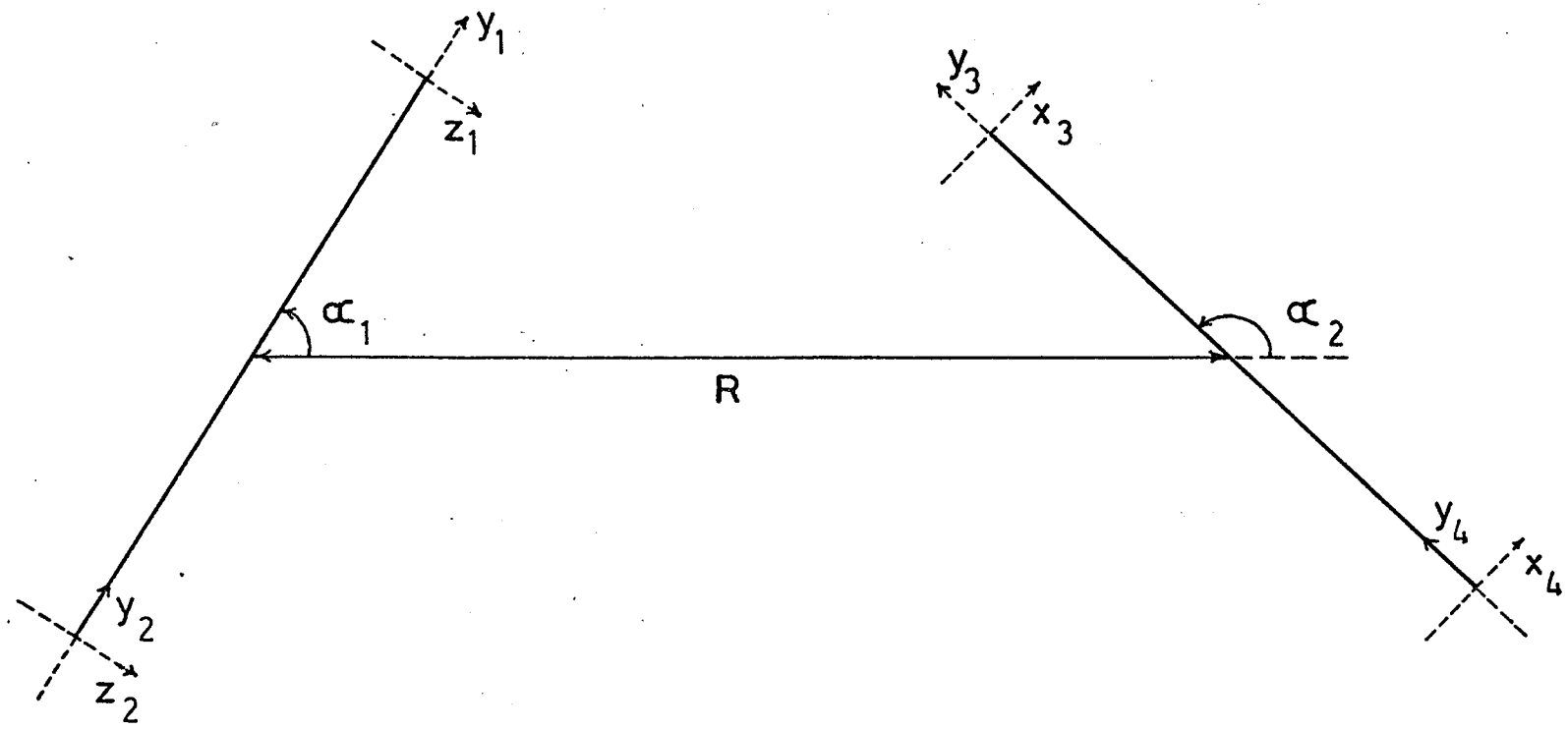


MOLECULE 1(π)

MOLECULE 2(ε)

$$V_{\pi\varepsilon} = \sum_{i}^{\pi} \sum_{n}^{\varepsilon} Z(R_{i_n})/r_{i_n} + \sum_{i}^{\varepsilon} \sum_{n}^{\pi} Z(R_{i_n})/r_{i_n} \qquad \text{(VII.2)}$$

and

$$V_{\sigma_1\sigma_2} = [64(1/R_{13} + 1/R_{14} + 1/R_{23} + 1/R_{24}) + (5.27 - 3.67 \sin^2\alpha_2)$$

$$\cdot(6.10 - 4.26 \sin^2\alpha_1)]\ 2.5\ e^{-.66R} \qquad \text{(VII.3)}$$

where $R_{mn}$ is the separation of m from n, $r_{in}$ is the distance of electron i from nucleus n and $Z(R_{in})$ is an empirical function whose form is given in Appendix F. The subscript i is associated with electrons while the subscript n is associated with the nuclei (center of mass of the methylene groups). For $R_{i_n}$ it is taken that electron i is associated with nucleus n.

The choice of basis functions becomes apparent by considering the form of (VII.1) at the asymptotic limit. Using (VII.2) and (VII.3) and the exponantly damped form of $Z(R_{i_n})$ given in Appendix F, the asymptotic Hamiltonian takes on the form

$$H\ (R = \infty) = H_\pi + H_\varepsilon$$

The proper choice of basis set for $H_\pi$ or $H_\varepsilon$ has been considered in Section VI.2. The resulting multi-electron functions for the two electron system are given in equation (VI.4). Remembering that inter-molecule electron exchange processes are not to be considered, an appropriate choice of multi-electron function for use with the operator given in (VII.1) is

$$|\psi_1(1,2,3,4)> = |S^o(1,2)>|S^o(3,4)> \qquad \text{(VII.4a)}$$

$$|\psi_2(1,2,3,4)> = |S^o(1,2)>|S^1(3,4)> \qquad \text{(VII.4b)}$$

$$|\psi_3(1,2,3,4)> = |S^1(1,2)>|S^o(3,4)> \qquad \text{(VII.4c)}$$

$$|\psi_4(1,2,3,4)> = |S^1(1,2)>|S^1(3,4)> \qquad \text{(VII.4d)}$$

where electrons 1 and 2 are associated with the π molecule and electron 3 and 4 with molecule ε. Having defined the Hamiltonian and electronic functions, the various matrices of (II.8) have been resolved and the equations of motion for the electrons are defined and take on the form

$$d_t\underline{b} = -i[\underline{H}_o + \underline{V} + \underline{I}\ V_{\sigma_1\sigma_2}]\underline{b} \tag{VII.5}$$

where

$$\underline{H}_o(i,j) = \langle\psi_i|H_\pi + H_\varepsilon|\psi_j\rangle \tag{VII.6a}$$

$$\underline{V}(i,j) = \langle\psi_i|V_{\pi\varepsilon}|\psi_j\rangle \tag{VII.6b}$$

and $\underline{I}$ is the identity matrix.

The neglect of exchange channels and restricted nuclear motion results in a null $\underline{G}$ matrix, and the electronic equations of motion (VII.5) are in the diabatic representation. The treatment of the ethylene molecules as rigid rotors can be expressed analytically in the form

$$\underline{H}_o = \underline{E} \tag{VII.7}$$

where $\underline{E}$ is a diagonal matrix of constants whose values are given in Appendix F. The size of these elements suggested the use of the transformations given by equations (II.20) and (II.21) to the time dependent basis set by choosing

$$\underline{U}(i,j) = e^{i\underline{E}(i,j)t} \tag{VII.8}$$

Then (VII.5) becomes

$$d_t\underline{b}' = -i(\underline{V}' + \underline{I}\ V_{\sigma_1\sigma_2})\underline{b}' \tag{VII.9}$$

The mean energy of the system (excluding nuclear kinetic energy) from (II.24) is

$$\bar{E}(\tilde{R}) = \underline{b}'^{+}(\underline{E} + \underline{V}' + \underline{I}\ V_{\sigma_1\sigma_2})\underline{b}' \tag{VII.10}$$

Figure 16

Typical energy surface for $\alpha_1 = 0^o$ ($\psi_2$)

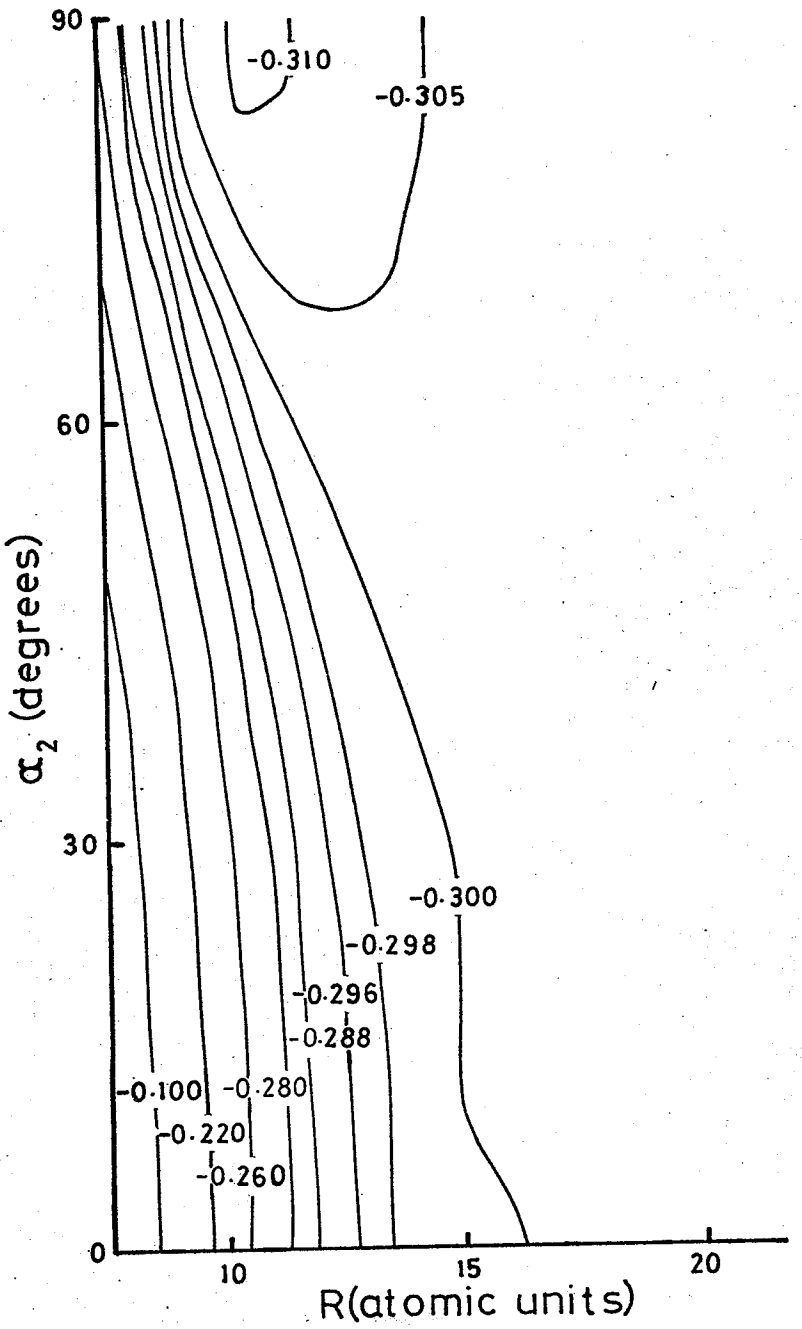
90
60
30
0
$\alpha_2$ (degrees)
-0·310
-0·305
-0·300
-0·298
-0·296
-0·288
-0·280
-0·260
-0·220
-0·100
10
15
20
R(atomic units)

The potential surfaces from (VII.10) are difficult to plot since $\bar{E}$ has a dependence on three independent co-ordinates (the constraints imposed at the start of this section reduce the number of degrees of freedom to this number). For one co-ordinate fixed, a typical surface is given in Figure 16.

The motion of the nuclei will be described in terms of the relative co-ordinates of Figure 15, where R is associated with the relative motion of the center of masses of the two rigid rotors while $\alpha_1$, describes the angular motion of molecule 1 about its center of mass and $\alpha_2$ has a similar role with respect to molecule 2. The application of Raff's (123) analysis of a four body system is given in Appendix G. The total classical Hamiltonian for the system can be written

$$H = 1/2\ m\ \nu^2 + 1/2\ I_1\ \omega_1^2 + 1/2\ I_2\ \omega_2^2 + \bar{E}(\tilde{R}) \qquad \text{(VII.11)}$$

where m is the reduced mass associated with relative velocity $\nu$, $I_1$ is the reduced inertia associated with angular velocity $\omega_1$, $I_2$ the reduced inertia for angular velocity $\omega_2$, and $\bar{E}(\tilde{R})$ is mean energy given by (VII.10). Then from (II.28) and (VII.11) the nuclear equations of motion are

$$d_t R = m\ \nu \qquad \text{(VII.12a)}$$

$$d_t \alpha_1 = m\ \omega_1 \qquad \text{(VII.12b)}$$

$$d_t \alpha_2 = m\ \omega_2 \qquad \text{(VII.12c)}$$

$$d_t \nu = -1/m\ \partial_R\ \bar{E}(\tilde{R}) \qquad \text{(VII.13a)}$$

$$d_t \omega_1 = -\ 1/I_1\ \partial_{\alpha_1}\ \bar{E}(\tilde{R}) \qquad \text{(VII.13b)}$$

$$d_t \omega_2 = -\ 1/I_2\ \partial_{\alpha_2}\ \bar{E}(\tilde{R}) \qquad \text{(VII.13c)}$$

Substituting (VII.10) and using (II.11b), (VII.13) becomes

$$d_t\nu = -\,1/m\; b'^{+}\,(\partial_R \underline{V}' + \underline{I}\;\partial_R\, V_{\sigma_1\sigma_2})\underline{b}' \qquad \text{(VII.14a)}$$

$$d_t\omega_1 = -\,1/I_1\; b'^{+}\,(\partial_{\alpha_1}\underline{V}' + \underline{I}\;\partial_{\alpha_1}\, V_{\sigma_1\sigma_2})\underline{b}' \qquad \text{(VII.14b)}$$

$$d_t\omega_2 = -\,1/I_2\; b'^{+}\,(\partial_{\alpha_2}\underline{V}' + \underline{I}\;\partial_{\alpha_2}\, V_{\sigma_1\sigma_2})\underline{b}' \qquad \text{(VII.14c)}$$

The matrices $\partial_x \underline{V}'$ may be obtained directly from the elements given in Appendix F and relations given in Appendix G, while the terms $\partial_x V_{\sigma_1\sigma_2}$ can be directly derived from (VII.3). The values for the reduced mass and inertias may be obtained from Appendix G.

## VII.3 Structure and Spatial Dependence of Coupling Matrices

First, this section will consider the matrix equation (VII.9). The analytic advantage of using the diabatic representation for this system is that analysis of the $\underline{V}$ matrix is a complete analysis of all transitions in the system. For an arbitrary configuration of the system the $\underline{V}$ matrix has the form

$$\underline{V} = \begin{bmatrix} X & X & X & 0 \\ X & X & 0 & X \\ X & 0 & X & X \\ 0 & X & X & X \end{bmatrix}$$

where X represents a non-zero element. The transitions resulting from the state couplings of such a $\underline{V}$ matrix can be presented pictorially

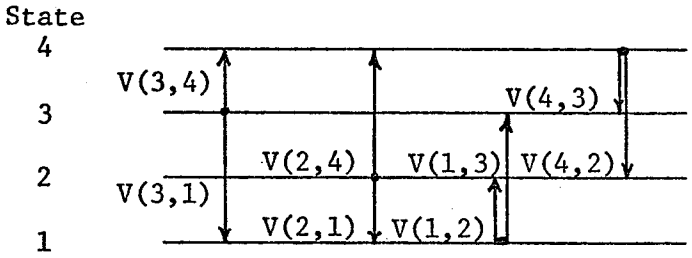


Figure 17

From Figure 17 it can be seen that

a) State 1 and 4 are directly coupled to states 2 and 3.

b) State 2 and 3 are directly coupled to states 1 and 4.

The process of interest, electronic energy transfer or exchange of probability between states 2 and 3, (2→3) therefore depends on indirect couplings rather than direct coupling as was the case with the ethylene study.

Therefore, the relative magnitude and spatial dependence of the various matrix elements will tend to be more signifigant than in the pre-

vious study. For instance, if

$$|\underline{V}(3,4)| >> |\underline{V}(1,2)|$$

the indirectly coupled channel 3→4→2 would play an insignificant role in the process 2→3 since $V^{+}(4,3) = V(3,4)$ or state 4 would transfer probability back to state 3 preferentially. Since the magnitude of the elements of $\underline{V}$ are dependent on the relative spatial orientation, the effectiveness of the indirect coupling depends heavily on this factor. Table 2 gives an example of each case.

Table 2

| R | $\alpha_1$ | $\alpha_2$ | V(1,2) | V(1,3) | V(2,4) | V(3,4) | Case |
|---|---|---|---|---|---|---|---|
| 8 | 90° | 0° | 0.05 | 0.0 | 0.0 | 0.092 | non-exchange |
| 8 | 0° | 0° | 0.067 | -0.067 | -0.134 | 0.174 | exchange |

It is to be noted that Table 2 contains elements of the matrix $\underline{V}$ defined by (VII.6b) rather than elements of the $\underline{V}'$ of (VII.9). To understand the effect of the transformation defined by (II.21) and (VII.8) two cases must be considered. If the complex phase factors of all elements of $\underline{V}'$ are the same, then the discussion of the previous paragraph applies. If, however, there are differences in the complex phase factors then the situation becomes more difficult, with the indirect coupling depending on a number of equally important elements. This problem will be considered in the actual studies undertaken in the next section.

## VII.4 System Studies

Equations (VII.9), (VII.12) and (VII.14) are a complete set of differential equations which quantitatively describe the behaviour of the model system defined at the start of section (VII.2). To determine the behaviour of the system it is only necessary to define the initial conditions and apply the numeric integration method of section (III.4). The accuracy of the solution is assured by checking for conservation of the energy defined by (VII.11). For later discussion it is useful to define the quantities

$$T_R = 1/2\ m\ v^2 \qquad \text{(VII.15a)}$$

$$T_{\omega_1} = 1/2\ I_2\ \omega_2^2 \qquad \text{(VII.15b)}$$

$$T_{\omega_2} = 1/2\ I_2\ \omega_2^2 \qquad \text{(VII.15c)}$$

where $T_R$ is the kinetic energy associated with the relative motion of the two centers of mass, $T_{\omega_1}$ is the angular kinetic energy about the center of mass of molecule 1 and $T_{\omega_2}$ is the angular kinetic energy about the second molecular center of mass.

Two general system were examined, these being

1) $\Delta E_\pi = \Delta E_\varepsilon$

2) $\Delta E_\pi = .65\ \Delta E_\varepsilon$

where

$$\Delta E_\pi = E_\pi - E_\pi^*$$

$$\Delta E_\varepsilon = E_\varepsilon - E_\varepsilon^*$$

with $E_\pi$ and $E_\varepsilon$ being the mean internal energy of the ground states for molecules 1 and 2 respectively and $E_\pi^*$ and $E_\varepsilon^*$ being the mean internal energies for the excited states for molecules 1 and 2 respectively.

For the first system a variety of initial conditions were employed since a strong dependence on relative spatial orientation was expected. The results are tabulated in Table 3. Initial conditions common to all runs were

$\omega_1 = 0 \quad (T_{\omega_1} = 0)$

$\omega_2 = 1 \times 10^{-5} \quad (T_{\omega_2} = 4 \times 10^{-6})$

$P(2) = 1.0$

$R = 30$ au

The conditions that were varied are listed in Table 3 along with the final probability for state 3 (P(3)) and the energy at the end of the event in the various modes of motion available to the nuclei.

An examination of these results reveals rather complex dependences and as a result few simple correlations. However, the following qualitative features are noted.

1) The initial kinetic energy $T_R$ has a moderate and unpredictible effect on the exchange probability.
2) The variation of the initial orientation of the two molecules has a strong effect on the exchange probabilities but the exact form of the behaviour is not clear. In general, runs with small initial angles $\alpha_1$, $\alpha_2$ have a large exchange probability.
3) Runs in which the kinetic energy $T_R$ is converted into the other modes, that is $T_{\omega_1}$ and/or $T_{\omega_2}$ become larger, tend to have signifigant exchange probabilities.
4) The time of a complete exchange process is of the order of $10^{-11}$ to $10^{-12}$ seconds.

Table 3

Bimolecular System Runs

Common Initial Conditions:

$\omega_1 = 0$, $\omega_2 = 1 \times 10^{-5}$, P(2) = 1, R = 30

| INITIAL CONDITIONS | | | FINAL CONDITIONS | | | | |
|---|---|---|---|---|---|---|---|
| $\alpha_1$ | $\alpha_2$ | $T_R$ | P(3) | $T_R$ | $T_{\omega_1}$ | $T_{\omega_2}$ | Time Elapsed (a.u.) |
| $0^o$ | $0^o$ | .02 | .846 | .00697 | .00196 | .011 | $.4 \times 10^5$ |
| $0^o$ | $0^o$ | .01 | .445 | .0052 | .0040 | .0004 | $.5 \times 10^5$ |
| $0^o$ | $10^o$ | .01 | .916 | .0029 | .0048 | .0026 | $3.8 \times 10^5$ |
| $0^o$ | $30^o$ | .01 | .368 | .0068 | .0051 | .0000 | $3 \times 10^5$ |
| $0^o$ | $45^o$ | .01 | .034 | .0077 | .0014 | .0009 | $.37 \times 10^5$ |
| $0^o$ | $60^o$ | .01 | .057 | .01 | 0.0 | 0.0 | $.32 \times 10^5$ |
| $0^o$ | $90^o$ | .01 | .005 | .01 | 0.0 | 0.0 | $.34 \times 10^5$ |
| $0^o$ | $0^o$ | .005 | Bound | -- | -- | -- | -- |
| $0^o$ | $90^o$ | .005 | .017 | .005 | 0.0 | 0.0 | $.4 \times 10^5$ |

The third feature can be more fully understood from Figure 18b. First, the energy transfer is taking place in the time of closest contact between the two molecules or near the turning point. Therefore, the time spent in the strongest interaction region is lengthened ($T_R$ small for longer time) and the relative spatial geometry changes signifigantly in this region ($T_{\omega_1}$ and $T_{\omega_2}$ no longer small). Both these factors will enhance the possibility that signifigant coupling will take place. For runs in which there is no signifigant net transfer of energy from $T_R$ to $T_{\omega_1}$ and/or $T_{\omega_2}$ it happens that there is little transitory transfer resulting in a constant nuclear configuration and a collision which is elastic in nature.

Figure 18a reveals that the indirect nature of the coupling is undetectible in the transition probabilities even in the interaction region. This suggests that the intermediary state can act only as a pathway from one state to the other and can not be highly populated then depopulated in turn which partially explains the strong dependence of the exchange probability on the configuration since only a limited number of nuclear configurations result in a $\underline{V}$ matrix with the proper structure for such an event.

The study of second system ($\Delta E_\pi = .65 E_\epsilon$) was guided by the results with the first system. Though not all of the initial conditions used in the first study were run for the second system, the results were conclusive. The probability for energy exchange in the second system is negligible. This change can be understood in terms of the transformation matrix (VII.8) applied to the matrix $\underline{V}$. The form of the resultant matrix $\underline{V}'$ depends on $\Delta E_\pi$ and $\Delta E_\epsilon$. The basic feature to be noted is that changing

Figure 18

For $\Delta E_{\pi} = \Delta E_{\varepsilon}$

a) The time variation of the probability for states 2 and 3. Result is energy exchange process.

b) The exchange of energy among the various nuclear modes with time. The three curves are: $T_R$ — — —

$T_{\omega_1}$ — · —

$T_{\omega_2}$ ————

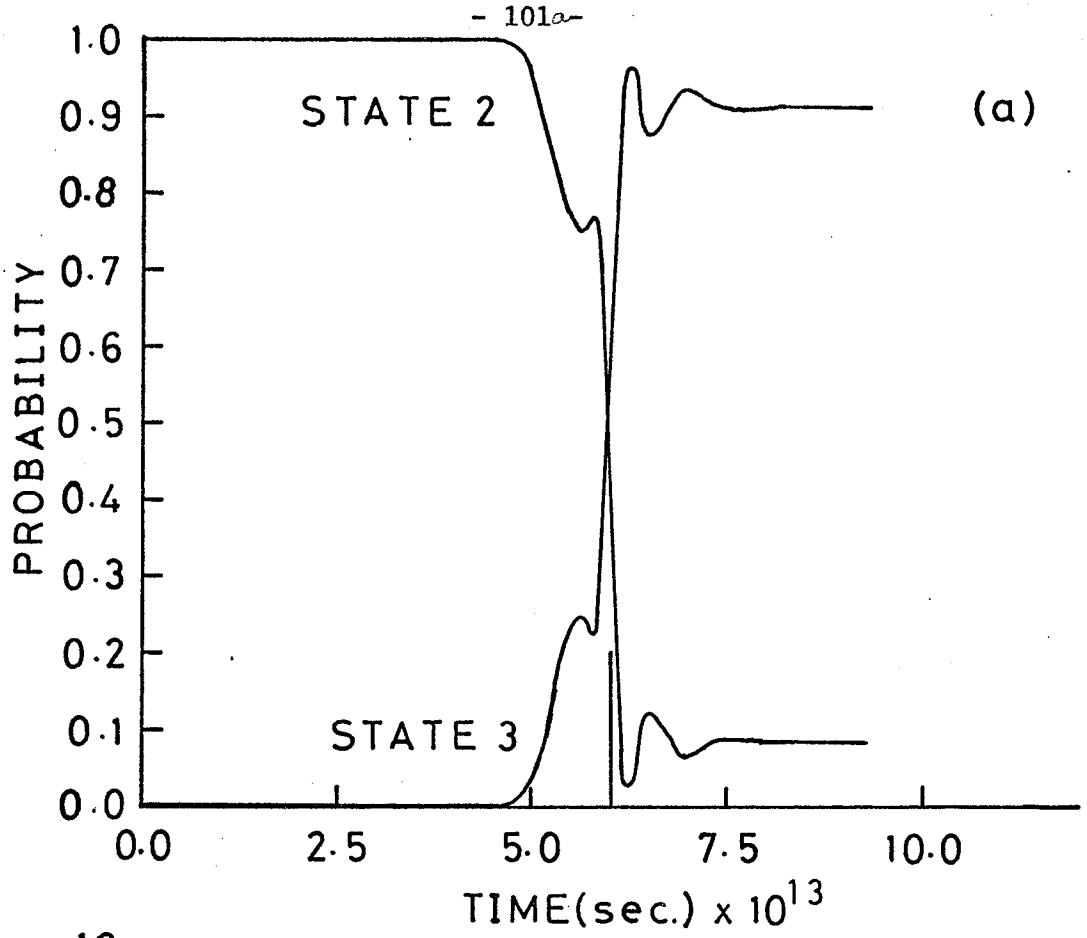
1.0
0.9
0.8
0.7
0.6
0.5
0.4
0.3
0.2
0.1
0.0
PROBABILITY
STATE 2
STATE 3
(a)
0.0
2.5
5.0
7.5
10.0
TIME(sec.) x 10^13

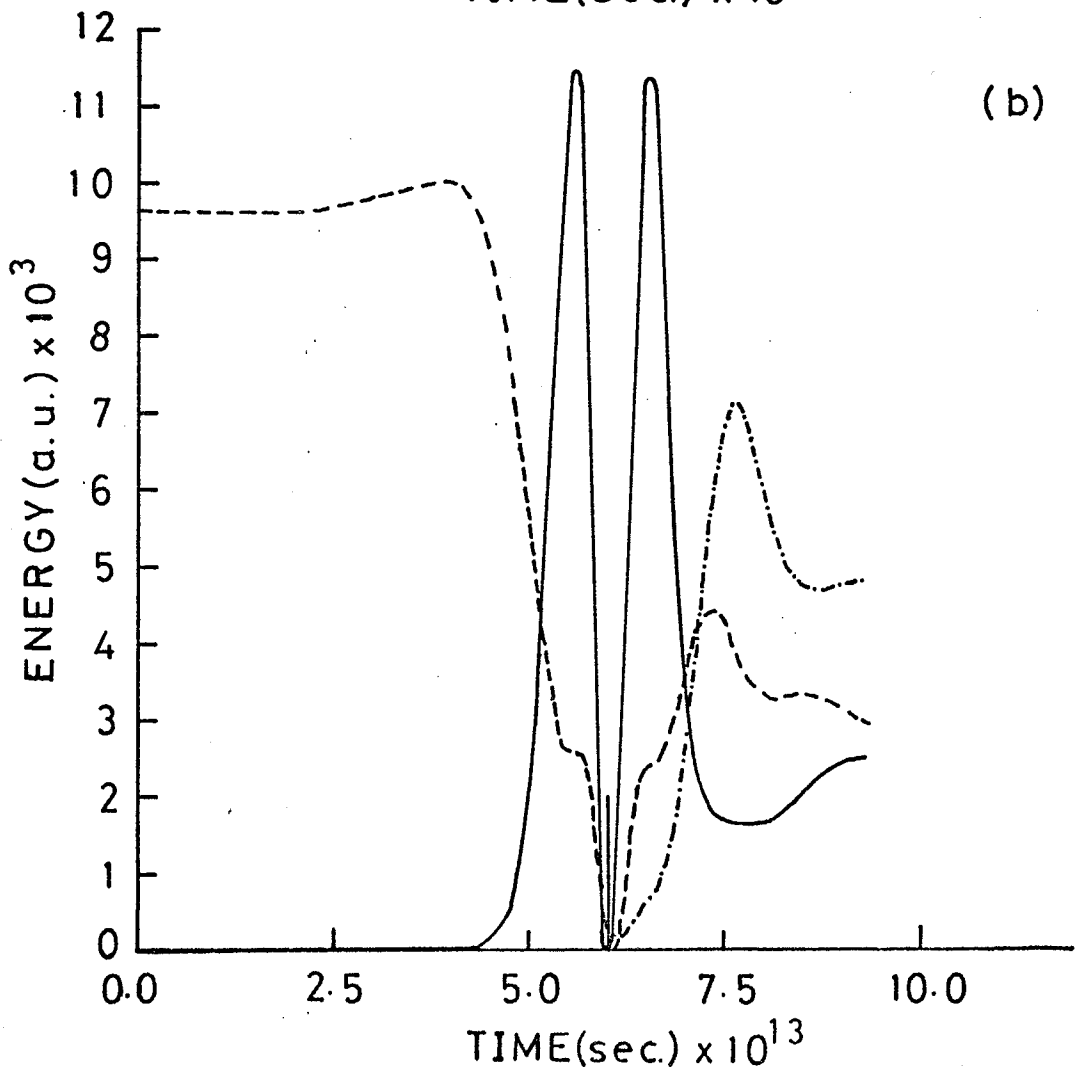
12
11
10
9
8
7
6
5
4
3
2
1
0
ENERGY(a.u.) x 10^3
(b)
0.0
2.5
5.0
7.5
10.0
TIME(sec.) x 10^13

$\Delta E_{\pi}$ produces a difference in the relative phases and magnitude of the matrix elements involved in the indirect coupling. This change is enough to result in a system in which energy exchange is improbable. That this factor is that important can be discerned from Figure 19 which shows the counterpart run of system one depicted by Figure 18. As in Figure 18 there is an exchange of energy from the mode $T_R$ to $T_{\omega_1}$ and $T_{\omega_2}$ but no large transitory or permanent exchange took place.

Figure 19

For $\Delta E_{\pi} = .65 \Delta E_{G}$

a) The change in the probability of state 2 with time. Result is no electronic energy exchange.

b) Displays the exchange of energy amongst the various nuclear modes with time. The three curves are: $T_R$ — — —

$T_{\omega_1}$ — · —

$T_{\omega_2}$ ————

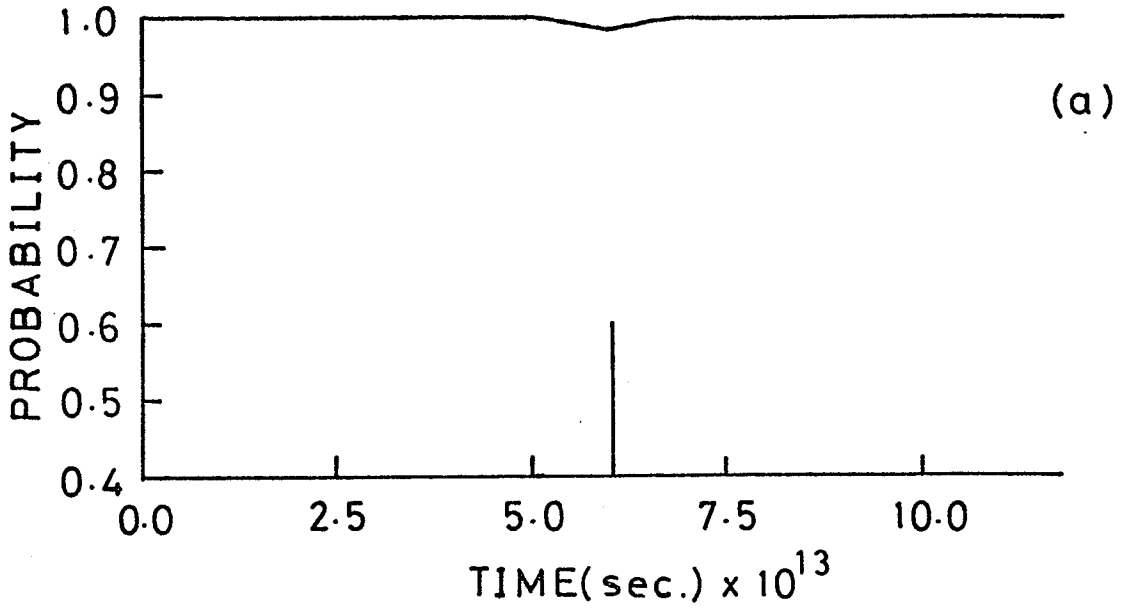
1·0
0·9
0·8
0·7
0·6
0·5
0·4
PROBABILITY
0·0
2·5
5·0
7·5
10·0
TIME(sec.) x 10^13

(a)

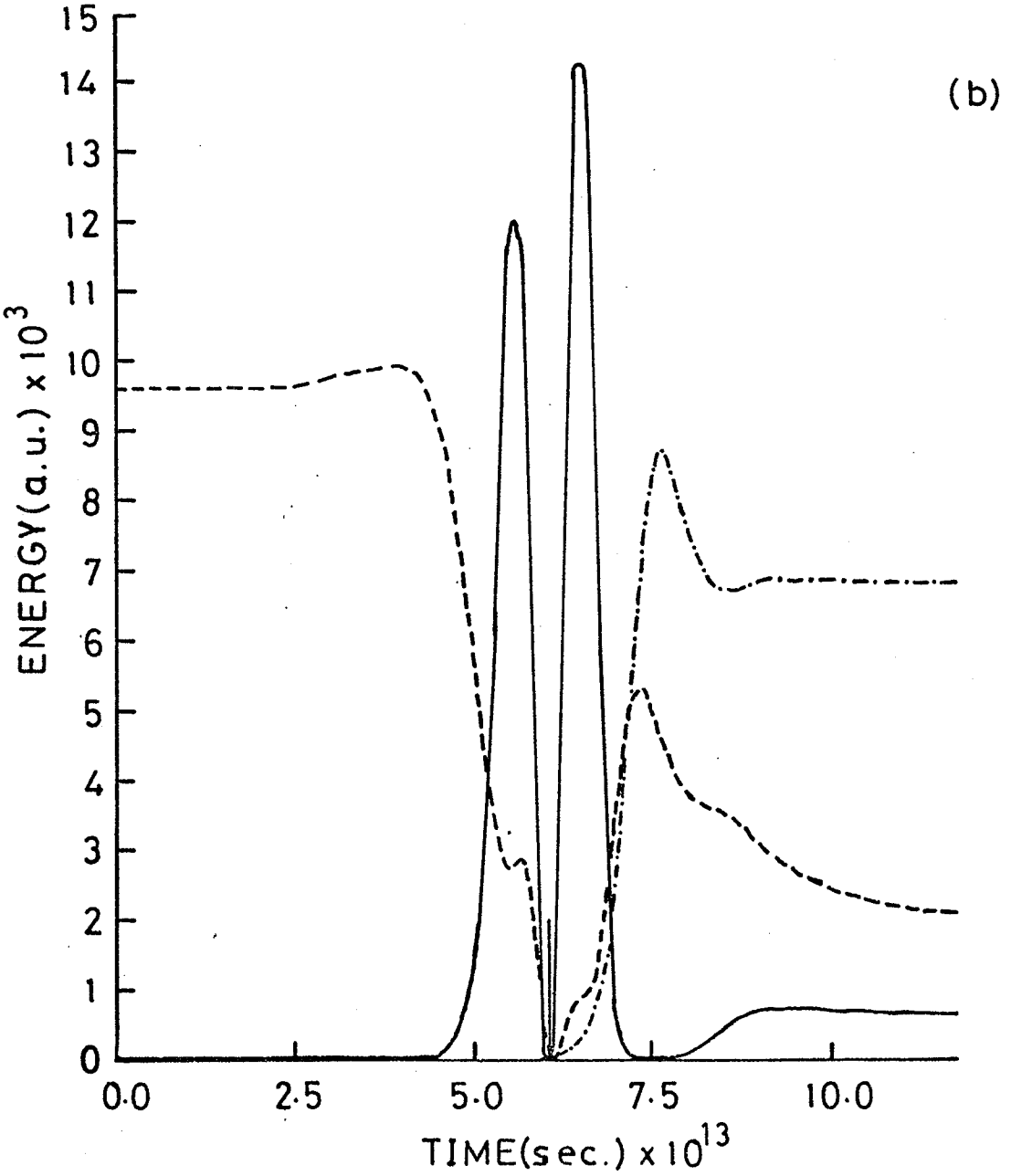
15
14
13
12
11
10
9
8
7
6
5
4
3
2
1
0
ENERGY(a.u.) x 10^3
0·0
2·5
5·0
7·5
10·0
TIME(sec.) x 10^13

(b)

VII.5 A discussion of the Results

The purpose of this study, as was stated in the introduction, was to determine whether short range coulombic interactions could lead to energy exchange processes. Since there is a dearth of information on this topic it was felt that even the most simplified analysis could be informative. Therefore, the present model was developed which considered only a fraction of the possible collisions possible for this system (result of approximations three and four) and examined only the simplest form of intermolecular interaction in the electronic treatment. There is no question that the introduction of other modes such as molecular vibrations could reveal other channels leading to energy exchange and perhaps modify or change the conclusions drawn to this point. Also, the use of a more sophisticated electronic treatment might result in similar changes. But neither of these extensions was possible at this time, and conclusions were drawn from the present model. Again, Monte Carlo averaging was not employed since the design of the model restricts the study to such a small range of the possible collisions that such an approach would not be fruitful. Instead, the study included runs with selected initial conditions, and two situations were examined, these being:

1) photo-sensitized cis-trans isomerizations in which the excitation energy (separation of excited state from ground state) of the sensitizer is the same as that of the ethylene molecule ($\Delta E_{\pi} = \Delta E_{\varepsilon}$).
2) photo-sensitized cis-trans isomerization in which the excitation energy of the sensitizer is much less than that of the ethylene molecule ($\Delta E_{\pi} = .65\Delta E_{\varepsilon}$).

The results of system studies of the last section combined with the results of Chapter VI indicate that the short range electrostatic coupling resulting from electron cloud penetration provides a channel with a significant probability for cis-trans isomerization. Also, the reaction time has been estimated and is of the order of $10^{-11}$ seconds. This result is consistent with the experiment in that no flourescence is observed. Finally, the model displays the correct behaviour for changes in the excitation energy of the sensitizer with the transition probability decreasing with decreasing sensitizer excitation energy.

It is hardly possible to conclude that the mechanism utilized in this model study is "the explanation" of the photo-sensitized cis-trans isomerization of ethylene like molecules. Besides the basic drawbacks of a classical nuclear model andthe related need for statistically averaged trajectories the major question is the correctness of the semi-empirical and empirical treatments employed. However, the model is a dynamic representation of the system which allows for the effect of nuclear motion on the electronic transitions and the lack of both experimental and theoretical information on these systems makes the present model a welcome if limited investigation of these systems.

# Chapter VIII

# CONCLUSION

## VIII.1 Some Closing Remarks on the Generalized Impact Parameter Method

The intent of this dissertation was to examine and evaluate the applicability of a generalization of the impact-parameter method to the field of reactive collision theory. Though the work is far from definitive some conclusions can be drawn.

First, the method is extremely flexible. It was applied with reasonable success to the study of

a) vibrational energy exchange in the classical limit

b) high and low energy collisions involving electron exchange

c) photo-decomposition

d) photo-induced cis-trans isomerization

e) bimolecular electronic energy exchange.

The results of each study correlated with available experimental data.

However, other aspects of the study were not so encouraging. It was suggested in Chapter IV that the use of empirical functions should be avoided in that parameterization often proved not to be unique, and this was in fact part of the motivation for developing the present semi-classical method. Unfortunately, computing restrictions necessitated the adoption of semi-empirical and empirical treatments for the study of the more complex systems attempted. In fact, these treatments tended to be "crude" or at best simplistic in nature as a result of the simple lack of employable descriptions of electronically excited states and intermolecular forces. These two sources of difficulty are likely to be around for some time. Also, the necessity for using a representation that simplifies the electronic equations of motion has been demonstrated, and the proper representation for a multi-channel problem is in

general not apparent.

One other area of difficulty is associated with the classical nature of the nuclear description. Of course, it invalidates the application of the GIP method to any process in which the nuclear behaviour is expected to exhibit quantum behaviour. More importantly, however, there is a practical limit on the number of nuclei that can be handled. This limitation stems from a quickly increasing number of variables whose significance would have to be investigated.

These two general difficulties are related in that they both reflect the difficulty of dealing with many-body interactions, and it is unlikely that a totally practical solution will be found in the near future.

The question then arises, should the GIP method be considered further? The answer is conditional. As a method of analyzing rearrangement collisions the answer at the present time would have to be no. However, for studies of simple molecule photo-decomposition and de-excitation the method can supply simple dynamic models. In general, it is suggested that the GIP method can provide the framework for simple semi-quantitative model studies of relatively complex systems.

# APPENDICES

A Definition of atomic units and their equivalence.

unit of charge=charge of electron= 1 a.u. = $4.80296 \times 10^{-10}$ esu.

unit of mass = mass of electron = 1 a.u.= $9.1091 \times 10^{-28}$ g.

unit of length = Bohr radius = $a_o$ = 0.529167 $A^o$.

unit of action = $h/2\pi$ = 1.

unit of time = 1 a.u. = $2.42 \times 10^{-17}$ sec.

unit of energy = 1 A.U. = 27.2107 e V. = 1 Debye(D)

## B.1 Computer Hardware and Software Considerations

The University of Manitoba Computer Center has made available to the university community the services of an IBM 360-65 high speed digital computer. A schematic representation of the present system (as of Aug., 1972) is given in Appendix B.3 as well as a definition of various abbreviations that will be used in this section. The computational capability provided by such an installation is quite extensive and is reflected in the facilities available to the user.

Besides, the necessary peripherals such as line printers, card readers and core, there are available teletype and typewriter terminals and adequate tape and disk storage.

Presently, the system is operating under OS-MVT with the HASP batch processing system. There is available to the user both time sharing languages such as APL and time sharing systems such as TSO and MUM as well as batch processing. A large number of languages are available for jobs run under batch processing but the present discussion will be limited to the more useful.

First there is the assembler language. This is the most fundamental language on the computer other than machine language. It would not be feasible to use this language exclusively for the programming being considered here but specialized segments can be made very efficient by use of this language. For language and system details one is referred to the I.B.M. manuals (74).

There are basically three languages to be considered in scientific programming, Fortran, Algol and PL/1 which are all high-level languages.

A high-level language is one which the command words are operation orientated rather than machine oriented, that is a high-level language is largely algebraic in nature and its structure is independent of machine specifics. Such a language can not be directly "understood" by a computer but must be translated into machine language. Programs called compilers are provided on larger computer systems to do this task. Unfortunately it is the available system support in the form of compilers and I/O (input-output) support programs, which determines the usefulness of a particular language.

Algol, the name being derived from algorithm, is probably the most appropriate of the three for scientific programming. It is a language which is consistent, flexible and completely machine independent in structure. Unfortunately, it was unfeasible to use this language at the University Computer Center until very recently because the available compiler was poor and the I/O support completely inadequate.

PL/1, a language established by IBM, is again a flexible if somewhat complex language incorporating the features of the languages Algol, Cobol (a business oriented data management language) and assembler (75). Unfortunately the language tends to reflect the hardware characteristics of the IBM 360 system. Until recently, the compilers were slow and produced comparatively inefficient coding. Recently this situation has changed but compilation is still rather lengthy and relatively expensive. On the other hand the I/O capabilities of this language are by far the best of the languages considered.

Fortran, the first universally accepted high level language is still in common use in the North American scientific community. Though

the language is limited in command words and form, it is capable of handling numeric computations quite efficiently. It is limited, however, if more complex operations such as algebraic manipulations are being considered. There are a minimum of three compilers available, WATFIV, IBM Fortran level G, and IBM Fortran level H. In particular, the Fortran H level compiler produces very efficient coding, that is the operation time is short. The I/O support, though limited in some aspects, is complete enough for most tasks. (76)

This concludes this brief description of the University of Manitoba computing facilities except for the question of cost. Though the academic researcher may not have to provide funds for his computer time, the computer costs are indicative of the available computing capacity. For this reason it is useful to estimate the relative cost of using different approaches. The computer center bases its charges on a formula which quantitatively relates the cost of various hardware facilities. This factor must also be given consideration before a final decision is made.

Before leaving this section it is necessary to mention unfortunate features of digital computer hardware. In representing a real and in particular an irrational number it is necessary to use a number of limited length. This error is termed round-off error and can become signifigant in certain mathematical operations. The IBM 360 has a hardware based double-length word facility which can be used to minimize this problem. Unfortunately resorting to this solution of the problem raises the program operating costs.

## B.2 Selection of Numeric Technique

The most logical starting point is to find the Jacobian matrix $\underline{A}$ since this would provide an analytic basis for the choice of a method. However, the evaluation of $\underline{A}$ as defined by (III.3) requires the definition of $f(t,\underline{y})$ or specification of the system of study and, therefore, it will vary quite extensively from system to system as well as for various choices of $(t,\underline{y})$. Also, it soon became apparent that an analytic evaluation of $\underline{A}$ is impractically difficult. Therefore, a first order estimate was made by taking that

$$\partial f_j\,(t,\underline{y}) \,/\, \partial y_i = \{f_j\,(t,y_1, \ldots, y_i + h, \ldots, y_n) - f_j\,(t,y_1, \ldots, y_i, \ldots, y_n)\}/h \qquad \text{(B.1)}$$

and the eigenvalues of $\underline{A}$ were determined for a typical system. It was found that for argument $(t,\underline{y})$, for which the system could be considered to be in the interaction region the dominant eigenvalues were totally imaginary. This information combined with the stability diagram of Crane and Klopfenstein (69) indicated that the Runge-Kutta methods were the most appropriate choice.

However, another important factor suggested the opposing choice. It is easy to demonstrate that a dominate element in the computation time is the evaluation of the functions $f_i\,(t,\underline{y})$. Since predictor-corrector methods on the average use half as many evaluations of the $f_i\,(t,\underline{y})$ as Runge-Kutta methods of the same order, one would expect the former to be the better choice.

The analysis being inconclusive, it was necessary to simply try a number of available methods of both the predictor-corrector (66, 69)

and Runge-Kutta (66, 70, 72, 73) types. On the basis of stability, cost, and ease of use the Runge-Kutta-Gill algorithm (a fourth-order method) was chosen (66). A method could not be found which was signifigantly more economic in the use of computer time. The lack of an error estimate caused little difficulty since it proved possible to use physical conservation laws to check the validity of the solution.

The Runge-Kutta-Gill algorithm is a four step method which incorporates a round-off error compensation. The procedure can be expressed in the form

Step One (B.2)

$$\underline{k}_1 = h\, f\,(t_o, \underline{y}_o)$$

$$\underline{q}_1 = \underline{q}_o + 3\,[1/2\,(\underline{k}_1 - 2\underline{q}_o)] - 1/2\,\underline{k}_1$$

$$\underline{y}_1 = \underline{y}_o + 1/2\,(\underline{k}_1 - 2\underline{q}_o)$$

Step Two

$$\underline{k}_2 = h\, f\,(t_o + h/2, \underline{y}_1)$$

$$\underline{q}_2 = \underline{q}_1 + 3^{o}[(1 - \sqrt{1/2})\,(\underline{k}_2 - \underline{q}_1)] - (1 - \sqrt{1/2})\,\underline{k}_2$$

$$\underline{y}_2 = \underline{y}_1 + (1 - \sqrt{1/2})\,(\underline{k}_2 - \underline{q}_1)$$

Step Three

$$\underline{k}_3 = h\, f\,(t_o + h/2, \underline{y}_2)$$

$$\underline{q}_3 = \underline{q}_2 + 3\,[(1 + \sqrt{1/2})\,(\underline{k}_3 - \underline{q}_2)] - (1 + \sqrt{1/2})\,\underline{k}_3$$

$$\underline{y}_3 = \underline{y}_2 + (1 + \sqrt{1/2})\,(\underline{k}_3 - \underline{q}_2)$$

Step Four

$$\underline{k}_4 = h\ f\ (t_o + h,\ \underline{y}_3)$$

$$\underline{q}_4 = \underline{q}_3 + 3\ [1/6\ (\underline{k}_4 - 2\underline{q}_2)] - 1/2\ \underline{k}_4$$

$$\underline{y}_4 = \underline{y}_3 + 1/6\ (\underline{k}_4 - 2\underline{q}_3)$$

The results of step four is the solution $(t_1, \underline{y}_1)$. These can be substituted into step one, and the procedure repeated to give $(t_2, \underline{y}_2)$. The $\underline{q}$ terms are related to round-off error correction. To start the method one initially sets these to zero.

B. 3 Basic core layout and machine configuration of the IBM 360/65 computer

The following discussion is from the August 1972 issue of MERCURY, newsletter of the University of Manitoba Computer Centre.

The diagram on this page shows the way in which the 360/65 core storage is used to accomodate the various operating system modules, time sharing systems, and other programs. Core is split into two main areas, these being the 024k of ECM (extended core memory) or slow core and 768k of high speed core. Since some of the abbreviations used may be unfamiliar to the reader, the following expansions are given.

MVT Multi-programming with a Variable number of Tasks

LPA Link Pack Area

HASP Houston Asynchronous Spooling Program

APL A Progamming Language (time sharing system)

MUM Manitoba University Monitor

TSO Time Sharing Option

OS Operating System

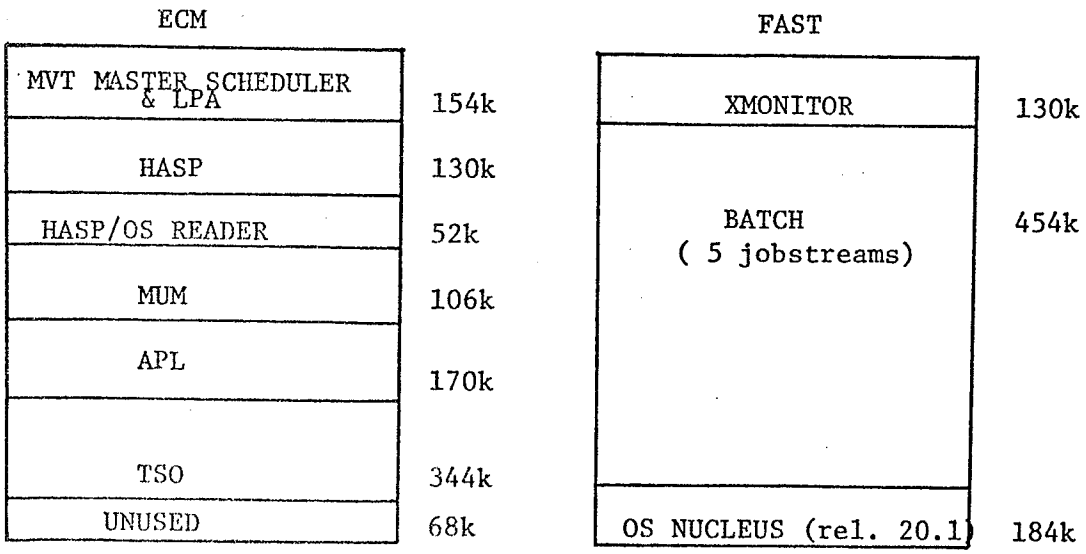

Diagram 20 shows the configuration of the 360/65, that is tha basic parts of the system, together with all the peripheral devises and remote terminals. For an explanation of the use of the various devises the reader is referred to the Computer Centre's library. The extensive list of manuals that is required to document this computer system would serve little purpose to the main intent of this thesis.

Figure 20

University of Manitoba Computer Centre 360/65 Configuration.

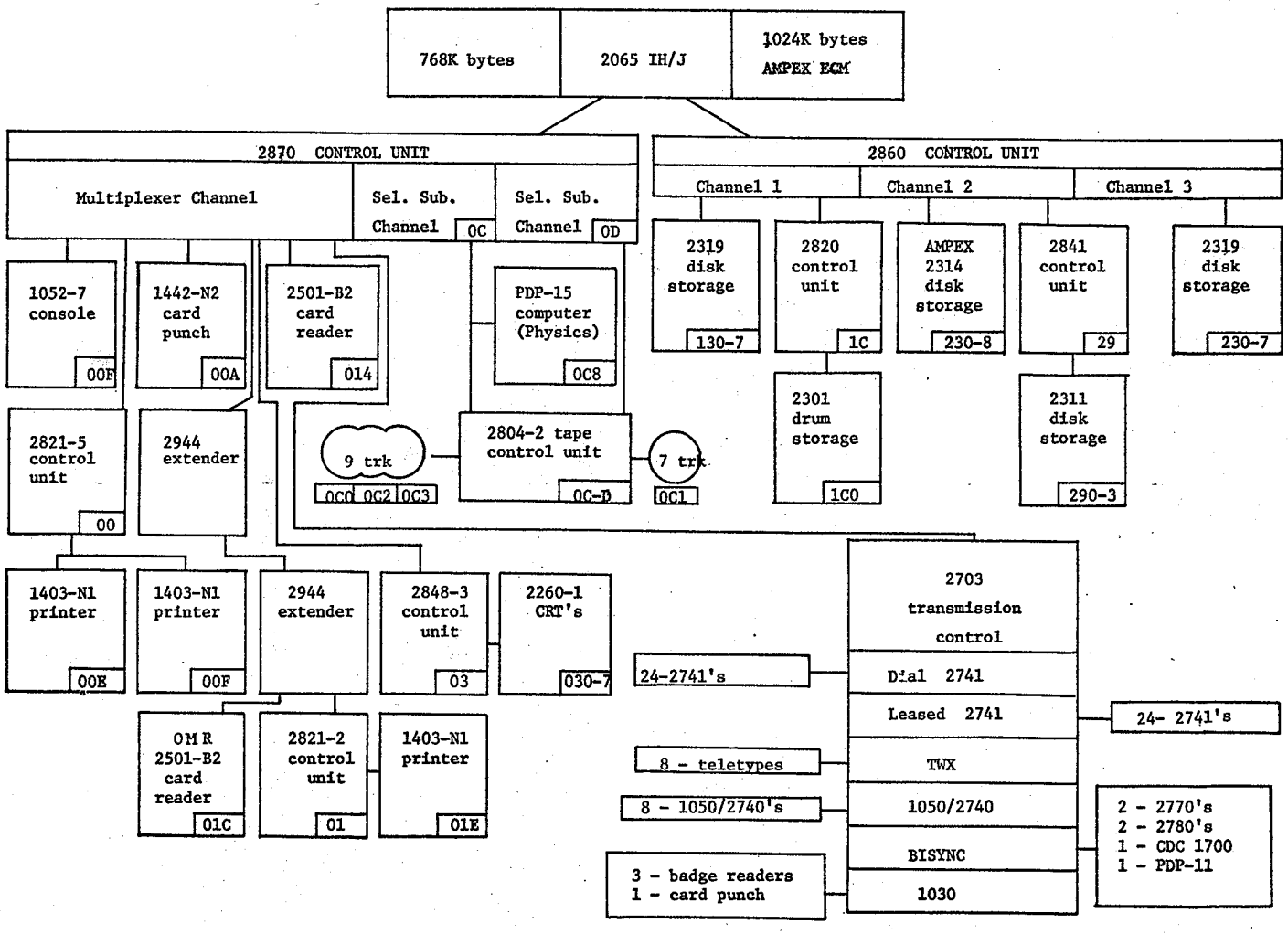
768K bytes
2065 IH/J
1024K bytes
AMPEX ECM
2870 CONTROL UNIT
Multiplexer Channel
Sel. Sub. Channel 0C
Sel. Sub. Channel 0D
2860 CONTROL UNIT
Channel 1
Channel 2
Channel 3
1052-7 console 00F
1442-N2 card punch 00A
2501-B2 card reader 014
PDP-15 computer (Physics) 0C8
2319 disk storage 130-7
2820 control unit 1C
AMPEX 2314 disk storage 230-8
2841 control unit 29
2319 disk storage 230-7
2821-5 control unit 00
2944 extender
9 trk 0C0 0C2 0C3
2804-2 tape control unit 0C-D
7 trk 0C1
2301 drum storage 1C0
2311 disk storage 290-3
1403-N1 printer 00E
1403-N1 printer 00F
2944 extender
2848-3 control unit 03
2260-1 CRT's 030-7
2703 transmission control
24-2741's
Dial 2741
Leased 2741
24- 2741's
8 - teletypes
TWX
8 - 1050/2740's
1050/2740
2 - 2770's
2 - 2780's
1 - CDC 1700
1 - PDP-11
BISYNC
3 - badge readers
1 - card punch
1030
OMR 2501-B2 card reader 01C
2821-2 control unit 01
1403-N1 printer 01E

B.4 Program Logic and Design

A number of different programs were employed to deal with the systems analyzed. However, there is a common design to all the programs used and this is presented in the form of flow diagrams in figures 21 and 22. The first figure presents a macro logic flow chart for the whole program while the second diagram presents two typical micro flow charts for subblocks of the program. The other micro flow charts can be easily constructed by reference to the appropriate equations.

Most of the programs incorporated a time interupt system, that is the program could be restarted without loss of the results accomplished to that point. This was necessary since the CPU time for integration of the equations for some systems was quite extensive, and the job could not be done in one step. This feature was achieved writing intermediary information on a permanent disk data set and retrieving the same to restart the program.

Although some programming was done in Assembler language the majority of the coding was done in Fortran IV. As a number of peripheral devises were used, the Job Control Language (JCL) was rather extensive. The aid of the Computer Centre staff in this and other matters too numerous to mention is gratefully acknowledged.

Figure 21

Total Program Macro Flow Chart

The major steps (blocks) and their interrelations are illustrated graphically
$\Delta E$ is the error in the energy in a given step.

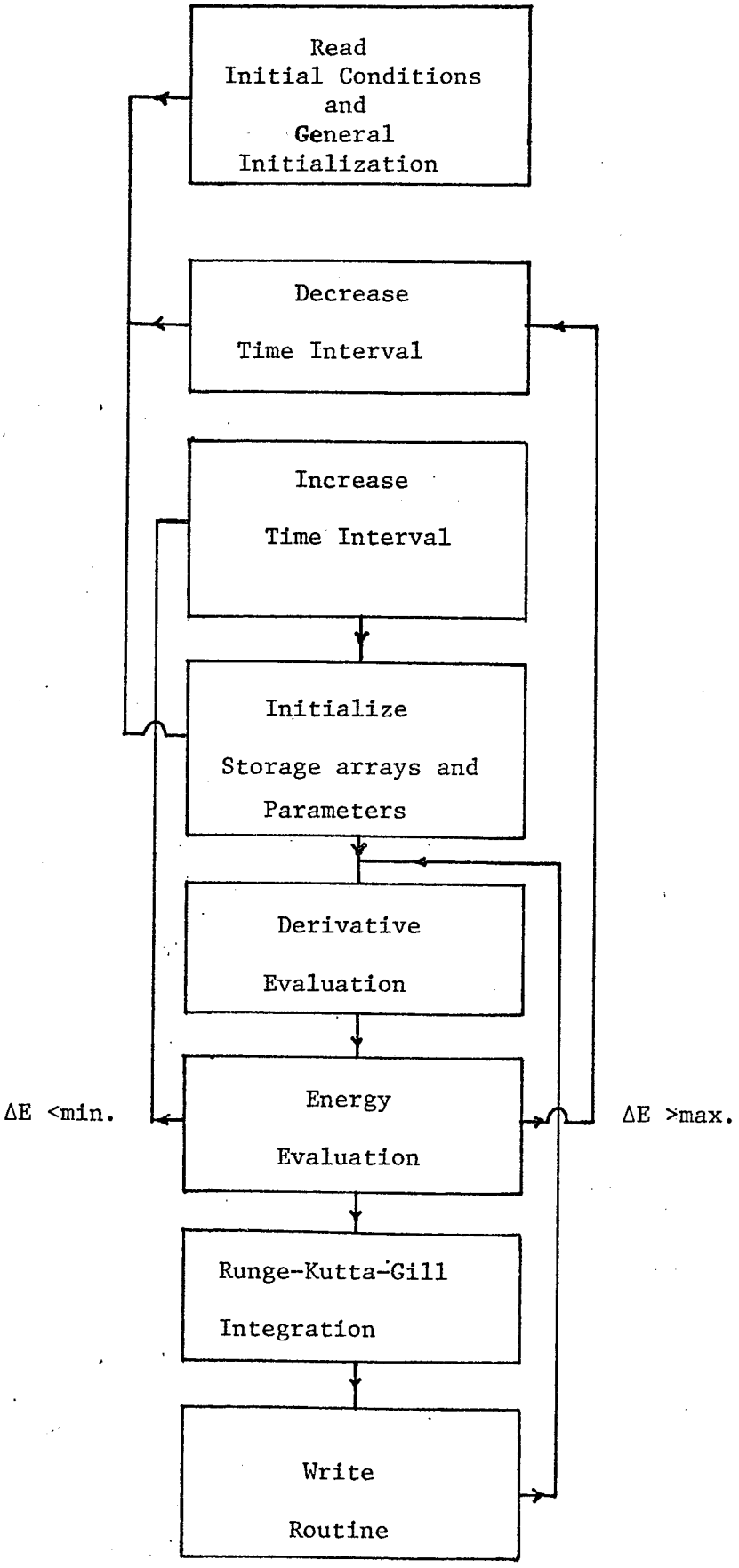
Read
Initial Conditions
and
General
Initialization
Decrease
Time Interval
Increase
Time Interval
Initialize
Storage arrays and
Parameters
Derivative
Evaluation
ΔE <min.
Energy
Evaluation
ΔE >max.
Runge-Kutta-Gill
Integration
Write
Routine

Figure 22

Typical Micro Flow Charts

(a) Read Block

(b) Write Block

(a)

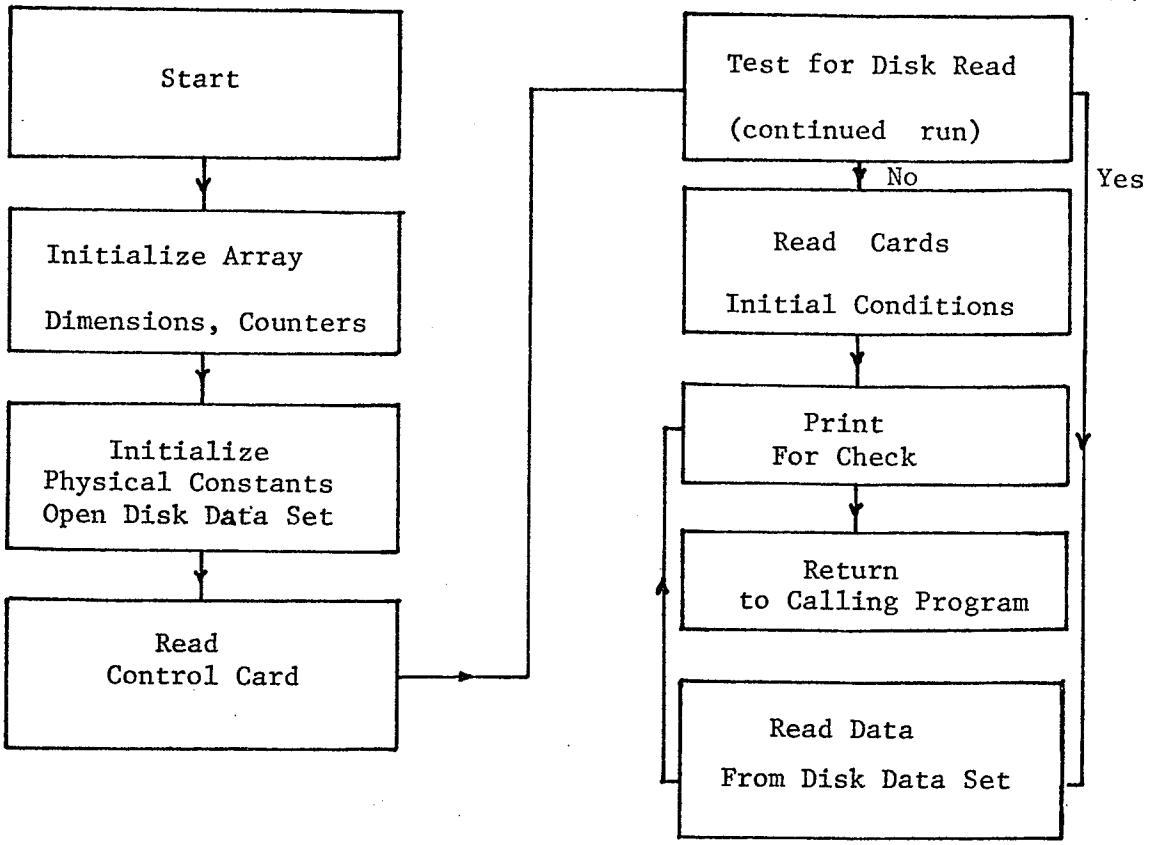
Start
Initialize Array
Dimensions, Counters
Initialize
Physical Constants
Open Disk Data Set
Read
Control Card
Test for Disk Read
(continued run)
No
Yes
Read Cards
Initial Conditions
Print
For Check
Return
to Calling Program
Read Data
From Disk Data Set

(b)

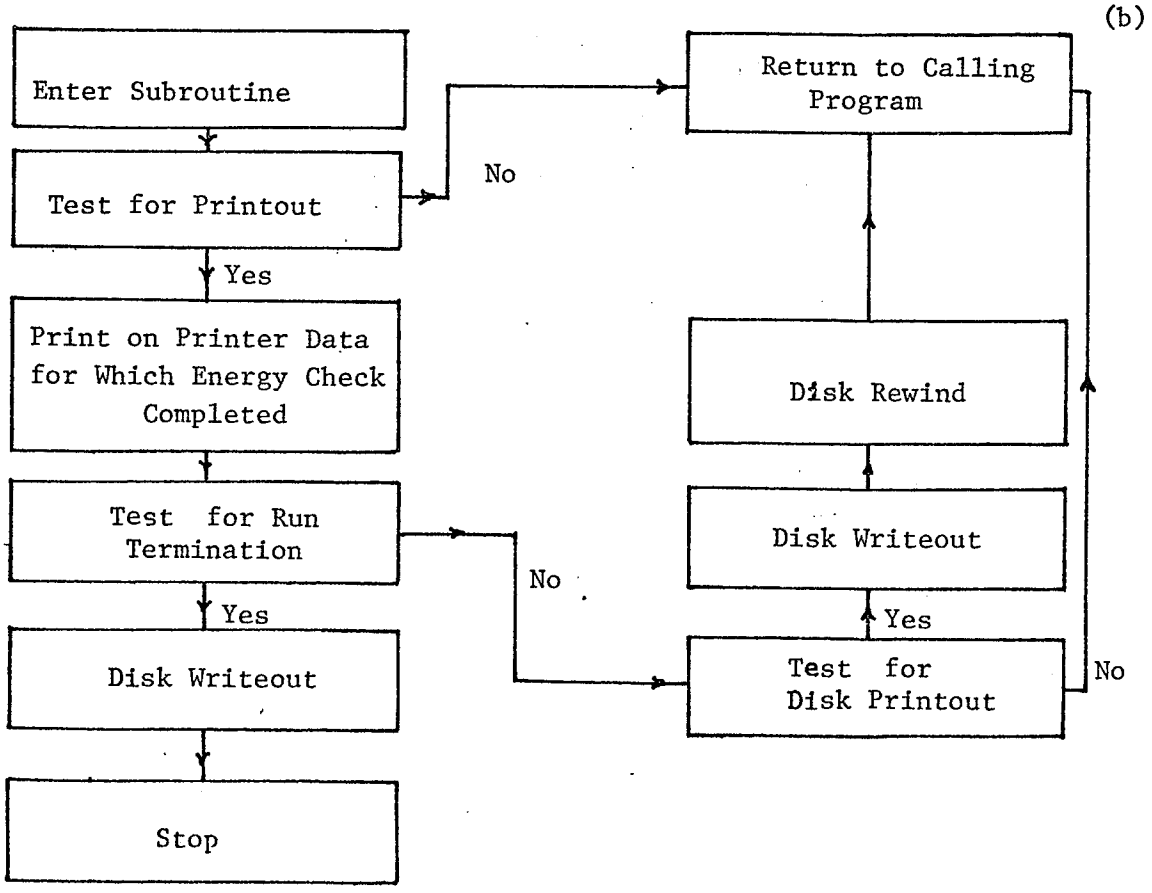
Enter Subroutine
Test for Printout
No
Yes
Print on Printer Data
for Which Energy Check
Completed
Test for Run
Termination
No
Yes
Disk Writeout
Stop
Return to Calling
Program
Disk Rewind
Disk Writeout
Yes
Test for
Disk Printout
No

## C Equations of Motion for Classical Molecular Models

Rewriting (IV.8) in cartesian coordinates the equations take the form

$$d_t\, x_i = p\ /M_i^x$$
$$d_t\, y_i = p\ /M_i^y$$
$$d_t\, z_i = p\ /M_i^z \qquad\qquad i=1,n$$
$$d_t\, p_i^x = -\partial_i^x\ V(\tilde{q})$$
$$d_t\, p_i^y = -\partial_i^y\ V(\tilde{q})$$
$$d_t\, p_i^z = -\partial_i^z\ V(\tilde{q})$$

where $(x_i,y_i,z_i)$ are the cartesian coordinates of particle i and $(p_i^x,p_i^y,p_i^z)$ are the cartesian components of the momentum of particle i. These equations are completely defined by the choice of the specific form of the potential $V(\tilde{q})$ and its derivatives. Since this potential has been expressed in terms of a series of potentials in section IV.2 it is only necessary to derive the derivatives of the generalized potentials discussed in IV.2 to complete this section. These are tabulated below.

1) Coulomb Potential

$$V_{ij}^C(\tilde{q}_i,\tilde{q}_j) = Q_iQ_j|\tilde{q}_i-\tilde{q}_j|^{-1}$$

$$-\partial_{x_i}\ V_{ij}^C = Q_iQ_j(x_i-x_j)|\tilde{q}_i-\tilde{q}_j|^{-3}$$
$$-\partial_{y_i}\ V_{ij}^C = Q_iQ_j(y_i-y_j)|\tilde{q}_i-\tilde{q}_j|^{-3}$$
$$-\partial_{z_i}\ V_{ij}^C = Q_iQ_j(z_i-z_j)|\tilde{q}_i-\tilde{q}_j|^{-3}$$

2) Morse Potential

$$V_{ij}^M(\tilde{q}_i,\tilde{q}_j) = D_{ij}\{1-K_{ij}\cdot\exp(-\beta_{ij}|\tilde{q}_i-\tilde{q}_j|)\}^2$$

$$-\partial x_i\ V_{ij}^M = -2\beta_{ij}K_{ij}D_{ij}\exp(-\beta_{ij}|\tilde{q}_i-\tilde{q}_j|)\{1-K_{ij}\exp(-\beta_{ij}|\tilde{q}_i-\tilde{q}_j|)\}(x_i-x_j)|\tilde{q}_i-\tilde{q}_j|^{-1}$$
$$-\partial y_i\ V_{ij}^M = -2\beta_{ij}K_{ij}D_{ij}\exp(-\beta_{ij}|\tilde{q}_i-\tilde{q}_j|)\{1-K_{ij}\exp(-\beta_{ij}|\tilde{q}_i-\tilde{q}_j|)\}(y_i-y_j)|\tilde{q}_i-\tilde{q}_j|^{-1}$$

$$-\partial_{z_i} V^m_{ij} = -2\beta_{ij}K_{ij}D_{ij}\exp(-\beta_{ij}|\tilde{q}_i-\tilde{q}_j|)\{1-K_{ij}\exp(-\beta_{ij}|\tilde{q}_i-\tilde{q}_j|)\}(z^i-z^j)|\tilde{q}_i-\tilde{q}_j|^{-1}$$

3) Lennard-Jones Potential

$$V^l_{ij}(\tilde{q}_i,\tilde{q}_j) = 4\varepsilon_{ij}\{(\sigma_{ij}/|\tilde{q}_i-\tilde{q}_j|)^{12} - (\sigma_{ij}/|\tilde{q}_i-\tilde{q}_j|)^6\}$$

$$-\partial_{x^i} V^l_{ij} = 24\varepsilon_{ij}\{2\sigma^{12}_{ij}/|\tilde{q}_i-\tilde{q}_j|^{14} - \sigma^6_{ij}/|\tilde{q}_i-\tilde{q}_j|^8\}(x^i-x^j)$$

$$-\partial_{y^i} V^l_{ij} = 24\varepsilon_{ij}\{2\sigma^{12}_{ij}/|\tilde{q}_i-\tilde{q}_j|^{14} - \sigma^6_{ij}/|\tilde{q}_i-\tilde{q}_j|^8\}(y^i-y^j)$$

$$-\partial_{z^i} V^l_{ij} = 24\varepsilon_{ij}\{2\sigma^{12}_{ij}/|\tilde{q}_i-\tilde{q}_j|^{14} - \sigma^6_{ij}/|\tilde{q}_i-\tilde{q}_j|^8\}(z^i-z^j)$$

4) General Potential

$$V^g_{ij}(\tilde{q}_i,\tilde{q}_j) = k_{ij}|\tilde{q}_i-\tilde{q}_j|^{-n}$$

$$-\partial_{x^i} V^g_{ij} = nk_{ij}|\tilde{q}_i-\tilde{q}_j|^{-n-2}(x^i-x^j)$$

$$-\partial_{y^i} V^g_{ij} = nk_{ij}|\tilde{q}_i-\tilde{q}_j|^{-n-2}(y^i-y^j)$$

$$-\partial_{z^i} V^g_{ij} = nk_{ij}|\tilde{q}_i-\tilde{q}_j|^{-n-2}(z^i-z^j)$$

5) Quadratic Angular Distortion Potential

$$V^a_{ijk}(\tilde{q}_i,\tilde{q}_j,\tilde{q}_k) = 1/2\cdot\delta_{ijk}\{\arccos(\tilde{q}_{ji}\cdot\tilde{q}_{jk})/|\tilde{q}_{ji}||\tilde{q}_{jk}| - \theta^o_{ijk}\}^2$$

$$= 1/2\cdot\delta_{ijk}\{\arccos f_{ijk}(\tilde{q}_i,\tilde{q}_j,\tilde{q}_k) - \theta^o_{ijk}\}^2$$

$$-\partial_{x^i} V^a_{ijk} = \delta\{\arccos f - \theta^o\}\{(x^k-x^j)/|\tilde{q}_{ji}||\tilde{q}_{jk}| - (x^i-x^j)\cdot f/|\tilde{q}_{ji}|^2\}/(1-f^2)^{1/2}$$

$$-\partial_{y^i} V^a_{ijk} = \delta\{\arccos f - \theta^o\}\{(y^k-y^j)/|\tilde{q}_{ji}||\tilde{q}_{jk}| - (y^i-y^j)\cdot f/|\tilde{q}_{ji}|^2\}/(1-f^2)^{1/2}$$

$$-\partial_{z^i} V^a_{ijk} = \delta\{\arccos f - \theta^o\}\{(z^k-z^j)/|\tilde{q}_{ji}||\tilde{q}_{jk}| - (z^i-z^j)\cdot f/|\tilde{q}_{ji}|^2\}/(1-f^2)^{1/2}$$

The equations for atom k are obtained by interchanging the coordinates of i and k on the right hand side of the above equations. Finally, the equations for atom j are as follows

$$-\partial_{x^j} V^a_{ijk} = s(x^i-x^j)/d\cdot\{c/|\tilde{q}_{ji}|^2-1\}+(x^k-x^j)/d\cdot\{c/|\tilde{q}_{jk}|^2-1\}$$

$$-\partial_{y^j} V^a_{ijk} = s(y^i-y^j)/d\cdot\{c/|\tilde{q}_{ji}|^2-1\}+(y^k-y^j)/d\cdot\{c/|\tilde{q}_{jk}|^2-1\}$$

$$-\partial_{z^j} V^a_{ijk} = s(z^i-z^j)/d\cdot\{c/|\tilde{q}_{ji}|^2-1\}+(z^k-z^j)/d\cdot\{c/|\tilde{q}_{jk}|^2-1\}$$

where

$$s = \delta(\arccos f - \theta^o)/(1-f^2)^{1/2}$$

and

$$d = |\tilde{q}_{ji}||\tilde{q}_{jk}|$$

$$c = (\tilde{q}_{ji} \cdot \tilde{q}_{jk})$$

D Functions and Matrix Elements for the proton-hydrogen Study

In atomic units, the basis functions have the form

$|\phi_1^\alpha(\tilde{r})> \equiv |1s(1)> = \sqrt{\pi}\cdot\exp(-r_1)$

$|\phi_2^\alpha(\tilde{r})> \equiv |2s(1)> = \sqrt{32\pi}\cdot(2-r_1)\cdot\exp(-r_1/2)$

$|\phi_3^\alpha(r)> \equiv |2pz(1)> = \sqrt{32\pi}\cdot r_1\cdot\exp(-r_1/2)\cdot\cos\theta$

The matrix elements involving the integration over two nuclear centers were evaluated by conversion to the elliptical coordinates. With reference to figure 4, these coordinates are defined as follows:

$\lambda = (r_1+r_2)/R$

$\mu = (r_1-r_2)/R$

and $\phi$ is the azimuthal angle round the axis $n_1n_2$. The ranges of these three variables are

$1 \leqslant \lambda \leqslant \infty$

$-1 \leqslant \mu \leqslant 1$

$0 \leqslant \phi \leqslant 2\pi$

Since the basis functions are orthonormal within the channels, only the cross channel elements of the matrix $\underline{N}$ need be evaluated. These elements follow.

$<1s(1)|1s(2)> = (1+R+R^2/3)\ e^{-R}$

$<2s(1)|2s(2)> = (1+R/2+R^2/12+R^3/240)\ e^{-R/2}$

$<2pz(1)|2pz(2)> = (-1-R/2-R^2/20+R^3/60+R^4/240)\ e^{-R/2}$

$<1s(1)|2s(2)> = C\{(-64/R+22-3R)+(64/R+10)\cdot e^{-R/2}\}e^{-R/2}$

$<1s(1)|2pz(2)> = C\{(64/R^2+32/R-16+3R)+(-64/R^2-64/R-8)e^{-R/2}\}e^{-R/2}$

$<2s(1)|2pz(2)> = -(R^3/120+R^4/240)e^{-R/2}$

where $C= 32/(27\sqrt{2})$.

For the matrix $\underline{V}$, the closed channel elements are as follows.

$\langle 1s(1)|V|1s(1)\rangle = (1+1/R)e^{-2R}$

$\langle 2s(1)|V|2s(1)\rangle = (1/R+3/4+R/4+R^2/8)e^{-R}$

$\langle 2pz(1)|V|2pz(1)\rangle = -12/R^3+(12/R^3+12/R^2+7/R+11/4+3R/4+R^2/8)e^{-R}$

$\langle 1s(1)|V|2s(1)\rangle = D(2+3R)e^{-3R/2}$

$\langle 1s(1)|V|2pz(1)\rangle = D\{64/9R^2+(-64/9R^2-32/3R-8-3R)e^{-3R/2}\}$

$\langle 2s(1)|V|2pz(1)\rangle = 3/R^2+(-3/R^2-3/R-3/2-5R/8-R^2/8)e^{-R}$

where $D = -2\sqrt{2}/27$ . The cross-channel elements of $\underline{V}$ follow.

$\langle 1s(1)|V|1s(2)\rangle = (1/R-2R/3)e^{-R}$

$\langle 2s(1)|V|2s(2)\rangle = (1/R+1/4-R/24+R^2/24-R^3/160)e^{-R/2}$

$\langle 2pz(1)|V|2pz(2)\rangle = (-1/R-1/4+3R/40+R^2/60-R^3/160)e^{-R/2}$

$\langle 1s(2)|V|2s(1)\rangle = C\{(-64/R^2+8/R)+(64/R^2+24/R+15/4)e^{-R/2}\}e^{-R/2}$

$\langle 1s(1)|V|2s(2)\rangle = C\{(-64/R^2+32/R-33/4+9R/8)+(64/R^2)e^{-R/2}\}e^{-R/2}$

$\langle 1s(2)|V|2pz(1)\rangle = C\{(64/R^3+48/R^2-8/R)+(-64/R^3-80/R^2-24/R-3)e^{-R/2}\}e^{-R/2}$

$\langle 1s(1)|V|2pz(2)\rangle = C\{(64/R^3+24/R^2+]2/R+6-9R/8)+(-64/R^3-56/R^2)e^{-R/2}\ e^{-R/2}$

$\langle 2s(2)|V|2pz(1)\rangle = \langle 2s(1)|V|2pz(2)\rangle = (-R/24-7R^2/240+R^3/160)e^{-R/2}$

The matrix $\underline{E}$ has the elements

$$\begin{bmatrix} -0.5 & 0.0 & 0.0 & 0.0 & 0.0 & 0.0 \\ 0.0 & -0.125 & 0.0 & 0.0 & 0.0 & 0.0 \\ 0.0 & 0.0 & -0.125 & 0.0 & 0.0 & 0.0 \\ 0.0 & 0.0 & 0.0 & -0.5 & 0.0 & 0.0 \\ 0.0 & 0.0 & 0.0 & 0.0 & -0.125 & 0.0 \\ 0.0 & 0.0 & 0.0 & 0.0 & 0.0 & -0.125 \end{bmatrix}$$

The matrices $\underline{N}', \underline{V}'$ are given by defining

$\underline{U}(i,j) = e^{i\underline{E}(i,j)t}$

where $\underline{E}(i,j)$ are the elements of the matrix $\underline{E}$ just defined and applying equation (II.21).

E Ethylene system-one-electron operators, functions and integrals

The Hamiltonian $H^o$ of (VI,2) deals only with the $\pi$ electron system, and it is taken that

$$H_i^o = -\nabla_i^2/2 - \sum_n z_n r_{ni}^{-1}$$

where the subscript i refers to the electron and n refers to the nuclei(methylene groups). $H_i^o$ is the effective one electron Hamiltonian since $z_n$ is the effective nuclear charge incorporating nuclear-nuclear and electron-electron repulsions and electron-nuclear attractions. It was found that $z_n = 1$ for n=1,2 was the most appropriate choice for the present treatment.

A common choice of one-electron functions for a hamiltonian such as $H_i^o$ are the Slater functions. In the present case only one function

$$|p_{x_n}\rangle = \eta r_n \sin\theta_n \cos\phi_n \, e^{-\zeta r_n}$$

where $\eta = \{(2\zeta)^5/4! \cdot 3/4\pi\}^{1/2}$ and $\zeta = 1.625$. The subscript refers to the nuclear centre. Then the normalization constants for the single electron molecular orbitals of (VI.3) are

$$N = 1/(2(1+S\cdot\cos\alpha))^{1/2}$$

$$N^* = 1/(2(1-S\cdot\cos\alpha))^{1/2}$$

where

$$S = \langle p_{x_a} | p_{x_b} \rangle = e^{-\rho}(1+\rho^3/15+2\rho^2/5+\rho)$$

$$\rho = \zeta R$$

The non-zero elements of the matrix $\underline{H}^o$ can now be solved. These lie only on the diagonal and the state involved is indicated in the bracket.

$$\underline{H}^o(S^o) = 4N(H_{aa}+H_{ab}\cos\alpha) + E_\sigma$$

$$\underline{H}^o(S^1) = 2N(H_{aa}+H_{ab}\cos\alpha)+2N^*(H_{aa}-H_{ab}\cos\alpha)+E_\sigma$$

$$\underline{H}^o(T_2^1) = \underline{H}^o(S^1) - 0.137$$

where

$$H_{aa} = \langle p_{x_a} | H_i^o | p_{x_a} \rangle = -\zeta^2/2-\zeta/2\rho^3\cdot(-3+2\rho^2+e^{-2\rho}(\rho^3+4\rho^2+6\rho+3))$$

$$H_{ab} = \langle p_{x_a} | H_i^o | p_{x_b} \rangle = -1.7\zeta^2/2\cdot S$$

The later integral was solved semi-empirically. The other triplet states were not evaluated since they did not couple to any other state.

The non-zero elements of the other matrices in (VI.5) are

$$-\underline{G}_\alpha(S^1,S^o) = \underline{G}_\alpha(S^o,S^1) = S\cdot\sin\alpha/\{2^{1/2}(1-S^2\cos^2\alpha)^{1/2}\}$$

$$-\underline{G}_R(S^1,S^o) = \underline{G}_R(S^o,S^1) = A\cdot\cos\alpha/(1-S^2\cos^2\alpha)^{1/2}$$

$$\underline{V}^{so*}(T_2^1,S^o) = \underline{V}^{so}(S^o,T_2^1) = \frac{iz}{2^{3/2}(137)^2(1-S^2\cos^2\alpha)} \langle p_{x_a} | r^{-3} | p_{x_b} \rangle \sin\alpha$$

$$= \frac{iz\ S\cdot\sin\alpha}{2^{3/2}(137)^2(1-S^2\cos^2\alpha)}$$

The approximate form taken for $\underline{V}^{so}$ is considered to have the correct order of magnitude and to exhibit the correct behavior or to be qualitatively correct. The integral A has the solution

$$A = \langle p_{x_a} | \partial_R | p_{x_b} \rangle = \frac{-\zeta e^{-\rho}(6\rho+6\rho^2+2\rho^3)}{60(1-S^2\cos^2\alpha)^{1/2}}$$

The derivatives needed for (VI.12) can be found directly.

The only quantities remaining to be defined explicitly are the reduced mass and inertia of the methylene groups. These were calculated by using standard weights from the Handbook of Chemistry and Physics(124) and the equilibrium configuration obtained from the calculation of Meza and Wahlgren(125) which is tabulated in table E-1. The resulting reduced mass and inertia are

$$\mu_{CH_2} = 1.276911863\cdot10^4 \text{ a.u.}$$

$$I'_{CH_2} = 5.640208385\cdot10^3 \text{ a.u.}$$

Table E-1.

| | Cartesian coordinates (a.u.) | | |
|---|---|---|---|
| atom | x | y | z |
| C | 0.0 | 0.0 | -1.263305 |
| C | 0.0 | 0.0 | 1.263305 |
| H | -1.752667 | 0.0 | -2.331023 |
| H | -1.752667 | 0.0 | 2.331023 |
| H | 1.752667 | 0.0 | 2.331023 |
| H | 1.752667 | 0.0 | -2.331023 |

F.1 Solution of one electron integrals

Two Slater functions are involved in the one-electron integrals required to solve the electronic equations of motion, these being the $|2p_y>$ and $|2p_z>$ functions which in sperical coordinates have the forms

$$|p_{y_n}> = \eta r_n \sin\theta_n \sin\phi_n e^{-\zeta r_n}$$
$$|p_{z_n}> = \eta r_n \cos\theta_n e^{-\zeta r_n}$$

where $\eta = \{(2\zeta)^5/4!\cdot 3/4\pi\}^{1/2}$ and $\zeta = 1.625$ .

Figure 23

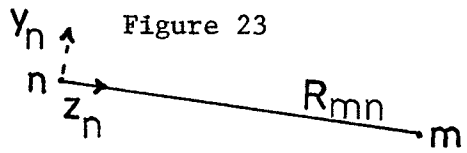


Referring to figure 23 which gives the relative spatial orientation of two nuclei, one in each molecule, and the functions associated with one centre there are two integrals of interest to this study, these being

$$I_{par}(m,n) = <p_{y_n} | Z_m/r_{mi} | p_{y_n}> = Z_m/(2R_{mn})\cdot\{e^{-2\delta}(\delta+4+6/\delta+3/\delta^2)+2-3/\delta^2\}$$

$$I_{perp}(m,n) = <p_{z_n} | Z_m/r_{mi} | p_{z_n}> = Z_m/R_{mn}\cdot\{-e^{-2\delta}(\delta^3+3\delta^2+11\delta/2+7+6/\delta+3/\delta^2) + 1+3/\delta^2\}$$

Then using the angles defined in figure 26 (appendix G) the following integrals are defined

$$I_\pi(m,n) = I_{par}(m,n)\cdot\sin^2\phi_{nm} + I_{perp}(m,n)\cdot\cos^2\phi_{nm}$$

$$I_\varepsilon(m,n) = I_{par}(m,n) \qquad \begin{matrix} m = 3,4 \\ n = 1,2 \end{matrix}$$

where m and n refer to the nuclear centre and $\delta = \zeta R_{mn}$.

F.2 Solution of the molecular orbital Integrals

Separating the operator defined by (VII.2) such that

$$V_\pi = \sum_i^\pi \sum_n^\epsilon Z(R_{ni})/r_{ni}$$

$$V_\epsilon = \sum_i^\epsilon \sum_n^\pi Z(R_{ni})/r_{ni}$$

the required M.O. integrals can be expressed in terms of the integrals defined in F.1 in the following fashion.

$$\langle S^o(1,2)|V_\pi|S^o(1,2)\rangle = N_\pi^2\{I_\pi(3,1)+I_\pi(4,1)+I_\pi(3,2)+I_\pi(4,2)\}$$

$$\langle S^1(1,2)|V_\pi|S^1(1,2)\rangle = N_\pi^{*2}\{I_\pi(3,1)+I_\pi(4,1)+I_\pi(3,2)+I_\pi(4,2)\}$$

$$\langle S^o(1,2)|V_\pi|S^1(1,2)\rangle = N_\pi N_\pi^*\{I_\pi(3,1)+I_\pi(4,1)-I_\pi(3,2)-I_\pi(4,2)\}$$

$$\langle S^o(3,4)|V_\epsilon|S^o(3,4)\rangle = N_\epsilon^2\{I_\epsilon(1,3)+I_\epsilon(1,4)+I_\epsilon(2,3)+I_\epsilon(2,4)\}$$

$$\langle S^1(3,4)|V_\epsilon|S^1(3,4)\rangle = N_\epsilon^{*2}\{I_\epsilon(1,3)+I_\epsilon(1,4)+I_\epsilon(2,3)+I_\epsilon(2,4)\}$$

$$\langle S^o(3,4)|V_\epsilon|S^1(3,4)\rangle = N_\epsilon N_\epsilon^*\{I_\epsilon(1,3)+I_\epsilon(1,4)-I_\epsilon(2,3)-I_\epsilon(2,4)\}$$

The normalization constants $N_\pi$ and $N_\epsilon$ are equivalent in form to N of appendix E and $N_\pi^*$ and $N_\epsilon^*$ to N*.

F.3 Definition of $Z(R_{mn})$.

This function was defined to have the empirical form

$$Z(R_{mn}) = -6.67e^{-.46R_{mn}}$$

The constants were obtained by use of the constraints imposed by energy cosiderations in the evaluation of the ethylene problem at the equilibrium configuration and observation of the resulting intermolecular surfaces for this system with changes in these constants. These surfaces were expected to reflect realistic potentials and do show such behavior. The form of the function was chosen on the basis of expected asymptotic behavior.

F.4 Matrix Elements for Electronic Equations of Motion

Using the M.O. integrals solved in appendix F.2 the non-zero matrix elements of $\underline{V}$ are (noting that $\underline{V}(i,j)=\underline{V}^*(j,i)$)

$$\underline{V}(1,1) = 2\langle S^o|V_\pi|S^o\rangle+2\langle S^o|V_\varepsilon|S^o\rangle$$

$$\underline{V}(2,2) = 2\langle S^o|V_\pi|S^o\rangle+\langle S^o|V_\varepsilon|S^o\rangle+\langle S^1|V_\varepsilon|S^1\rangle$$

$$\underline{V}(3,3) = \langle S^o|V_\pi|S^o\rangle+\langle S^1|V_\pi|S^1\rangle+2\langle S^o|V_\varepsilon|S^o\rangle$$

$$\underline{V}(4,4) = \langle S^o|V_\pi|S^o\rangle+\langle S^1|V_\pi|S^1\rangle+\langle S^o|V_\varepsilon|S^o\rangle+\langle S^1|V_\varepsilon|S^1\rangle$$

$$\underline{V}(1,2) = 2^{1/2}\langle S^o|V_\varepsilon|S^1\rangle$$

$$\underline{V}(1,3) = 2^{1/2}\langle S^o|V_\pi|S^1\rangle$$

$$\underline{V}(2,4) = 2^{3/2}\langle S^o|V_\pi|S^1\rangle$$

$$\underline{V}(3,4) = 2^{3/2}\langle S^o|V_\varepsilon|S^1\rangle$$

Choosing the equilibrium carbon-carbon separation for the two ethylene molecules (R=2.52 a.u.) it was calculated from the relations given in appendix E that

$$E_\pi = E_\varepsilon = -0.1454 \text{ a.u.}$$

Then using the experimentally determined separation(116) of the two singlet states ( 0.2815 a.u.)

$$E_{\varepsilon^*} = 0.1361 \text{ a.u.}$$

and $E_{\pi^*}$ is defined by the relations given in (VII.4). The matrix $\underline{E}$ (non-zero elements) is defined

$$\underline{E}(1,1) = 2E_\pi+2E_\varepsilon$$

$$\underline{E}(2,2) = E_\pi+E_{\pi^*}+2E_\varepsilon$$

$$\underline{E}(3,3) = 2E_\pi+E_\varepsilon+E_{\varepsilon^*}$$

$$\underline{E}(4,4) = E_\pi+E_{\pi^*}+E_\varepsilon+E_{\varepsilon^*}$$

## G.1 Derivation of Relative Coordinate System

The analysis presented here is a simplified version of that of Raff et al(123). One starts by defining the two dimensional cartesian coordinates in the laboratory frame for the four particles(methylene groups) as shown in figure 24.

Figure 24

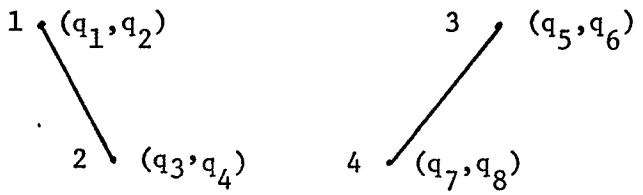


Then the relative coordinates are

$$Q_j = q_{j+2} - q_j$$

$$Q_{j+2} = q_{j+6} - q_{j+4} \qquad j = 1,2$$

$$Q_{j+4} = [(m_1 q_{j+4} + m_2 q_{j+6})/(m_3+m_4) - (m_3 q_j + m_4 q_{j+2})/(m_1+m_2)]$$

$$Q_{j+6} = M^{-1}(m_1 q_j + m_2 q_{j+2} + m_3 q_{j+4} + m_4 q_{j+6})$$

where $M=m_1+m_2+m_3+m_4$. The last set of coordinates describes the motion of the center of mass of the four patricles and will not be considered further since the present interest is in the relative motion. Now noting that $m_1=m_2=m_3=m_4=m$, the masses associated with the relative coordinates are

$$\mu_j = m/2$$

$$\mu_{j+2} = m/2$$

$$\mu_{j+4} = m$$

Since only the colinear motion of the two molecules(their centres of mass) is going to be considered, the following constraints are introduced.

$$Q_1^2+Q_2^2 = \text{constant}$$

$$Q_3^2+Q_4^2 = \text{constant}$$

$|Q_5| = R$

$Q_6 = 0$

This is followed by the transformation to the coordinates of figure 15 and the relation between the two coordinate systems is

$Q_1 = -2r\cos\alpha_1$

$Q_2 = -2r\sin\alpha_1$

$Q_3 = -2r\cos\alpha_2$

$Q_4 = -2r\sin\alpha_2$

Relating the kinetic energy in the two frames

$1/2\mu_j(\{d_tQ_1\}^2+\{d_tQ_2\}^2) = 1/2I_1\{d_t\alpha_1\}^2 = 1/2\ I_1\omega_1^2$

it is found that $I_1 = I_2 = 2mr^2$ where 2r is the carbon-carbon bond length in one of the molecules. The choice of constraints has given the third relative coordinate $R = |Q_5|$, and the associated mass is m, the methylene group mass. Then

$I_1 = I_2 = 8.100752074 \cdot 10^4$ a.u.

$m = 2.553823727 \cdot 10^4$ a.u.

## G.2 Solution of Angle Relations for Angles $\phi_{mn}$ in terms of $(R_{12}-R_{34})$

The internuclear distances $R_{mn}$ are defined by figure 25. It is taken that $R_{12}$ and $R_{34}$ are fixed

Figure 25

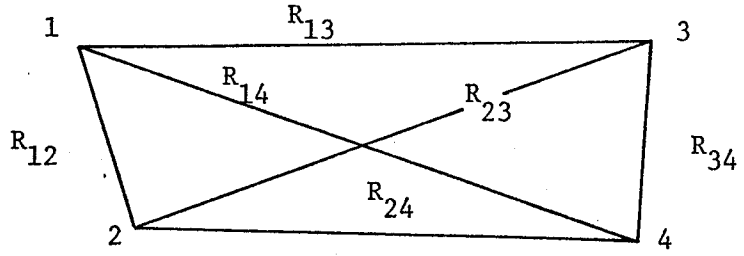


Figure 26 gives a graphical definition for $\phi_{14}$ .

Figure 26

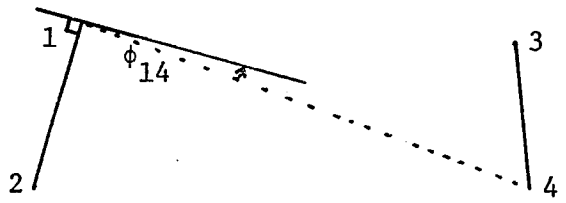


Noting that the other angles are defined similarly it follows that

$$\sin \phi_{14} = (R_{12}^2+R_{14}^2-R_{24}^2)/(2R_{12}R_{14})$$

$$\sin \phi_{13} = (R_{12}^2+R_{13}^2-R_{23}^2)/(2R_{12}R_{13})$$

$$\sin \phi_{23} = (R_{12}^2+R_{23}^2-R_{13}^2)/(2R_{12}R_{23})$$

$$\sin \phi_{24} = (R_{12}^2+R_{24}^2-R_{14}^2)/(2R_{12}R_{24})$$

and defining $a= R_{12}/2$ and $b=R_{34}/2$

$$R_{13} = ((-R+a\cos\alpha_1-b\cos\alpha_2)^2+(a\sin\alpha_1-b\sin\alpha_2)^2)^{1/2}$$

$$R_{14} = ((-R+a\cos\alpha_1+b\cos\alpha_2)^2+(a\sin\alpha_1+b\sin\alpha_2)^2)^{1/2}$$

$$R_{23} = ((-R-a\cos\alpha_1-b\cos\alpha_2)^2+(-a\sin\alpha_1-b\sin\alpha_2)^2)^{1/2}$$

$$R_{24} = ((-R-a\cos\alpha_1+b\cos\alpha_2)^2+(-a\sin\alpha_1+b\sin\alpha_2)^2)^{1/2}$$

## Bibliography


1. A. Messiah; "Quantum Mechanics", Wiley, 1966.

2. N. F. Mott, H. S. W. Massey; "The Theory of Atomic Collisions", Third Edition, Oxford University Press, 1965.

3. P. Roman; "Advanced Quantum Theory", Addison-Wesley, 1965.

4. M. L. Goldberger, K. M. Watson; "Collision Theory", Wiley, 1964.

5. R. D. Levine; "Quantum Mechanics of Molecular Rate Processes", Oxford University Press, 1969.

6. E.W. McDaniel; "Collision Phenomenum in Ionized Gases", Wiley, 1964.

7. A. O. Barut; "Scattering Theory", Gordon and Breach Science Publ., 1969.

8. K. Takayanagi; Prog. Theor. Phys. Suppl. 25,60(1963).

9. D. Rapp, T. Kassel; Chem Rev. 69, 61(1969).

10. R. D. Levine; "Molecular Collisions and Reactive Scattering", MTP International Review of Science, Phy. Chem., Series one, Volume 1, 229 (1972).

11. A. Burgess, I. C. Percival; "Classical Theory of Atomic Scattering", Adv. in Atomic and Molecular Phys. 4, 109 (1968).

12. D. R. Bates, A. E. Kingston; "Use of Classical Mechanics in the Treatment of Collisions between Massive Systems", Adv. in Atomic and Molecular Phys. 6, 269 (1970).

13. J. C. Keck; "Monte Carlo Trajectory Calculations of Atomic and Molecular Excitation in Thermal Systems", Adv. in Atomic and Molecular Phys. 8, 39 (1972).

14. W. Kolos; "Adiabatic Approximation and Its Accuracy", Adv. in Quantum Chem. 5, 99 (1970).

15. B. Corrigall, B. Kuppers, R. Wallace; Phys. Rev. A, 4, 977 (1971).

16. R. B. Gerber; Proc. Roy. Soc. A, 309, 221 (1969).

17. H. Rosenthal, Phy. Rev. A, 4, 1030 (1970).

18. J. Krenos, R. Preston, R. Wolfgang, J. C. Tully; Chem. Phys. Lett 10, 17 (1971).

19. W. L. McMillan; Phys. Rev. A, 4, 69 (1971).

20. R. Wallace; Phys. Rev. A, 2, 1711 (1970).

21. B. R. Johnson, D. Secrest; J. Math. Phys., 7, 2187 (1968).

22. A. P. Clark, A. S. Dickinson; J. Phys. B: Atom. Mol. Phys., 6, 164 (1973).

23. D. J. Diestler; J. Chem. Phy. 54, 4547 (1971).

24. E. A. McCullough, R. E. Wyatt; J. Chem. Phys., 54, 3578 (1971).

25. J. Jortner, M. Bixon; J. Chem. Phys., 48, 715 (1968).

26. J. Jortner, M. Boxon; J. Chem. Phys., 50, 3284 (1969).

27. J. Jortner, M. Bixon; J. Chem. Phys., 50, 4061 (1969).

28. A. Nitzan, J. Jortner; J. Phys. Lett., 11, 458 (1971).

29. R. Abrines, I. C. Percival; Proc. Phys. Soc., 88, 861 (1966).

30. R. Abrines, I. C. Percival; Proc. Phys. Soc., 88, 873 (1966).

31. R. A. Pettitt, Master's Thesis, "A Study of Atomic and Molecular Collision Theory", Sept. 1970, Univ. of Manitoba.

32. P. Pechukas; Phys. Rev., 181, 166, 174 (1969), J. Chem. Phys., 56, 4970 (1972).

33. W. H. Miller; J. Chem. Phys., 53, 3578 (1970), Chem. Phys. Lett., 7, 431 (1970).

34. A. P. Penner, personal communication.

35. A. P. Penner, Ph.D. thesis, May, 1974, Univ. of Manitoba.

36. A. P. Penner, R. Wallace; Phys. Rev. A, 7, 1007 (1973).

37. J. C. V. Chen, K. M. Watson; Phys. Rev., 174, 152 (1968).

38. J. C. V. Chen, K. M. Watson; Phys. Rev., 188, 236 (1969).

39. J. C. V. Chen, C.-S. Wong, K. M. Watson; Phys. Rev. A, 1, 1150 (1970).

40. P. J. Kuntz, M. H. Mak, J. C. Polanyi; J. Chem. Phys., 50, 4623 (1969).

41. P. J. Kuntz, E. M. Nemeth, J. C. Polanyi; J. Chem. Phys., 50, 4607 (1969).

42. J. C. Polanyi, W. H. Wong; J. Chem. Phys., 51, 1439 (1969).

43. P. J. Kuntz, E. M. Nemeth, J. C. Polanyi, W. H. Wong; J. Chem. Phys., 52, 4654 (1970).

44. M. H. Mak, J. C. Polanyi; J. Chem. Phys., 51, 1451 (1969).

45. M. H. Mak, J. C. Polanyi; J. Chem. Phys., 53, 4588, (1970).

46. N. Blais; J. Chem. Phys., 49, 9 (1968).

47. M. Godfrey, M. Karplus; J. Chem. Phys., 49, 3602 (1968).

48. L. Wilets, D. F. Gallaher; Phy. Rev., 147, 13 (1966), 169, 139 (1968).

49. D. R. Bates, D. S. F. Crothers; Proc. Roy. Soc. (London), A315, 465 (1970).

50. J. B. Delos, W. R. Thorson, S. K. Knudson; Phys. Rev. A, 6, 709 (1972), 6, 720 (1972).

51. R. Parr; "Quantum Theory of Molecular Electronic Structure", W. A. Benjamin, Inc. (1964).

52. L. C. Allen; Ann. Rev. of Phys. Chem., 20, 315 (1969).

53. L. Radom, J. A. Pople; MTP Review of Science, Phys. Chem. Series One, Vol. 1, 71 (1972).

54. H. Weinstein, R. Pauncz, M. Cohen; Adv. in Atomic and Mol. Phys., 7, 97 (1971).

55. M. B. Robin, R.R. Hart, N. A. Kuebler; J. Chem. Phys., 44, 1803 (1966).

56. R. J. Buenker, S. D. Peyerimhoff, W. E. Kammer; J. Chem. Phys., 55, 814 (1971).

57. R. J. Buenker, S. D. Peyerimhoff, H. L. Hsu; Chem. Phys. Lett., 11, 65 (1971).

58. J. A. Pople, D. L. Beveridge ; 'Approximate Molecular Orbital Theory',McGraw-Hill, 1970.

59. F. T. Smith; Phys. Rev., 179, 111 (1969).

60. R. D. Levine, Johnson, Bernstein; J. Chem. Phys., 1694 (1969).

61. D. J. Locker, P. F. Endres; J. Chem. Phys., 51, 5482 (1969).

62. D. J. Locker, D. J. Wilson; J. Chem. Phys., 52, 271 (1970).

63. B. W. Goodwin, Ph.D. thesis, University of Manitoba, May, 1974.

64. B. W. Goodwin, R. Wallace; J. Magn. Res., 8, 41 (1972), 9, 280 (1973).

65. C. E. Froberg; "Introduction to Numerical Analysis", Addison-Wesley, Second Edition, 1969.

66. A. Ralston, H. S. Wilf; "Mathematical Methods for Digital Computers", Wiley, 1967.

67. F. B. Hildebrand; "Introduction to Numerical Analysis", McGraw-Hill, Second Edition, 1974.

68. P. Henrici; "Discrete Variable Methods in Ordinary Differential Equations", Wiley, 1962.

69. R. L. Crane, R. W. Klopfenstein; J. Assoc. Comp. Mach., 12, 227 (1965).

70. H. A. Luther; SIAM Review, 8, 374 (1966).

71. J. D. Lawson; SIAM J. Num. Anal., 4, 620 (1967).

72. H. A. Luther, H. P. Konen; SIAM Review, 7, 551 (1965).

73. S. Gill; Proc. Camb. Phil. Soc., 47, 96 (1951).

74. Assembler Language; IBM Manual C28-514-8.
Principles of Operation; IBM Manual A22-6821-8.

75. PL/1 Programmer's Guide; IBM Manual C28-6594-8.
IBM System 360 Operating System PL/1 Language Ref. Man.;
IBM Manual C28-8201-4.

76. Basic Fortran Language; IBM Manual C28-6629-2.
IBM SYS/360 Fortran IV(G & H) Programmer's Guide;
IBM Manual C28-6817-4.

77. G. Herzberg; "Infrared and Raman Spectra", Van Nostrand, 1945, P. 168.

78. P. M. Morse; Phys. Rev., 34, 57 (1929).

79. J. Mathews, R. L. Walker; "Mathematical Methods of Physics", Benjamin, 1965.

80. B. H. Brandson; "Atomic Rearrangement Collisions", Adv. in Atomic and Mol. Phys., 1, 85, Academic Press, 1965.

81. J. O. Hirschfelder, C. F. Curtiss, R. B. Bird; "Molecular Theory of Gases and Liquids", Wiley 1954, P. 22.

82. G. Herzberg; "Spectra of Diatomic Molecules", Van Nostrand 1950.

83. Calculated from anharmonicity in (82).

84. R. Boyd; private communication.

85. H. K. Shin; J. Chem. Phys., 49, 3964 (1968).

86. J. G. Parker; J. Chem. Phys., 41, 1600 (1964).

87. S. W. Benson, G. C. Berend; J. Chem. Phys., 44, 470 (1966).

88. S. L. Thompson; J. Chem. Phys., 49, 3400 (1968).

89. J. B. Calvert, R. C. Amne; J. Chem. Phys., 45, 4710 (1966).

90. S. W. Benson, G. C. Berend, J. C. Wu; J. Chem. Phys., 37, 1386 (1962).

91. S. W. Benson, G. C. Berend; J. Chem. Phys., 40, 1289 (1964).

92. S. W. Benson, G. C. Berend; J. Chem. Phys., 44, 4247 (1966).

93. G. C. Berend, S. W. Benson; J. Chem. Phys., 51, 1480 (1969).

94. R. F. Stebbings, R. A. Young, C. L. Orley, H. Ehrhardt; Phys. Rev., 138, A1312 (1965).

95. L. Wilets, D. F. Gallaher; Phys. Rev., 147, 13 (1966).

96. D. F. Gallaher, L. Wilets; Phys. Rev., 169, 139 (1966).

97. I. M. Cheshire; J. Phys. B, 1, 428 (1968).

98. I. M. Cheshire, D. F. Gallaher, A. J. Taylor; J. Phys. B, 3, 813 (1970).

99. D. Rapp, D. Dinwiddie, D. Storm, T. E. Sharp; Phys. Rev. A, 5, 1290 (1972).

100. D. Rapp, D. Dinwiddie; J. Chem. Phys., 57, 4919 (1972).

101. H. Tai, E. Gerjuay; J. Phys. B, Atom. Mol. Phys., 6, 1426 (1973).

102. A. P. Penner; personal communication.

103. S. Geltman; "Topics in Atomic Collision Theory", Academic Press, New York, 1969.

104. B. Corrigall; M. Sc. thesis, University of Manitoba, February, 1970.

105. B. Corrigall, R. Wallace; unpublished, private communication.

106. B. Corrigall, R. Wallace; J. Phys., B, 4, 1013 (1971).

107. R. Wallace; Molec. Phys., 15, 249 (1968).

108. H. F. Helbig, E. Everhart; Phys. Rev., 140, A715 (1965).

109. W. E. Kaupilla, P. J. O. Teubner, W. L. Fite, R. J. Girnius; Phys. Rev. A, 2, 1759 (1970).

110. A. A. Lamala, N. J. Turro; "Energy Transfer and Organic Photochemistry", Vol. XIV of Tech. of Org. Chem., Interscience, 1969.

111. O. L. Chapman, Ed.; "Organic Photochemistry", Vol. I, Marcel-Dekker, 1967.

112. N. J. Turro; "Molecular Photochemistry", W. A. Benjamin, 1965.

113. M. Bixon, J. Jortner; J. Chem. Phys., 48, 715 (1968).

114. R. S. Mulliken, C. C. J. Roothaan; Chem. Rev., 41, 219 (1947).

115. M. B. Robin, R. R. Hart, N. A. Kuebler; J. Chem. Phys., 44, 1803 (1966).

116. R. J. Buenker, S. D. Peyerimhoff, W. E. Kammer; J. Chem. Phys., 55, 814 (1971).

117. R. J. Buenker, S. D. Peyerimhoff, H. L. Hsu; Chem. Phys. Lett., 11, 65 (1971).

118. J. A. Ryan, J. L. Whitten; Chem. Phys. Lett., 15, 119 (1972).

119. B. Levy, J. Ridard; Chem. Phys. Lett., 15, 49 (1972).

120. S. Meza, U. Wahlgren; Theor. Chim. Acta(berl), 21, 323 (1971).

121. H. Goldstein; "Classical Mechanics", Addison-Wesley, Reading, 1965.

122. W. M. Gelbart, K. F. Freed, S. A. Rice; J. Chem. Phys., 52, 2460 (1970).

123. L. M. Raff, D. L. Thompson, L. B. Sims, R. N. Porter; J. Chem. Phys., 56, 5998 (1972).

124. R. C. Weast, S. M. Selby, C. D. Hodgman;editors,' Handbook of Chemistry and Physics', 46th Ed.,Chem. Rubber Co., 1965-1966.

125. S. Meza, U. Wahlren; Theor. Chin. Acta(Berl), 21, 323 (1971).

126. B. C. Eu; J. Chem. Phy., 52,1882(1970), 52, 3903(1970), 55, 5600(1971), 56, 2507(1972), 56, 5202(1972), 58,472(1973).

127. B. C. Eu, T. P. Tsien; Chem. Phy. Lett, 17, 256 (1971).

128. R. A. Marcus, J. Chem. Phy., 54, 3965 (1972), 56, 311 (1972), 56, 3548 (1972).

129. R. J. Cross, Jr.; J. Chem. Phy., 58, 5178 (1973).

130. R. J. Cross, Jr.; J. Chem. Phy., 47, 3724 (1967), 48, 4338 (1968), 51, 5163 (1969).

131. D. R. Bates, R. McCarroll; Proc Roy Ser (London), A245, 175 (1968).